Purdue University
Purdue e-Pubs

Open Access Dissertations | Theses and Dissertations

January 2016

INVESTIGATING RHEOLOGICAL TECHNIQUES TO MODEL AND PREDICT OPERATING CONDITIONS OF A SINGLE SCREW EXTRUDER WITH INTERNAL RESTRICTIONS

Amudhan Ponrajan
Purdue University

Follow this and additional works at: https://docs.lib.purdue.edu/open_access_dissertations

Recommended Citation
Ponrajan, Amudhan, "INVESTIGATING RHEOLOGICAL TECHNIQUES TO MODEL AND PREDICT OPERATING CONDITIONS OF A SINGLE SCREW EXTRUDER WITH INTERNAL RESTRICTIONS" (2016). *Open Access Dissertations*. 1267.
https://docs.lib.purdue.edu/open_access_dissertations/1267

This document has been made available through Purdue e-Pubs, a service of the Purdue University Libraries. Please contact epubs@purdue.edu for additional information.

Graduate School Form
30 Updated 12/26/2015

PURDUE UNIVERSITY
GRADUATE SCHOOL
Thesis/Dissertation Acceptance

This is to certify that the thesis/dissertation prepared

By Amudhan Ponrajan

Entitled

INVESTIGATING RHEOLOGICAL TECHNIQUES TO MODEL AND PREDICT OPERATING CONDITIONS OF A SINGLE SCREW EXTRUDER WITH INTERNAL RESTRICTIONS

For the degree of Doctor of Philosophy

Is approved by the final examining committee:

Dr. Martin R. Okos
Chair

Dr. Osvaldo H. Campanella

Dr. Bruce R. Hamaker

Dr. Ganesan Narsimhan

To the best of my knowledge and as understood by the student in the Thesis/Dissertation Agreement, Publication Delay, and Certification Disclaimer (Graduate School Form 32), this thesis/dissertation adheres to the provisions of Purdue University's "Policy of Integrity in Research" and the use of copyright material.

Approved by Major Professor(s): Dr. Martin R. Okos

Approved by: Dr. Bernard A. Engel 7/11/2016

Head of the Departmental Graduate Program Date

INVESTIGATING RHEOLOGICAL TECHNIQUES TO MODEL AND PREDICT OPERATING CONDITIONS OF A SINGLE SCREW EXTRUDER WITH INTERNAL RESTRICTIONS

A Dissertation

Submitted to the Faculty

of

Purdue University

by

Amudhan Ponrajan

In Partial Fulfillment of the

Requirements for the Degree

of

Doctor of Philosophy

August 2016

Purdue University

West Lafayette, Indiana

To my parents

ACKNOWLEDGEMENTS

I would like to start by thanking my advisor, Dr. Martin Okos for his continued guidance and never ending support throughout my Ph.D. Through his mentorship, I have acquired several academic and professional skills during my time here at Purdue University. His support has been critical in my experiences with developing country projects, which are unique and very valuable.

I would like to thank my graduate advisory committee members, Dr. Campanella, Dr. Narsimhan and Dr. Hamaker. They have all been very supportive, were willing and were open and available to discuss the various aspects of my dissertation, without which this work would not have been possible. I would like to thank Dr. Campanella for his teachings on capillary rheometry and extrusion which were very crucial for this work. His training on critical thinking and questioning previous work done in this area has truly led to paradigm shifting work through this dissertation. Dr. Narsimhan's classes on basic and advanced transport phenomena laid the foundation for the analytical modeling work in this dissertation. I would like to thank him for the numerous meetings and for his patience in working with me on modeling. I would like to express my sincerest gratitude to Dr. Hamaker for his support not only on my dissertation but also for allowing me to work on developing countries projects with direct application of my research topic. Taking the small-scale extruder to Senegal, Niger and Kenya through his projects and working

in-person, hands-on with researchers from these countries was truly a once in a lifetime experience and I'm very thankful for having the opportunity. I'm entirely certain that this work will play a crucial role in shaping my future career.

I would like to thank the tremendous and timely support I've received from the ABE department machine shop under Scott Brand and Garry Williams. I would like to thank the Food Science department pilot plant maintained by Steve Smith and Mathias Bohn, where all my extrusion experiments were conducted. I would like to thank all the professors who have allowed me to use their laboratories during the last 4 years for several aspects of my work. I would like to thank the friendliest staffs in the ABE business office, especially Barb, Becky and Pam and the Food Science staff for their support.

I would also like to thank my numerous friends near and far who have been constantly supporting me throughout my Ph.D. And last but not the least, I would like to thank my family members for their constant support during the last four years, especially my parents.

TABLE OF CONTENTS

Page

Page

LIST OF TABLES

Table Page

LIST OF FIGURES

Figure Page

Figure Page

Figure Page

Figure Page

Figure Page

ABSTRACT

Ponrajan, Amudhan. Ph.D., Purdue University, August 2016. Investigating Rheological Techniques to Model and Predict Operating Conditions of a Single Screw Extruder with Internal Restrictions. Major Professor: Martin Okos.

Understanding rheology of raw materials and the numerous transformations they undergo is an essential aspect of modeling and predicting extrusion conditions. Both off-line capillary rheometry and in-line extruder fed rheometry techniques have been used to model rheology of materials during extrusion. Investigations on use of an off-line capillary rheometer to model apparent viscosity of full fat soy flours revealed inability of the capillary rheometer to handle food/biological materials high in oil content (20%) at high temperature (80^{o}C) and low moisture content (15% wet basis). The lack shear degradation in the capillary rheometer also resulted in over-prediction of corn flour viscosities at high temperatures (80 to 120^{o}C), shear rates (1 to 100 s^{-1}) and low moisture contents (35 to 40%). A novel two-opening die attached to a small scale extruder operating at 100 to 300 rpm was used to measure in-line viscosities of cornmeal at 32.5 to 37.5% moisture during extrusion. Comparison of off-line versus in-line cornmeal viscosities at similar conditions consistently indicated that for food/biological materials sensitive to shear degradation, in-line viscosities were lower. Pasting property measurement revealed differences in material transformation which could be used to explain differences between techniques. Mechanistic model for the small-scale

extruder with screw restrictions was built by considering a modified plane Couette flow setup with varying gaps and heat fluxes leaving at both plates, for one screw, one restriction and a die setup. The model successfully predicts the effect of screw restriction gap, extrusion pressure, viscous dissipation and heat fluxes.

Keywords: Extrusion, rheology, modeling, grains

CHAPTER 1. INTRODUCTION

Extrusion processing has become a versatile and valuable technology for polymer & plastics, food & feed, and paper milling industries. Since its introduction, the technology has evolved over time to adapt to various needs. Tremendous amount of research has been carried out in understanding and development of extruders from piston or ram-type extruders, to the most advanced twin screw extruders with precision control at every stage of the process. Understanding the rheology of raw materials and the numerous transformations they undergo during extrusion has been proven to be an essential aspect of understanding the process. It is necessary for modeling various components of the extrusion process, which in turn can help predict and optimize operating conditions, design and scale-up processes, define final product characteristics and reduce cost (Bouvier and Campanella, 2014; Harper, 1981; Mercier et al., 1989).

1.1 Rheological techniques

Both in-line and off-line rheometry techniques have been used to understand the rheology of a material during extrusion. Capillary rheometry is one of the most common off-line techniques used in polymer processing, mainly to measure viscosities at high shear rates. Compared to rotational rheometers which are limited to liquids, gels or pastes, capillary rheometers can be used to measure high viscosities of polymer melts at high

temperatures, similar to conditions during extrusion (Bird et al., 1987; Morrison, 2001). Capillary rheometers have also been used to quantify viscosities of different food materials/biopolymers, which exhibit a non-Newtonian pseudoplastic behavior, under a range of conditions similar to extrusion (Bagley et al., 1998; Dautant et al., 2007; Fraiha et al., 2011; Remsen and Clark, 1978; Sandoval and Barreiro, 2007; Singh and Smith, 1999; Xie et al., 2012).

The most common in-line technique involves a single-screw or a twin-screw extruder feeding directly into a slit die or a capillary die viscometer which is fitted with multiple pressure transducers along its length to measure pressure drop, flow rate and hence viscosity at different conditions. In the case of food materials/biopolymers, this technique has been used primarily in high temperature, shear and low moisture conditions (Fletcher et al., 1985; Harper et al., 1971; Li et al., 2004; Robin et al., 2010; Vergnes et al., 1993; Wang et al., 1990). As an alternate to in-line slit die or capillary die viscometer, which is challenging to operate especially with biopolymers, a dual orifice die has also been investigated (Drozdek and Faller, 2002). More recently, off-line capillary rheometer measurements and in-line extruder die pressure and flow rate measurements have been utilized in combination to quantify the viscosity of food doughs with varying composition at low temperature, high moisture conditions in pasta extrusion (de la Pena et al., 2014).

Modeling of extruders began in the plastic/polymer industry, but have been adopted in food/biopolymer industry over the years. Single screw extruders have been modeled mechanistically and numerically, whereas twin screw extruders have primarily been modeled numerically due to the complex flow patterns between the screws. The basic

mechanistic model is of the metering section in a single screw extruder where the screw is considered as a long channel peeled off the screw root and approximating it to a two dimensional plane Couette flow. Velocity profiles in the channel, operating characteristics such as flow rate and pressure build-up at the die, leakage flow due to clearance between the barrel and screw channel, presence of barrel grooves and tapered channels in specialized extruders have been successfully accounted for by this approach, for Newtonian fluids. In the case of non-Newtonian fluids, complications arise in the solution of the equation of motion, hence often, they are carefully approximated as Newtonian within certain defined conditions (Harper, 1981). In the case of foods/biopolymers, during extrusion processing, they undergo a structural transformation in a short period of time. Hence, along with the non-Newtonian behavior, the raw material undergo various transformations such as starch gelatinization or melting or fragmentation, protein denaturation, binding of macromolecules and other such transformations which complicate modeling their behavior under various extrusion conditions. Various approaches to account for the aforementioned challenges with food/biopolymer extrusion modeling have been documented in several texts (Bouvier and Campanella, 2014; Harper, 1981; Kokini et al., 1992; Mercier et al., 1989).

1.2 Small-scale single screw extruder development

A 30 kg/hr small-scale single screw extruder, with restrictions on the screw was developed at Purdue University (West Lafayette, Indiana), in partnership with Insta-Pro International (Des Moines, Iowa), for the National Aeronautical and Space Administration (NASA; Figure 1.1). The design of the extruder was based on the scale-

down of a 300 kg/hr extruder by Insta-Pro International. It was part of a small-scale multipurpose seed processor project to serve NASA in long duration Advance Life Support system missions beyond Low Earth Orbit. The temperature rise of raw materials is purely based on the viscous dissipation during extrusion and no external heat was provided (Insta-ProInternational, 2004).

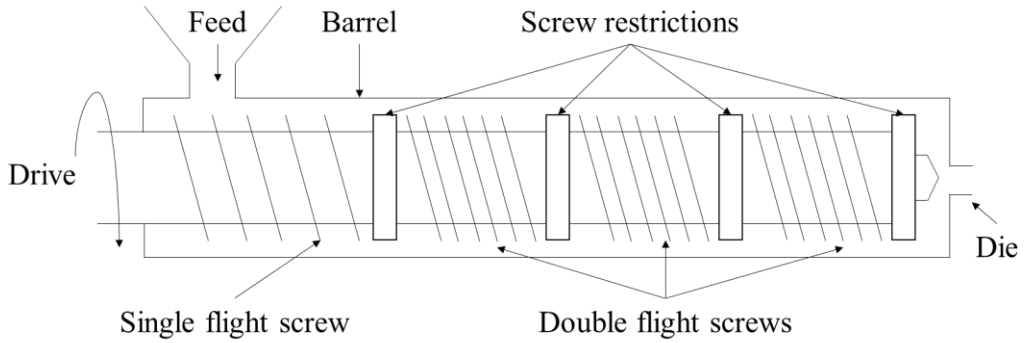

Figure 1.1. Schematic of the small-scale single-screw extruder with restrictions on the screw.

The potential application of this small-scale extruder in developing countries is being investigated. One of the main interests is in producing pre-cooked flours from raw grains using this extruder. Through a project on process development for ready-to-use therapeutic foods (RUTF) for developing countries, nine different grains/grain blends, including cereals, legumes and oil seeds were extruded in the small-scale extruder, to produce pre-cooked flours. The key operating parameters of the extruder identified based on a trial and error approach through this work is tabulated in Table 1.1.

Table 1.1. Extrusion parameters for different grains extruded for the RUTF project

Grain	Moisture content (% wet basis)	Screw speed (RPM)	Die Temperature (^{o}C)
Full fat + defatted soybean meal (13% oil content)	10	950	160
Oats groats	35	700	115
Whole grain yellow corn + Green peas	30	300	115
Whole grain teff	35	500	115
Dehulled pearl millet	35	700	120
Whole grain white corn	35	900	120
Emmer wheat grits	35	600	115
Garbanzo beans	35	750	120
Lentils	35	550	115

1.3 Problem Statement

The current challenge is the lack of a systematic method to predict operating conditions of the extruder, so a trial and error approach can be minimized and more informed decisions can be made when presented with a new grain to extrude.

Capillary rheometry is an off-line technique that can be used to measure, model and predict viscosity of solid materials at high shear rates and temperatures, similar to conditions in the extruder. In-line techniques such as an extruder fed slit or capillary die viscometer could also be used to measure and model viscosity at various extrusion conditions. Viscosity models thus developed could be used to mechanistically model extruders and predict various operational and product parameters.

The advantage of capillary rheometry technique is relatively low sample requirement and shorter experimentation times. As first objective, full fat soybeans, whole grain yellow corn and whole grain white corn, which operated at different conditions in the extruder, were chosen for measuring and modeling viscosity using a capillary rheometer at high shear rates, temperatures and low moisture contents. Preliminary results for soy beans showed the inability of the capillary rheometer to handle raw material with high oil content, due to pressure instability. In the case of corn, although consistent results were obtained with replications, viscosity models for the two types of corn failed to show significant differences between them, as evidenced in extruder operating conditions. The model was also over predicting the viscosity compared to other in-line models published in literature at similar extruder operating conditions (Li et al., 2004).

The lack of shear degradation in the capillary rheometer compared to the extruder was hypothesized to be the main reason for its inability to accurately measure the apparent viscosity of the material used. In-line techniques, such as a slit-die or capillary-die viscometer at the extruder die, on the other hand, have offered better resolution in measuring viscosity of various food materials and can also detect changes in shear history of the extrusion process (Li et al., 2004; Vergnes et al., 1993; Wang et al., 1990). Using in-line rheometers in conjunction with the small-scale extruder pose operational challenges in terms of maintaining a continuous flow through the rheometer and preventing the product from plugging the rheometer. Hence a different approach was needed for in-line viscosity measurement for the small-scale extruder. Use of specially designed dies with multiple openings was a possibility for this purpose (Drozdek and Faller, 2002). de la Pena et al. (2014) while comparing in-line extrusion measurements with capillary rheometry, showed the possibility of using a capillary rheometer to predict process parameters during pasta extrusion process in a region of low temperature, low shear and high moisture content. Hence as second objective, the apparent viscosity of dehulled, degermed yellow corn was measured and modeled off-line in a capillary rheometer and in-line with a two opening die for the small scale extruder, in a region of high temperature, high shear and low moisture content.

There has been no research investigating the differences in product transformation that the material goes through during apparent viscosity measurements between an off-line and an in-line technique. Hence as a part of the second objective, the difference in product transformation that occurs in the capillary rheometer versus the extruder

measurement was also investigated, to further understand the limitations of off-line measurements. Pasting properties, differential scanning calorimetry and size exclusion chromatography of the native and processed material could be used to quantify these differences (Moussa et al., 2011; Núñez et al., 2010).

Mechanistic models that have been developed thus far for single screw extruders have looked at the screw as a continuous channel unwound from the screw root. Variations in the width and height of the channel have also been modeled (Harper, 1981). But there is a lack of literature in mechanistic models for single screw extruders with restrictions on the screw. Hence as a third objective, a one-dimensional modified plane Couette flow with varying widths was investigated as a basic mechanistic model for a single screw extruder with restrictions.

1.4 Hypothesis

The working hypothesis of this research is that, given the feed material properties, extruder process conditions can be predicted based on desired final product characteristics.

1.5 Goal and objectives

The overall goal of this proposal is to develop a methodology to model and predict operating conditions, such as raw material moisture content and extruder screw speed which influence die temperature, of the small-scale extruder with restrictions on the screw, based on the rheological properties of a given grain, which is measured by either

off-line or in-line rheometry techniques. This research goal will be achieved through the following three primary objectives:

1. Develop rheological models for various grains using off-line capillary rheometry at high temperature, shear and low moisture extrusion conditions
    a. Study the effect of temperature, moisture content and shear rate on the viscosity of grains in an off-line capillary rheometer
    b. Develop master curve Power-law viscosity models that account for change in temperature, moisture content and shear rate for various grains
2. Compare off-line capillary rheometer and in-line extruder-fed capillary rheometer at high temperature, shear and low moisture extrusion conditions
    a. Study the use of dies with two openings of different diameters, as an in-line viscosity measurement technique for the small-scale extruder
    b. Compare in-line and off-line viscosity measurements
    c. Use pasting properties to quantify differences in product transformation during in-line and off-line viscosity measurements
3. Build a fundamental mechanistic model for a small-scale single screw extruder with restrictions on the screw
    a. Develop an analytical model for one double flight screw section and shear bushing using one-dimensional plane Couette flow with varying width between the two plates
    b. Understand the effect of pressure, heat fluxes and viscous dissipation for a Newtonian fluid on velocity and temperature profiles

1.6 References

Bagley, E.B., Dintzis, F.R., Chakrabarti, S., (1998). Experimental and conceptual problems in the rheological characterization of wheat flour doughs. Rheologica Acta. 37(6), 556-565.

Bird, R.B., Armstrong, R.C., Hassager, O., (1987). *Dynamics of polymeric liquids: Volume 1 - Fluid Mechanics*. John Wiley & Sons, New York, USA.

Bouvier, J., Campanella, O.H., (2014). *Extrusion processing technology: food and non-food biomaterials*. John Wiley & Sons, Ltd, West Sussex, UK.

Dautant, F.J., Simancas, K., Sandoval, A.J., Muller, A.J., (2007). Effect of temperature, moisture and lipid content on the rheological properties of rice flour. Journal of Food Engineering. 78(4), 1159-1166.

de la Pena, E., Manthey, F.A., Patel, B.K., Campanella, O.H., (2014). Rheological properties of pasta dough during pasta extrusion: Effect of moisture and dough formulation. Journal of Cereal Science. 60(2), 346-351.

Drozdek, K.D., Faller, J.F., (2002). Use of a dual orifice die for on-line extruder measurement of flow behavior index in starchy foods. Journal of Food Engineering. 55(1), 79-88.

Fletcher, S., McMaster, T., Richmond, P., Smith, A., (1985). Rheology and extrusion of maize grits. Chemical Engineering Communications. 32(1-5), 239-262.

Fraiha, M., Biagi, J.D., Ferraz, A.C.d.O., (2011). Rheological behavior of corn and soy mix as feed ingredients. Food Science and Technology (Campinas). 31(1), 129-134.

Harper, J., Rhodes, T.P., Wanninger, L., (1971). Viscosity model for cooked cereal doughs, *Chemical Engineering Progress Symposium Series*, pp. 40-43.

Harper, J.M., (1981). *Extrusion of foods: Volume I*. CRC Press, Boca Raton, Florida.

Insta-ProInternational, (2004). NASA SBIR Phase I Proposal. Purdue Univeristy and Insta-Pro International, West Lafayette, Indiana.

Kokini, J.L., Ho, C., Karwe, M.V., (1992). *Food extrusion science and technology*. Marcel Dekker, Inc., New York, New York.

Li, P.X., Campanella, O.H., Hardacre, A.K., (2004). Using an in-line slit-die viscometer to study the effects of extrusion parameters on corn melt rheology. Cereal Chemistry. 81(1), 70-76.

Mercier, C., Linko, P., Harper, J.M., (1989). *Extrusion cooking*. American Association of Cereal Chemists, Inc., St. Paul, Minnesota, USA.

Morrison, F.A., (2001). *Understanding rheology*. Oxford University Press, Inc., New York, USA.

Moussa, M., Qin, X., Chen, L.F., Campanella, O.H., Hamaker, B.R., (2011). High-quality instant sorghum porridge flours for the West African market using continuous processor cooking. International Journal of Food Science & Technology. 46(11), 2344-2350.

Núñez, M., Della Valle, G., Sandoval, A.J., (2010). Shear and elongational viscosities of a complex starchy formulation for extrusion cooking. Food research international. 43(8), 2093-2100.

Remsen, C.H., Clark, J.P., (1978). A viscosity model for a cooking dough. Journal of Food Process Engineering. 2(1), 39-64.

Robin, F., Engmann, J., Tomasi, D., Breton, O., Parker, R., Schuchmann, H.P., Palzer, S., (2010). Adjustable Twin-Slit Rheometer for Shear Viscosity Measurement of Extruded Complex Starchy Melts. Chemical Engineering & Technology. 33(10), 1672-1678.

Sandoval, A.J., Barreiro, J.A., (2007). Off-line capillary rheometry of corn starch: Effects of temperature, moisture content and shear rate. Lwt-Food Science and Technology. 40(1), 43-48.

Singh, N., Smith, A.C., (1999). Rheological behaviour of different cereals using capillary rheometry. Journal of Food Engineering. 39(2), 203-209.

Vergnes, B., DellaValle, G., Tayeb, J., (1993). A sprcific slit die rheometer for extruded starchy products - Design, validation and application to maize starch. Rheologica Acta. 32(5), 465-476.

Wang, S., Bouvier, J., Gelus, M., (1990). Rheological behaviour of wheat flour dough in twin-screw extrusion cooking. International Journal of Food Science & Technology. 25(2), 129-139.

Xie, F.W., Halley, P.J., Averous, L., (2012). Rheology to understand and optimize processibility, structures and properties of starch polymeric materials. Progress in Polymer Science. 37(4), 595-623.

CHAPTER 2. RHEOLOGICAL MODELING OF VARIOUS GRAINS USING OFF-LINE CAPILLARY RHEOMETRY AT HIGH TEMPERATURE, SHEAR AND LOW MOISTURE EXTRUSION CONDITIONS

2.1 Introduction

Rheological modeling of food materials is essential in understanding and modeling food extrusion processes, to predict operating conditions and define final product properties. A number of food materials, from pure starches and cereal grains to grain blends with multiple ingredients have been studied for their rheological behavior under high temperature and low moisture extrusion conditions. Based on the composition of the individual components such as starches, proteins, lipids and fiber, the behavior of these materials vary widely (Harper, 1981; Mercier et al., 1989).

2.2 Literature review

Both off-line and in-line techniques have been employed for this purpose. Off-line measurements were primarily made using capillary rheometers. Remsen and Clark (1978) were among the first to report a viscosity model at extrusion conditions for a soy flour dough system using a capillary rheometer. Since then, rheology of several different food materials have been studied and modeled using a capillary rheometer, including corn (maize) starch (Mackey and Ofoli, 1990; Sandoval and Barreiro, 2007; Vergnes and Villemaire, 1987), maize grits, potato powder (Senouci and Smith, 1988), potato granule

pastes (Halliday and Smith, 1995), wheat dough (Bagley et al., 1998), wheat meal, wheat starch, with or without added wheat germ oil and oat flour (Singh and Smith, 1999), rice flour (Dautant et al., 2007), complex starchy ready-to-eat formula (Núñez et al., 2010), corn and soy mix (Fraiha et al., 2011) and pasta dough (de la Pena et al., 2014). In most cases, there is no mechanical treatment in the capillary rheometer, as in the case of an extruder. Vergnes and Villemaire (1987) were the first to use a novel capillary rheometer with pre-shearing treatment called Rheoplast®, for modeling maize starch viscosity and the same was used by Núñez et al. (2010) for modeling viscosity of a complex starchy formula.

In-line techniques have also been used to model viscosity of various food materials, in the form of an extruder fed slit-die or capillary-die rheometer mounted with pressure transducers and temperature control options. The use of in-line rheometers have evolved over a period time with better understanding of thermomechanical history the product has experienced in the extruder before in-line measurements (Harper et al., 1971; Lai and Kokini, 1990; Li et al., 2004; Robin et al., 2010; Senouci and Smith, 1988; Vergnes et al., 1993).

Regardless of the technique used, food melts at extrusions conditions have exhibited a non-Newtonian pseudoplastic behavior, which have been fitted to a Power law model. Temperature, moisture content and shear rate are among the most common critical parameters that are modeled to describe the viscosity of a food melt. The effect of temperature is expressed by an Arrhenius-type equation, whereas moisture content and shear rate can be fitted with exponential expressions, incorporated into the power law

model. Dautant et al. (2007) developed a Power law model for rice flour using a capillary rheometer which accounts for change in lipid content (3, 5 and 7%) through an exponential expression along with temperature (90, 100, 130 and 150^{o}C), moisture content (21, 25 and 29 % wet basis) and shear rate (50 to 500 s^{-1}) variations. Similarly, Sandoval and Barreiro (2007), reported the effect of temperature (85, 100 and 120^{o}C), moisture content (27 to 30% wet basis) and shear rate (100 to 2000 s^{-1}) on corn starch rheology using off-line capillary rheometry. More recently, Fraiha et al. (2011) modeled the viscosity of a blend of corn and soybean (70:30 weight basis) in a capillary rheometer at various temperatures (80, 120 and 160^{o}C), moisture contents (26.5, 30.4 and 33.4 % wet basis) and shear rates (30.4, 72.9, 304.3 and 728.6 s^{-1}).

The application of a 60 lb/hr small-scale extruder (Insta-Pro International, now Technochem Inc., Boone, IA) to produce pre-cooked flours from various grains is currently being investigated. The grains cook in the extruder based on viscous dissipation of mechanical energy supplied through the extruder screw speed. Restrictions on the screw help enhance viscous dissipation and hence temperature of the material increases before it exits through the die. Preliminary studies on identifying extruder operating conditions for different grains showed that the full fat soy beans, whole grain yellow corn and whole grain white corn can be extruded at 900, 300 and 900 rpm, respectively to get a desired final product. Modeling the rheology of these grains would help understand and model the various extruder operating parameters, which in turn can be used to predict operating conditions for new grains. The continued interest in use of an off-line capillary rheometer in this study is because of the relatively low sample requirement compared to

in-line measurements. Measurements over a wide range of shear rates can also be made, in a relatively short time period. They are also versatile in terms of the type of material they can handle and they are relatively simple to operate and maintain compared to in-line rheometers. The main objective of this study is to study the effect of temperature, moisture content and shear rate on the viscosity of full fat soy flour, whole grain yellow corn flour and whole grain white corn flour using the capillary rheometer and fit the data hence generated to Power law viscosity models which account for these three variables.

2.3 Materials and Methods

2.3.1 Raw materials

Full fat soy flour (completely passes through US mesh size 40) was obtained by milling commercially available soybean grits (Soy Innovations International, Indianola, Iowa) in a pin mill (Alpine Augsburg 160Z, Augsburg, Germany). The initial moisture content and oil content of soy flour were determined to be 8.5% and 20% (wet basis), respectively. Whole grain yellow corn meal was obtained from Agricor Inc., (Marion, Indiana) and milled using the pin mill to make fine flour (completely passes through US mesh size 40). Whole grain white corn (Woodland foods Inc., Waukegan, Illinois) was first milled to coarse grits in a roller mill and then to fine flour in the pin mill. The initial moisture content of whole grain yellow corn and white corn flours was approximately 13%.

2.3.2 Sample preparation

For rheological studies, the moisture content of soy flour was adjusted to 15, 20 and 25% wet basis, while yellow and white corn flour moisture contents was adjusted to 35, 37.5

and 40% wet basis. The moisture addition was carried out by slow addition of distilled water during continuous mixing at a medium speed, in a benchtop laboratory mixer (KitchenAid Mixer, Benton Harbor, Michigan) at room temperature (21.7^{o}C). The moisture adjusted samples were then packed in plastic bags (Ziploc bags, S.C. Johnson & son, Racine, Wisconsin) and kept in a cold room (7.2^{o}C) overnight for equilibration. On the day of the experiment, the samples were removed from the cold room and allowed to equilibrate to room temperature before the experiment. The moisture content of the samples was verified after equilibration by standard hot-air oven method for moisture determination (103^{o}C for 24hrs).

2.3.3 Capillary rheometer measurements

A twin-bore Rosand RH2000 capillary rheometer (Bohlin Instruments, now Malvern Instruments Ltd, Worcestershire, UK) was used in this study. The experiments were carried out at three different bore wall temperatures (80, 100 and 120^{o}C) for all samples. The bores were fitted with 4 mm capillaries of two different length/diameter (L/D) ratios of 4 and 8, respectively, for all experiments. Approximately, 110 g of sample was loaded in each bore, after the bore wall reached testing temperature. Using the Flowmaster® software (Version 8.5, Malvern Instrments), samples were initially compressed at a piston speed of 10 mm/min until the pressure transducers in each bore read a constant maximum pressure, then the piston was stopped and samples were equilibrated for 10 minutes at the test temperature. After equilibration, samples were compressed again at 10 mm/min until a constant maximum pressure was reached in each bore (product was flowing out of the capillaries in both compression steps). Immediately following this, two sweeps (high to

low shear rate and vice versa) of viscosity measurements were made at pseudo wall shear rates of 100, 50, 20, 10, 5, 2 and 1 s^{-1}. The pressure recorded from each bore at each shear rate was an average of 8 pressure readings (100 readings per minute) when variability was within 2%. All the experiments were done is triplicate.

Shear stress at the capillary wall was determined using the pressure measurements as,

$$\tau_w = \frac{\Delta P \,.D}{4\,.\,L} \tag{2.1}$$

The data was analyzed with and without the Bagley correction, which corrects wall shear rate for entrance and exit pressure loss (Bagley, 1957). To apply Bagley correction, difference in pressure and L/D between the two bores was used in the above formula.

The pseudo wall shear rate was calculated from,

$$\dot{\gamma}_{ow} = \frac{4\,.Q}{\pi\,.\,R^3} \tag{2.2}$$

where, Q is the volumetric flow rate, calculated from piston speeds and bore dimensions and R is the radius of the capillary. The true wall shear rate was then obtained by applying the Rabinowitsch correction as,

$$\dot{\gamma}_w = \left(\frac{3n+1}{4n}\right).\dot{\gamma}_{ow} \tag{2.3}$$

where, n = d(ln τ_w)/d (ln $\dot{\gamma}_{ow}$).

The apparent shear viscosity was calculated as,

$$\eta = \frac{\tau_w}{\dot{\gamma}_w} \quad (2.4)$$

Power-law model was used to determine the rheological behavior of the different samples:

$$\eta = k(\dot{\gamma}_w)^{n-1} \quad (2.5)$$

where n is the power law or flow behavior index and k is the consistency coefficient in $Pa.s^n$.

2.3.4 Rheological modeling

The effect of temperature, moisture content and shear rate on the viscosity of the different samples was modeled using two methods. The first approach is using the method of reduced variables or time-temperature superposition described by Bird et al. (1987) to build master curves, where shift factor for each variable and their interdependence is found by progressively shifting the curves. The final model is of the format:

log viscosity = slope [log (shear rate) + log a1 + log a2 +…] + intercept (2.6)

where, log ai is the shift factor for parameter i.

The second approach, more commonly reported in literature, is using the model (Eq. 2.7) proposed by Harper et al. (1971) where the combined effect of temperature (using an Arrhenius equation) and moisture content (by exponential equation) is calculated through multiple linear regression analysis. It was performed by the Data Analysis add-on in Excel 2013 (Microsoft Inc.).

$$\eta = K_o \exp\left(\frac{E_a}{RT}\right).\exp(-aMC).(\dot{\gamma}_w)^{n-1} \quad (2.7)$$

where, K_o (Pa s^n) and a ($\%^{-1}$) are constants, E_a is the activation energy for a molten sample to flow (J/g mol), R is the universal gas constant (J/g mol/K), T is the absolute temperature (K) and MC is the moisture content of the sample (% wet weight basis).

2.4 Results and discussion

2.4.1 Full fat soy flour

Wall slip was a challenge in quantifying the apparent viscosity of full fat soy flour. Even at the lower limits of moisture content (15%) and temperature (80^{o}C) tested, the pressure inside capillary rheometer bores did not stabilize, as shown in Figure 2.1. This is attributed to the high oil content (20%) of the soy flour, which separates from the flour and accumulates at the capillary wall at these high temperatures.

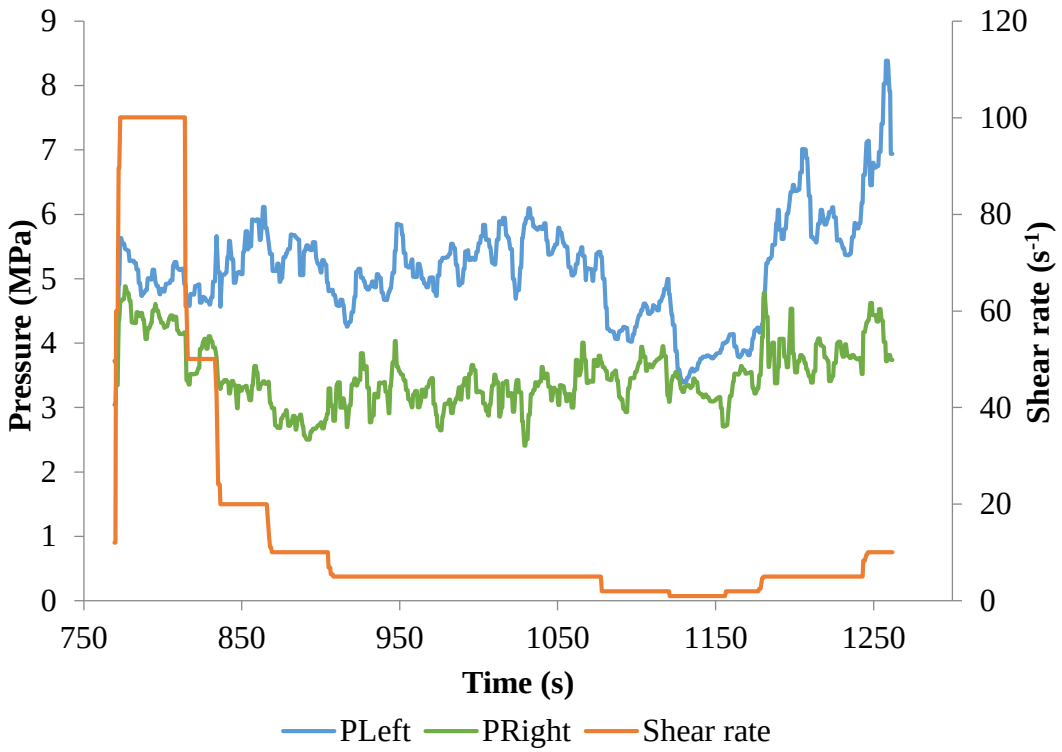

Figure 2.1. Pressure readings from two bores of the capillary rheometer while testing full fat soy flour at 80°C, 15% moisture and different shear rates.

Wall slip in polymers has been reported by several researchers and have been summarized by (Hatzikiriakos, 2012). Food rheology studies using capillary rheometer have also reported wall slip over the years. Halliday and Smith (1995) attempted to quantify wall slip in capillary flow of potato granule pastes at temperatures up to 80°C using a modified Mooney (1931) method. A critical wall shear stress of the order of 0.1 MPa, similar to some polymeric material, was determined to cause slip, but the heterogeneity of the food matrix and the interaction of various components at different conditions were also reported to complicate wall slip determination. Similar observations were made by Bagley et al. (1998) while attempting to characterize wheat dough

rheology in a constant pressure rheometer. At a constant pressure of 60 psi, using a capillary with radius 0.152 cm (L/R = 49.4), large variations in flow rate was recorded, which made it impossible to obtain precise pressure drop and hence dough properties. The change in wheat dough properties with time also interfered with consistent replication of measurements. Fluctuation in extrudate diameter as the filaments emerged from the die was also visually observed. In another study, during the measurement of power law index and consistency index for rheological modeling of wheat starch, wheat meal and oat flour, the capillary diameter had a significant effect on these parameters (Singh and Smith, 1999). Capillaries with smaller diameter gave lower viscosity values for the same material indicating the occurrence of wall slip. Rice flour with added lipids (7%) was qualitative shown to exhibit a very similar pressure fluctuation as the current study due to wall slip at moisture contents between 21 and 29% (Dautant et al., 2007). Fraiha et al. (2011) reported negative power law index (-0.05) during capillary rheometry measurements for a corn soy blend (70:30; mass) at 33.4% moisture and 120^{o}C and hypothesized that wall slip may be one of the reasons behind this erroneous result.

Viscosity measurements made using the same capillary rheometer used in this study for soy flour at different oil contents have been reported by Leung (2004). A 5% variability of pressure was allowed during measurements and samples were not equilibrated in the bores before measurements, which could explain how stable pressure readings were obtained. Based on the observations made in this study and evidences documented from previous literature, it was concluded that full fat soy flour viscosity cannot be

successfully measured at temperature and moisture conditions used in this study because of wall slip.

2.4.2 Whole grain yellow and white corn flour

For all the temperatures, moistures and shear rates, pressure stability was reached in both the bores for both the corn flour samples in the capillary rheometer. Figure 2.2 shows the pressure stability reached within the bores when testing 35% moisture content yellow corn at 80°C.

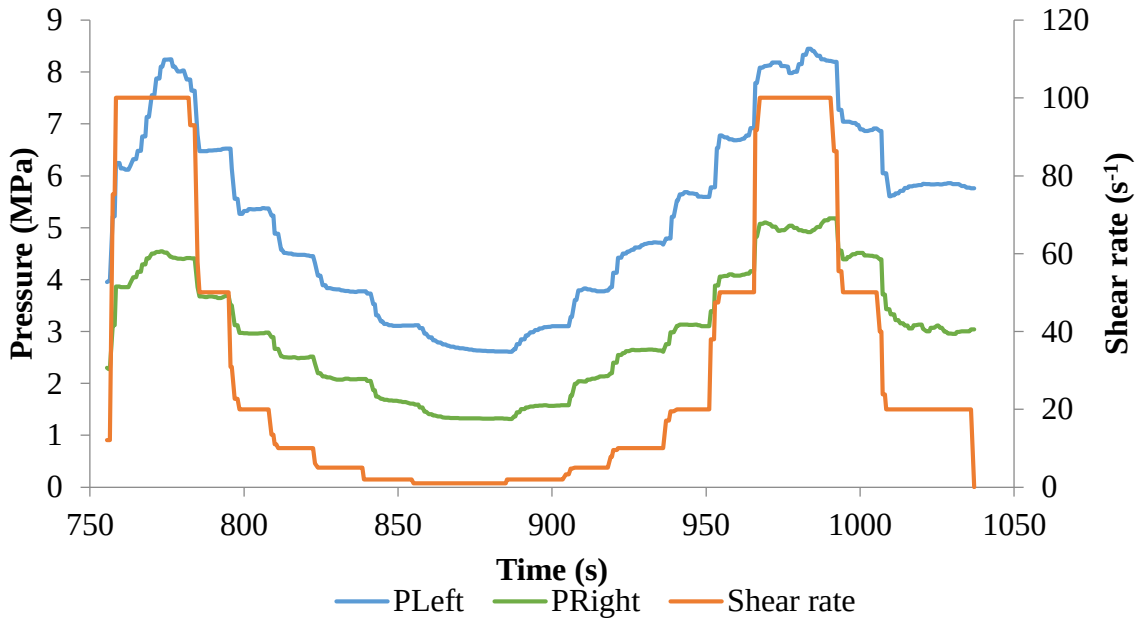

Figure 2.2. Pressure readings from two bores of the capillary rheometer when testing yellow corn flour at 80°C, 35% moisture and different shear rates.

Based on the bore pressure measurement and preset piston speeds in the capillary rheometer, shear stress and pseudo wall shear rate calculations were made using Eqs.

(2.1) and (2.2). Power law indicies (n) were calculated for each replicate from the slope of log-log plots of these values and actual wall shear rate was calculated by applying Rabinowitsch correction in Eq. (2.3). Bagley correction was not initially applied for the data analysis (data from L/D = 8 is first analyzed below). The impact of the Bagley correction is discussed later on. The data for each replicate was fit to a power law model described in Eq. (2.5), to calculate consistency index (k).

Overall, both the corn flours displayed a pseudoplastic behavior at the shear rates, temperatures and moisture contents tested (Figures 2.3 and 2.4). Increase in moisture content and temperature led to a decrease in viscosity of both the corn flours, under the conditions tested, agreeing with conclusions reported by several others who studied similar food/biological systems at these extrusion conditions, using both off-line and in-line rheometers (Dautant et al., 2007; de la Pena et al., 2014; Fraiha et al., 2011; Halliday and Smith, 1995; Harper et al., 1971; Lai and Kokini, 1990; Li et al., 2004; Núñez et al., 2010; Sandoval and Barreiro, 2007; Senouci and Smith, 1988; Vergnes et al., 1993; Vergnes and Villemaire, 1987).

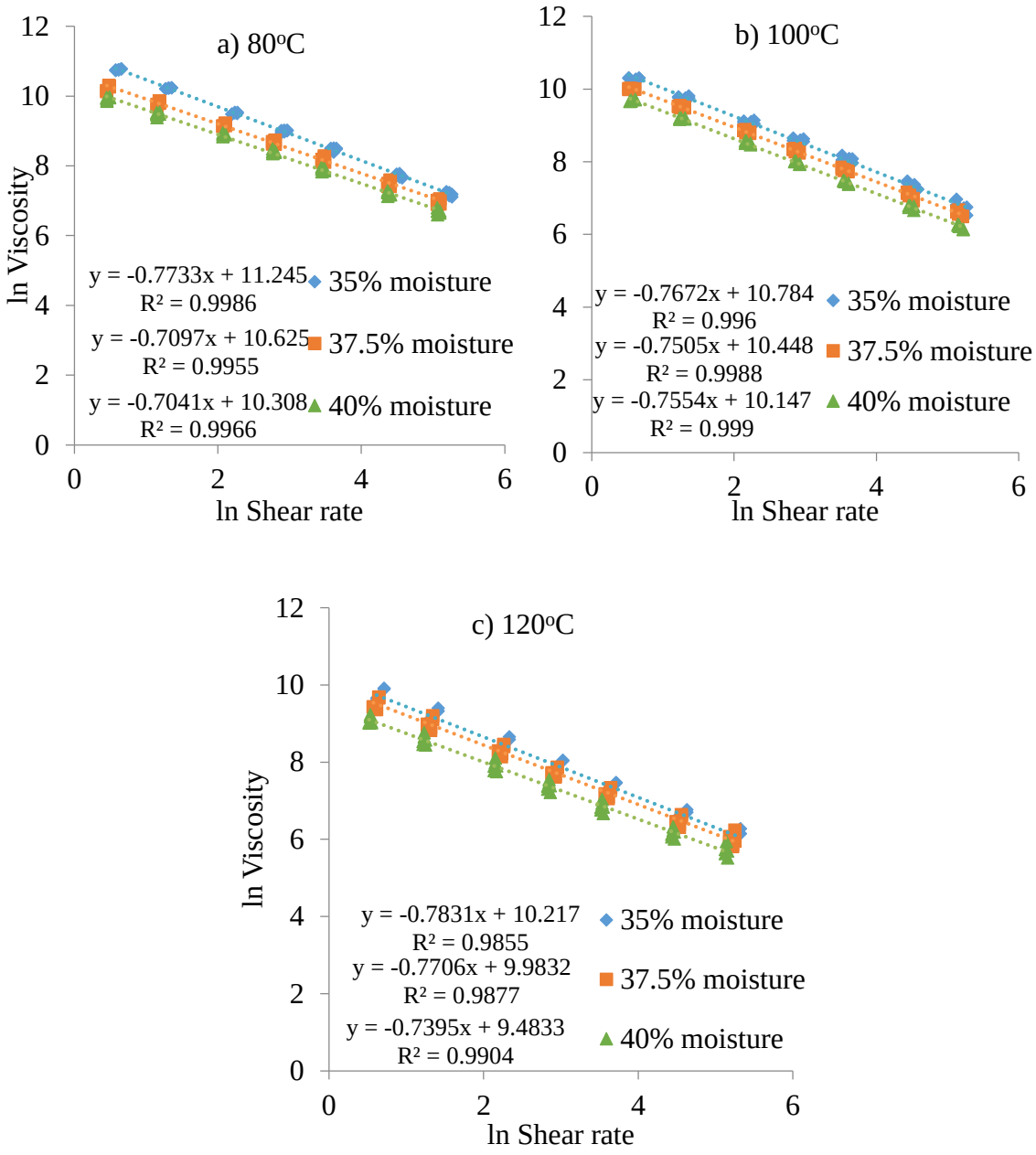

Figure 2.3. Viscosity vs shear rate (natural log) plots of whole grain yellow corn flour at temperature a) 80°C, b) 100°C and c) 120°C and 35%, 37.5% and 40% moisture contents.

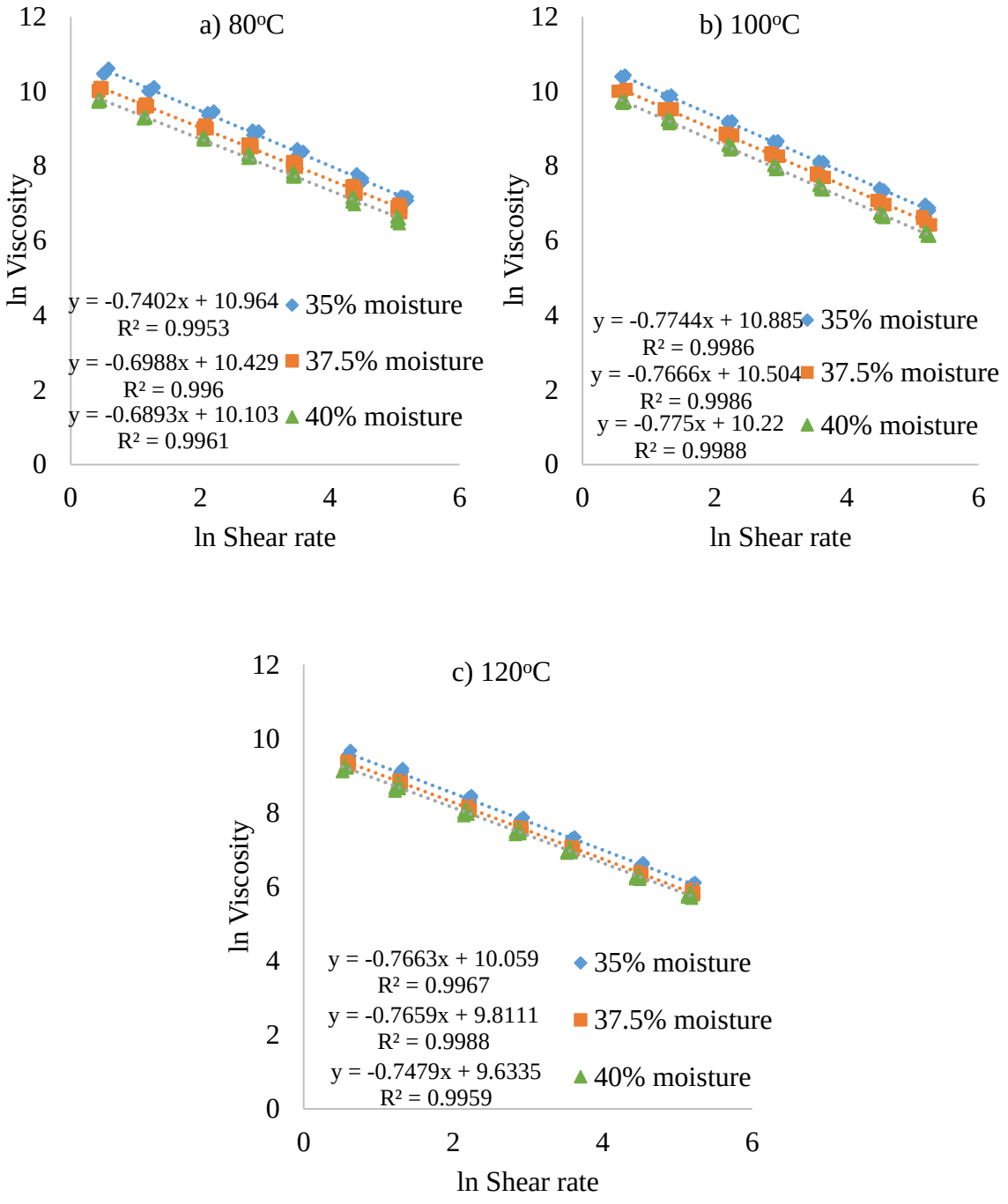

Figure 2.4. Viscosity vs shear rate (natural log) plots of whole grain white corn flour at temperature a) 80°C, b) 100°C and c) 120°C and 35%, 37.5% and 40% moisture contents.

The consistency coefficient, k, also decreased with increasing temperature and moisture content whereas the power law index, n, did not follow a particular trend, as shown in Table 2.1. This is also in agreement with rheological studies conducted on food materials by several others (Dautant et al., 2007; Fraiha et al., 2011; Sandoval and Barreiro, 2007). On the contrary, while using a pre-shearing rheometer, Vergnes and Villemaire (1987) and while using a novel in-line rheometer, Vergnes et al. (1993) and DellaValle et al. (1996), reported and modeled dependence of n value on temperature, moisture content and specific mechanical energy.

Table 2.1. Power law indices (n) and consistency coefficients (k) for whole grain yellow and white corn flours, at different temperatures and moisture contents

		Yellow corn		White corn	
Temperature (^oC)	Moisture content (% wet basis)	n	k ($kPa.s^n$)	n	k ($kPa.s^n$)
80	35	0.23	76.6	0.26	57.9
80	37.5	0.29	41.2	0.30	33.8
80	40	0.30	30.0	0.31	24.4
100	35	0.23	48.3	0.23	53.4
100	37.5	0.25	34.5	0.23	36.5
100	40	0.24	25.5	0.23	27.4
120	35	0.21	27.6	0.23	23.4
120	37.5	0.23	21.7	0.23	18.2
120	40	0.26	13.1	0.25	15.3

2.4.3 Rheological Modeling

2.4.3.1 Master curves

In order to build master curves, the viscosity data from both the corn flours was modeled by the method of reduced variables to fit in Eq. 2.6 (Bird et al., 1987). The procedure to build the master curve and to calculate shift factors for temperature and moisture content is described in the next few sections by using the whole grain yellow corn flour data, without Bagley correction. The data at each temperature was first shifted for a reference moisture content of 35%. The values by which the shear rates had to be shifted, in order to superposition to the reference moisture content was calculated for the 37.5% and 40% moisture contents, at each temperature. These values are plotted to obtain curves for the moisture shift factors (aM) at each temperature (Figure 2.5).

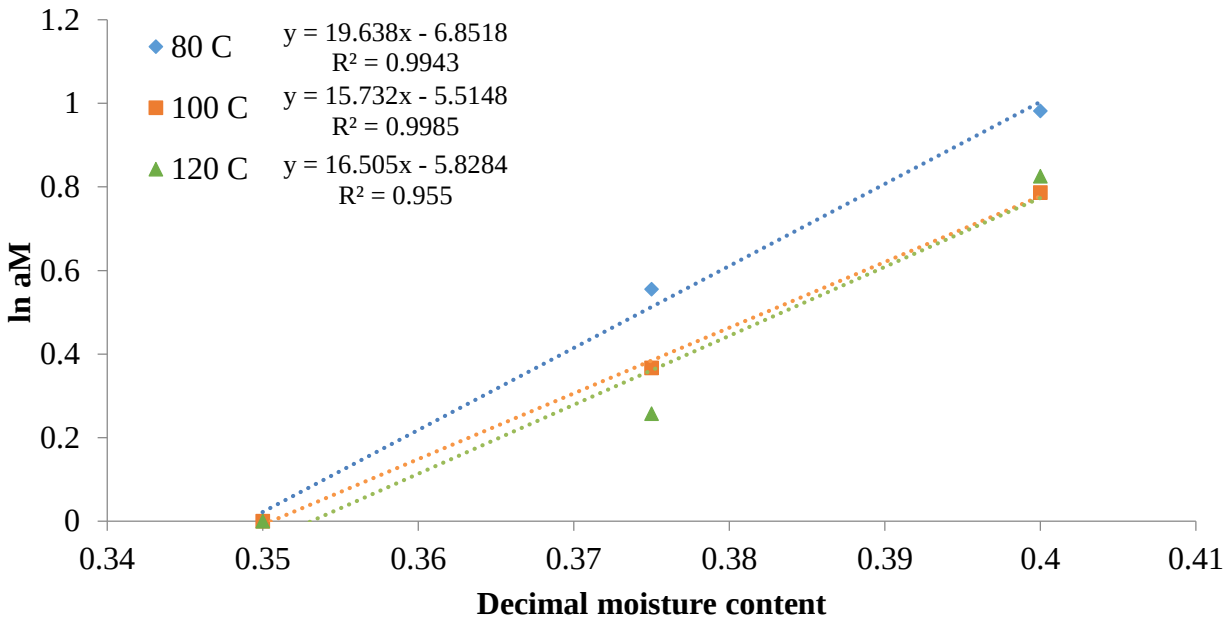

Figure 2.5. Moisture shift factors (aM) for whole grain yellow corn flour at different temperatures (80, 100 and 120^{o}C) plotted for the different moisture contents (35, 37.5 and 40%, expressed as decimal moisture content) with 35% as the reference moisture content.

A reference temperature of 80^{o}C is chosen for the master curve. To determine the temperature dependence of aM, they are plotted against different temperatures for a reference aM value (Figure 2.6). From the plot, it can be inferred that aM is dependent on temperature (R^2=0.87). Hence the equation for calculating aM, (linear fit equation at reference temperature) is written as,

ln (aM) = 19.638 (M+b) – 6.8518, where b = -0.0002 (T) + 0.0153, M is decimal moisture content and T is the temperature in ^{o}C. (2.8)

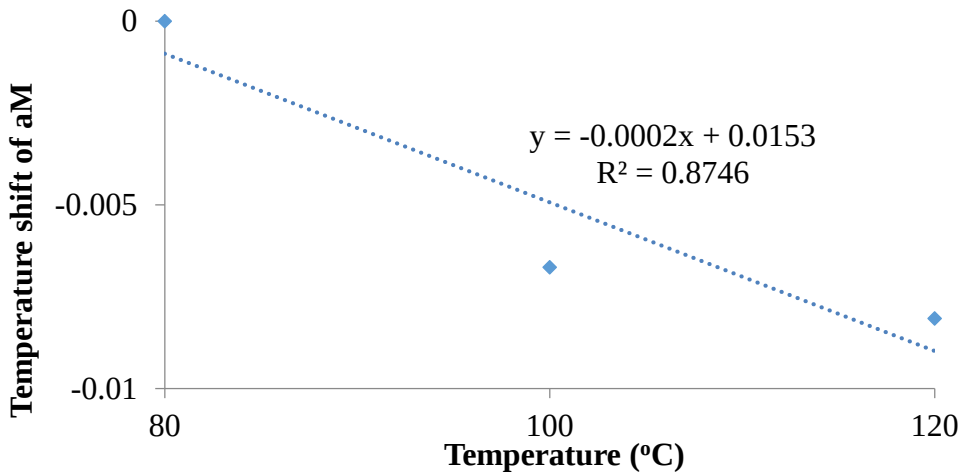

Figure 2.6. Temperature dependence of moisture shift factor (aM) for whole grain yellow corn flour at different temperatures (80, 100 and 120ºC).

Using Eq. 2.8, all the shear rate data at different moisture contents are shifted to reference moisture content of 35%, at all temperatures. The moisture shifted curves at different temperatures are shown in Figure 2.7.

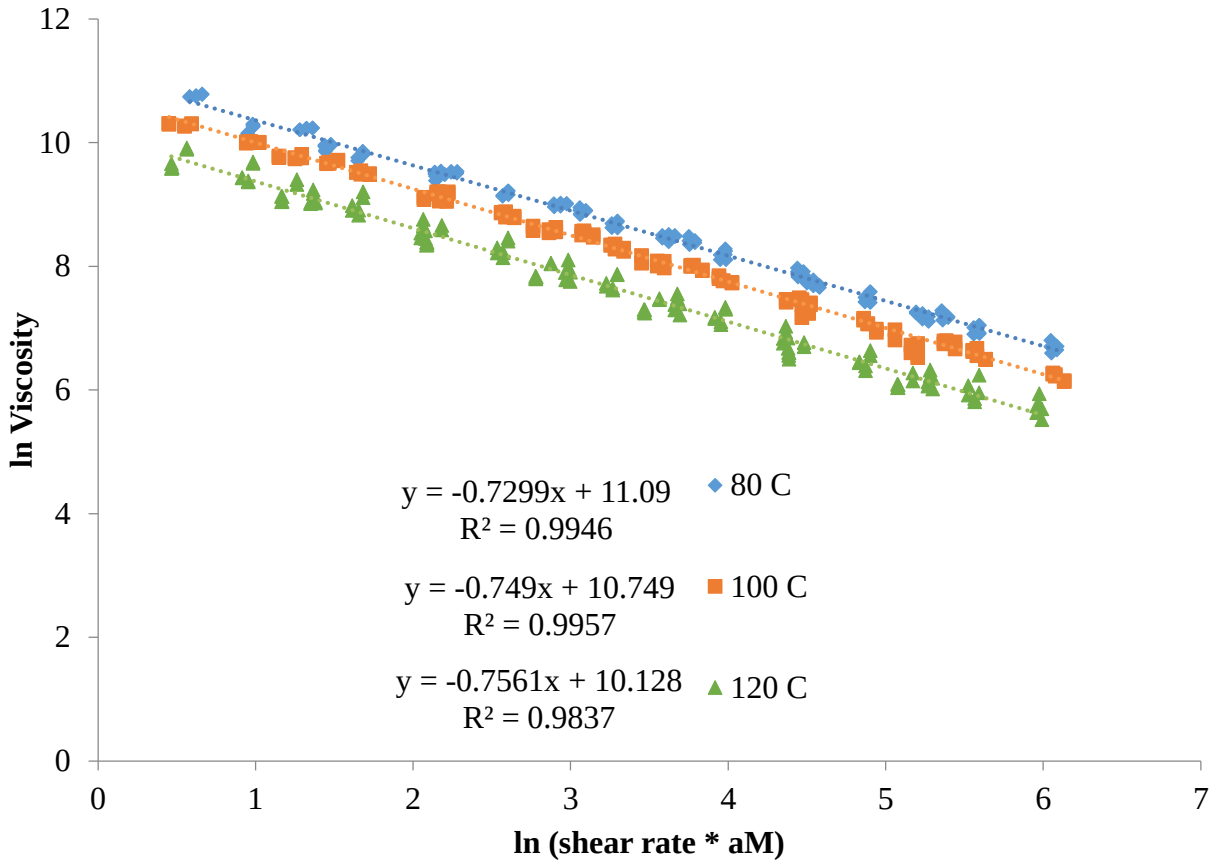

Figure 2.7. Moisture shifted curves for whole grain yellow corn flour at different temperatures (80, 100 and 120^{o}C) with 35% reference moisture content.

Temperature shift factors were calculated for 100^{o}C and 120^{o}C by shifting the curves to the reference temperature of 80^{o}C, by using the linear fit equation obtained for each temperature from the moisture shifted curves (Figure 2.7). These shift factors were then plotted against temperature (Figure 2.8) to get the equation for temperature shift (aT) as,

$$\ln (aT) = 0.0355 (T) - 2.8868 \qquad (2.9)$$

where T is temperature in ^{o}C.

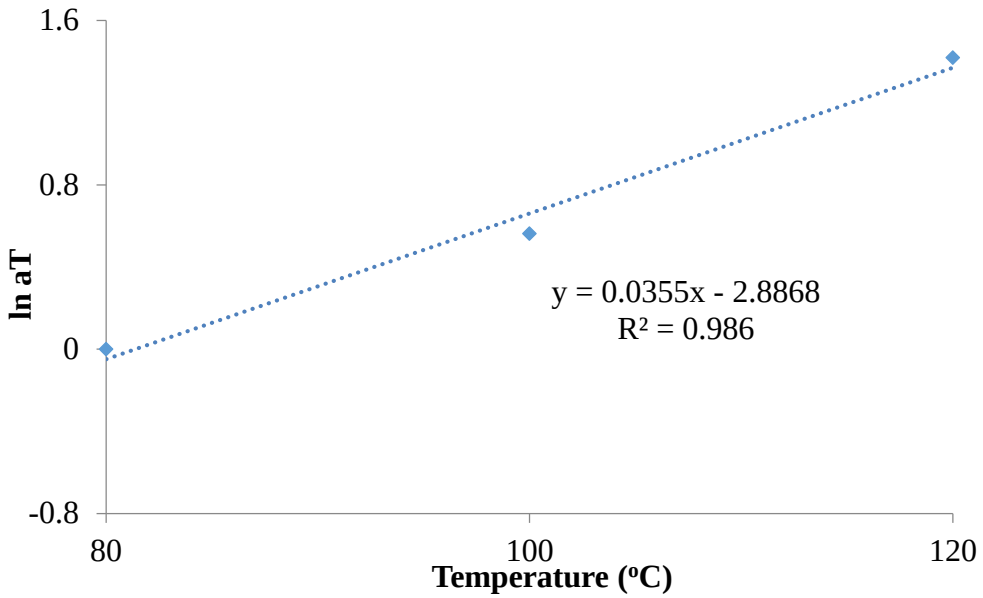

Figure 2.8. Temperature shift factors plotted for whole grain yellow corn flour at different temperatures (80, 100 and 120ºC) with 80ºC as the reference temperature.

Using Eq. 2.9, the moisture shifted shear rate data is shifted to the reference temperature of 80ºC to get the master curve for whole grain yellow corn flour (Figure 2.9).

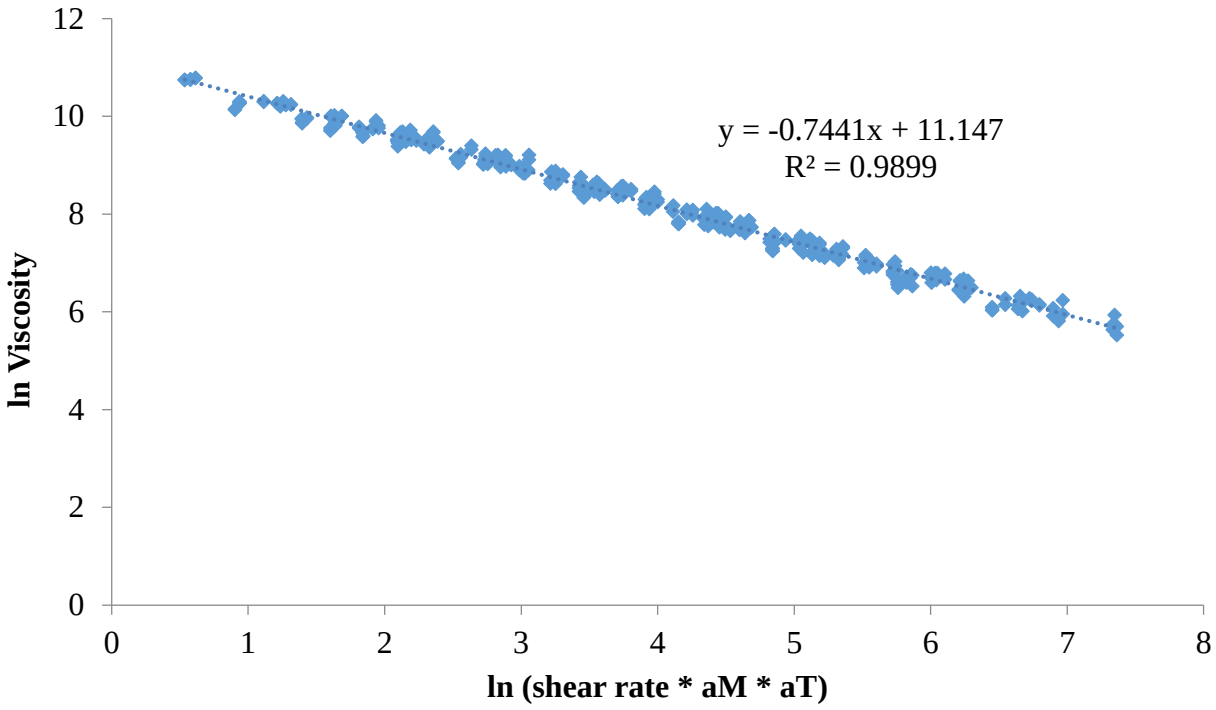

Figure 2.9. Master curve for whole grain yellow corn flour at a range of shear rates, temperatures (80, 100 and 120^{o}C) and moisture contents (35, 37.5 and 40%) shifted against a reference temperature of 80^{o}C and reference moisture content of 35%.

In order to understand the importance of Bagley correction, the whole grain yellow corn flour data was re-analyzed (using data from both bores, at L/D = 8 and 4). The data was used to build a master curve following the same steps described above. A comparison of master curves with and without Bagley correction for entrance and exit effects is presented in Figure 2.10. From this figure, it can be inferred that, applying Bagley correction does not significantly impact the viscosity master curve for whole grain yellow corn in the range of conditions tested in the capillary rheometer, but the R^2 value drops to 0.96 from 0.99. Analysis of data for whole grain white corn flour also resulted in a

similar observation (data not shown). Hence for further analysis of data and modeling, Bagley correction was omitted.

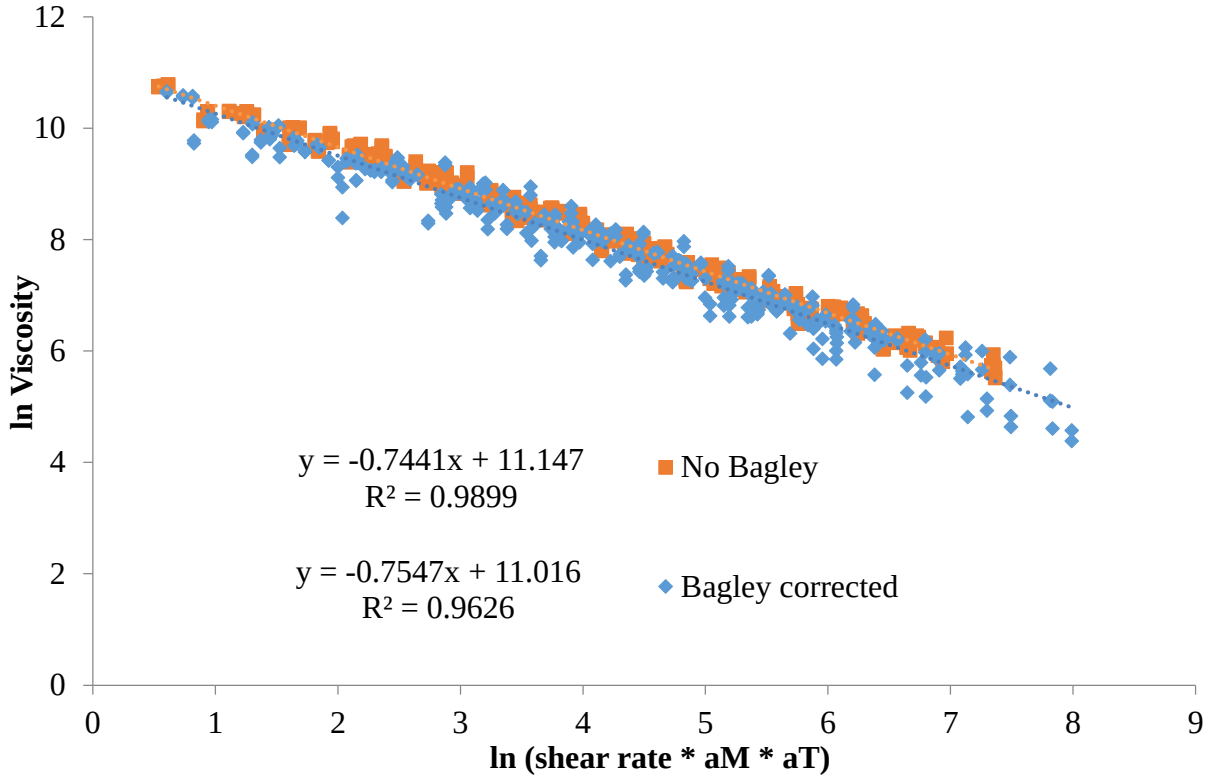

Figure 2.10. Comparison of whole grain yellow corn flour master curves with and without Bagley correction in the range of conditions tested.

The viscosity data for whole grain white corn was modeled in the same approach described and the data is compared with whole grain yellow corn in Figure 2.11. The values of constants obtained by modeling both the corn data to build viscosity master curves is given in Table 2.2.

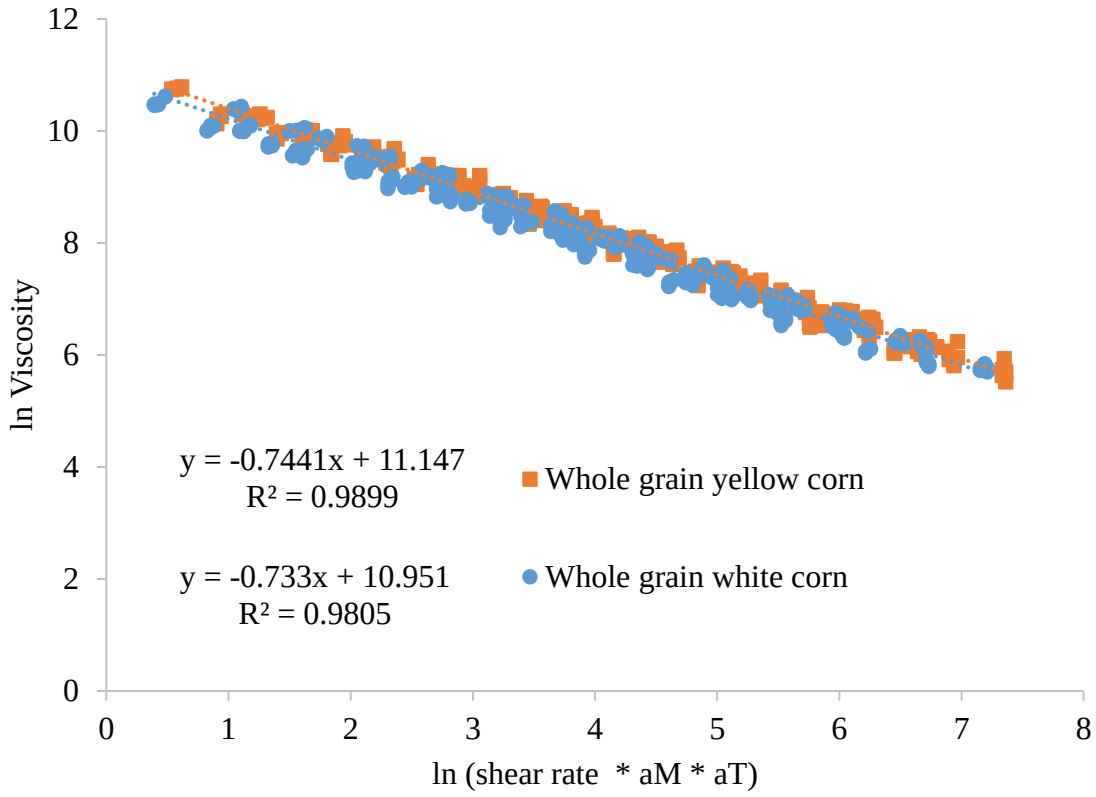

Figure 2.11. Comparison of whole grain yellow and white corn flour viscosity master curves in the range of conditions tested.

Table 2.2. Estimated values of constants in the viscosity master curve represented by Eq. 2.6, for whole grain yellow and white corn flour.

	Slope	**ln aM**	**ln aT**	**Intercept**
Whole grain yellow corn	-0.7441	19.638 (M+b) – 6.8518, where, b = -0.0002 T) + 0.0153	0.0355 (T) – 2.8868	11.147
Whole grain white corn	-0.733	20.066 (M+b) – 7.0007 where, b = -0.0005 (T) + 0.0391	0.0381 (T) – 3.156	10.951

aM - moisture shift factor

aT - temperature shift factor

M - decimal moisture content (wet basis)

T - temperature in ^{o}C

2.4.3.2 Multiple linear regression modeling

The viscosity data for both corn flours was also fit in Harper's model (Eq. 2.7) using multiple linear regression analysis. The parameter estimates for this model for both corn flours is shown in Table 2.3.

Table 2.3. Estimated values of parameter using multiple linear regression for the power law viscosity model represented by Eq. 2.7, for whole grain yellow and white corn flours.

	K_o	E_a/R	a	n
Whole grain yellow corn	6.60	3212	0.12999	0.25
Whole grain white corn	7.30	2754	0.11775	0.26

K_o in Pa. s^n

a in $\%^{-1}$

E_a/R in K

2.4.4 Challenges observed

The key observation made from tables 2.2, 2.3 and fig. 2.11 is that there is no significant difference in viscosity between whole grain yellow and white corn flours in the range of conditions measured using the capillary rheometer. The whole grain yellow and white corn were extruded at 300 and 900 rpm, at 98 and 170 W.h/kg of specific mechanical energy respectively, in the small scale extruder, at a feed moisture of 35% to give die temperature rise of around 120^{o}C to produce pre-cooked products. This is a clear indication of difference in rheology of these two types of corn which is the underlying

premise of this work. But the lack of difference in the viscosity models developed from the capillary rheometer led to a deeper investigation to explain these results.

2.4.5 Raw material composition

Starch is the major component of most cereal grains. Native starches occur in multilevel structures called granules, containing alternative amorphous and crystalline regions. Starch is a polysaccharide comprised of D-glucose units. The two major components of starch are – long chain unbranched amylose and short chain highly branched amylopectin. Amylose is sparsely branched where the glucose units are connected with α(1-4) bonds and can have a degree of polymerization as high as 600 with a molecular weight of 10^5 to 10^6 Da. Amylopectin on the other hand, is highly branched because of the presence of 5% α(1-6) bonds between the glucose molecules which also gives it a high molecular weight of 10^7 to 10^9 Da and the degree of polymerization is around 15 in each branched chain (Xie et al., 2012).

One of the initial hypotheses is that the corn flours used in this study could have different composition of amylose and amylopection. Waxy corn is rich in amylopectin and has very little amylose (~3%), whereas dent corn has a relatively higher amylose content (~25%). This difference in starch composition can have a significant impact on their behavior under various processing conditions, since amylopectin is relatively more sensitive to processing compared to amylose (Xie et al., 2012). Han et al. (2002) documented the effect of starch damage by ball milling on its rheological behavior. A significant decrease in shear stress and viscosity was observed in both waxy and normal maize starch, but waxy starch underwent more pronounced changes than normal starch.

Both the corn flours used in the study were analyzed for amylose content (Amylose/Amylopectin assay procedure, Megazyme, Ireland). The assay revealed that amylose content of the yellow (29.1%) and white (27.2%) corn flour were not significantly different. This eliminates the difference in starch composition as a possible reason for difference in their rheological behavior.

2.4.6 Effect of particle size

Both the whole grain yellow corn and white corn were milled to fine flour before use in the capillary rheometer. But the whole grain yellow corn was obtained as a corn meal from the corn milling company (Agricor Inc.) and extruded as a meal. The particle size of the meal, including the individual components – endosperm, germ and bran or pericarp was uniform since it was industrially milled. Whereas the whole grain white corn was obtained as corn kernels and milled in the laboratory. Milling all the components white corn to a uniform particle size was a challenge since the appropriate equipments were not available. The pericarp or bran particles were challenging to mill and were larger compared to the endosperm. This variation in particle size of the components can have a significant effect on the material rheology within the extruder. This is possibly hypothesized as one of the reasons behind the difference in operating extrusion operating condition between the two corns.

2.4.7 Shear fragmentation of starch during extrusion

As extrusion cooking is primarily carried out at relatively low moisture content, compared to the amount of moisture required for completely gelatinization (60%),

majority of the starch in the feed material is not gelatinized but melted. From experiments performed on a Brabender single screw extruder and a capillary rheometer, shear activation energies calculated for starch conversion were found to be orders of magnitude smaller compared to thermal activation energies. This increased efficiency of shear energy is a very important factor in making extrusion an efficient cooking method (Wang, 1993; Zheng and Wang, 1994). Lai and Kokini (1991) have compiled the various physiochemical changes that starch undergo during the extrusion process, such as gelatinization, melting and fragmentation. Among these main changes, fragmentation is primarily caused by shear, which is directly co-related to the operating conditions of the extruder namely, screw speed, temperature and feed moisture content. The fragmentation also varies based on the type of starch used. The larger size and hyper branched connectivity of amylopectin reduces its ability to withstand deformation without breaking hence making it more susceptible to shear degradation. Selective scission and maximum stable size concept were proposed as possible mechanisms of shear degradation of starch. Size exclusion chromatography was used to show the fragmentation mechanism of amylose and amylopectin starches in twin screw extruder (Liu et al., 2010). While studying extrusion cooking of wheat starch, Colonna et al. (1984) reported the degradation of amylose and amylopectin by random chain splitting which was quantified by intrinsic viscosity, gel-permeation chromatography and average molecular weight measurements. Wen et al. (1990) reported maximal fragmentation at low moisture content (20%), low temperature (100^{o}C) and high screw speed (300 rpm), when the mechanical energy was at its peak, during twin screw extrusion of corn meal. Measuring specific mechanical energy (SME) has been used as a method to quantify the amount

shear energy that has been supplied to the material during extrusion (Lai and Kokini, 1991).

2.4.8 Shear degradation during in-line vs. off-line rheological measurements

In off-line rheological measurements using capillary rheometers, the sample is not subject to shear degradation prior to viscosity measurements; hence they cannot reproduce the shear history experienced by a material in an extruder fed in-line rheometer. Senouci and Smith (1988) compared shear viscosity measurements of maize grits, potato powder and low density polyethylene made using an extruder-fed slit die viscometer and a capillary rheometer. A strong dependence of viscosity on extrusion processing history for maize grits and potato powder was reported which was associated with the macromolecular degradation of the food material inside the extruder. A comparison of the maize grits viscosity data with model developed in the current study is shown in Figure 2.12. There is a reasonable agreement in the capillary rheometer measurements made between the two studies. But the in-line measurements made by Senouci and Smith (1988) is clearly much lower than compared to either of the capillary rheometry measurement. This is a clear indication of the impact of the shear degradation/history experienced by the material or the lack of, on its viscosity.

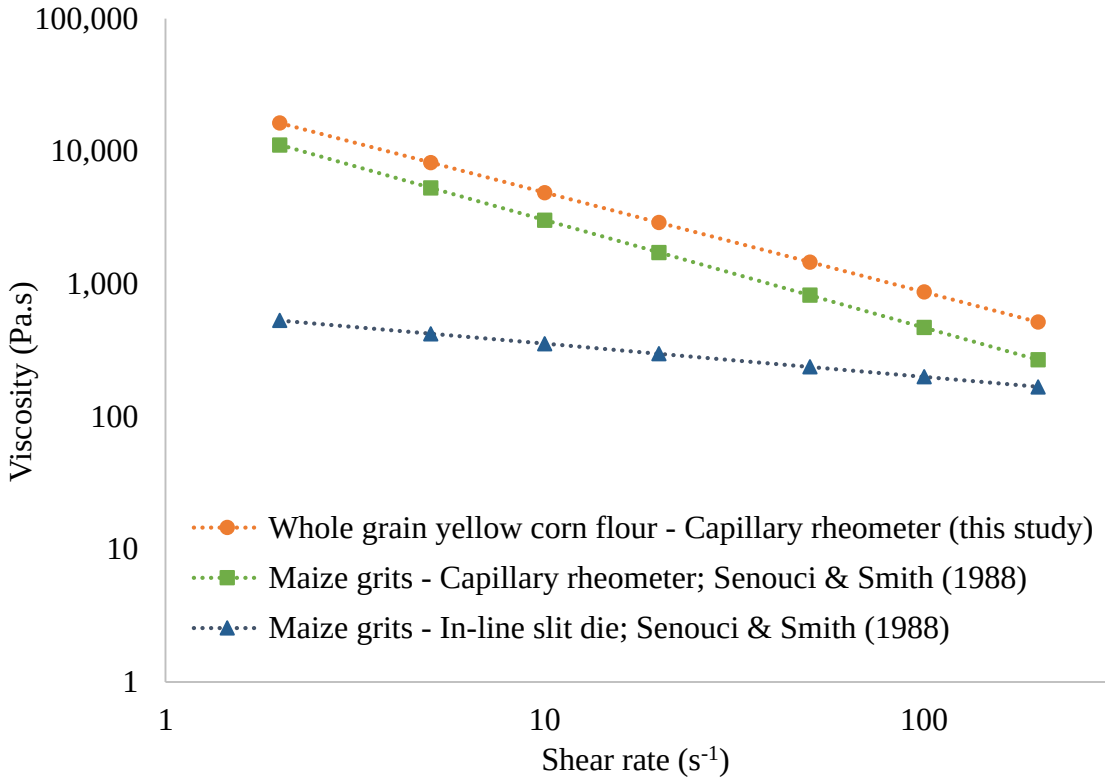

Figure 2.12. Comparison of viscosity model built for whole grain yellow corn flour in the current study with in-line and capillary rheometer models built for maize grits by Senouci and Smith (1988) at a reference temperature (120°C) and moisture content (35%).

In special off-line rheometers like a pre-shearing rheometer (Rheoplast), a material could be subject to a specific, defined pre-shearing treatment before viscosity measurement in the Couette zone of the rheometer after the material is melted, but there are challenges associated even in this approach especially when working with foods/biopolymers (Martin et al., 2003; Núñez et al., 2010; Vergnes and Villemaire, 1987; Vergnes et al., 1987). During the pre-shearing process inside the Rheoplast, the moisture content of the material might change when water is used as a plasticizer, at high temperature. Also

during discontinuous runs, material from the previous trial may continue to cook/melt and form a plug in the capillary or the convergent entrance of the injection pot. These issues make it challenging to get perfectly reproducible results; hence the experiments were repeated several times to get good results. Comparison of the Power law viscosity model built by Vergnes and Villemaire (1987) for maize starch with yellow corn flour model in the current study (Figure 2.13), showed that the pre-shearing rheometer model was predicting a higher viscosity. This could be because the measurements were made on pure maize starch whereas in the current study whole grain flour was used instead. The challenges with material from previous runs plugging in the pre-shearing rheometer could also result in higher viscosities reported.

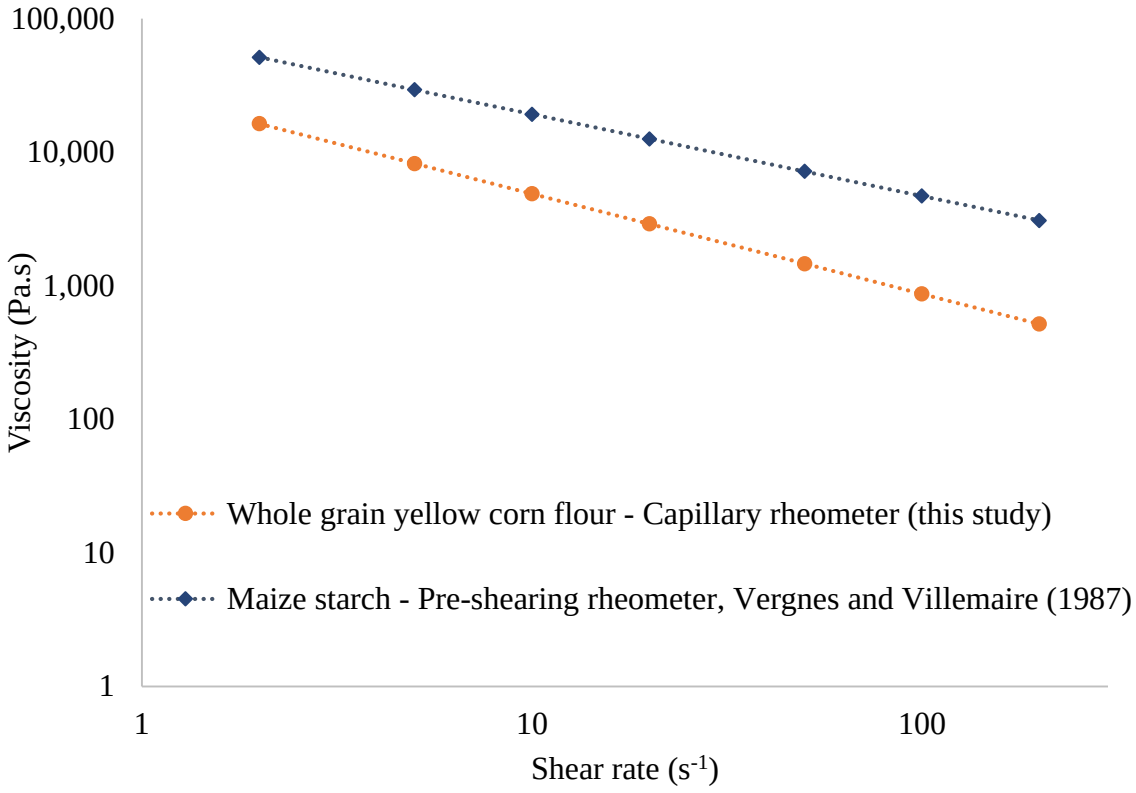

Figure 2.13. Comparison of viscosity model built for whole grain yellow corn flour in the current study with pre-shearing off-line rheometer (Rheoplast) model built for maize starch by Vergnes and Villemaire (1987) at a reference temperature (120^{o}C) and moisture content (35%).

The viscosity of the same maize starch used by Vergnes and Villemaire (1987) was measured by Vergnes et al. (1993) in a specific slit die rheometer (Rheopac) which maintains a constant thermomechanical history for the material at a given condition. The in-line viscosity measurements (Rheopac) were lower compared to the off-line measurement (Rheoplast) and this was attributed to the higher specific mechanical energy received by the maize starch during the in-line measurement. When comparing Rheopac and Rheoplast viscosity measurements for wheat starch, Martin et al. (2003) also reported

discrepancies between the two measurement techniques and attributed it to differences in specific mechanical energy and temperature.

The effect of amylose content (70, 47, 23 and 0%) on the viscous behavior of maize starch blends at low moisture contents (20 to 36%, wet basis) and high temperatures (100 to 190^{o}C) was studied using the Rheopac (DellaValle et al., 1996). From the data collected, viscosity models for each amylose content was developed. A comparison of these models with the yellow corn flour from the current study is shown in Figure 2.14. It indicates that the capillary rheometer model for whole grain yellow corn flour in the current study is over predicting viscosity. From Figure 2.14, it can also be seen that 0% amylose starch has the lowest viscosity among all the maize starch blends and a correlation between increase in amylose and increase in viscosity can be noted.

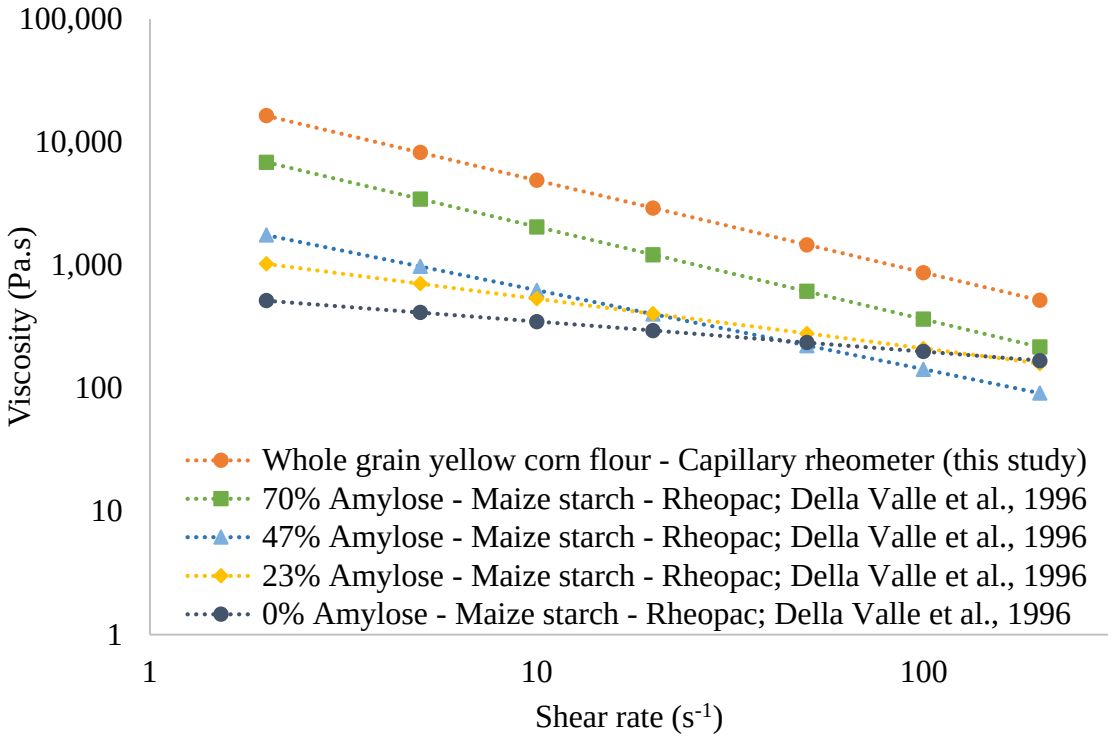

Figure 2.14. Comparison of viscosity model built for whole grain yellow corn flour in the current study with in-line rheometer (Rheopac) model built for maize starch blends with varying amylose content (70, 47, 23 and 0%) by DellaValle et al. (1996) at a reference temperature (120ºC), moisture content (35%) and specific mechanical energy (150 W.h/kg).

Li et al. (2004), measured viscosity of corn grits in another type of in-line slit die rheometer with a bypass which also ensures that the thermomechanical history experienced by the product remains constant during the measurement. The effects of moisture content, barrel temperature, screw speed, feed rate and degree of fill of the Clextral BC21 extruder have been reported in this study. The n and K values calculated from the slit-die rheometer measurements, reported for feed moisture of 35%, barrel

temperature of 120°C, screw speed of 400 rpm and feed rate of 7.5 kg/hr, was used to compare with the yellow corn in the current study (Figure 2.15). Once again, viscosity measurements made in-line were lower compared to the off-line measurements in the current study, similar to the comparison with the in-line model by Senouci and Smith (1988).

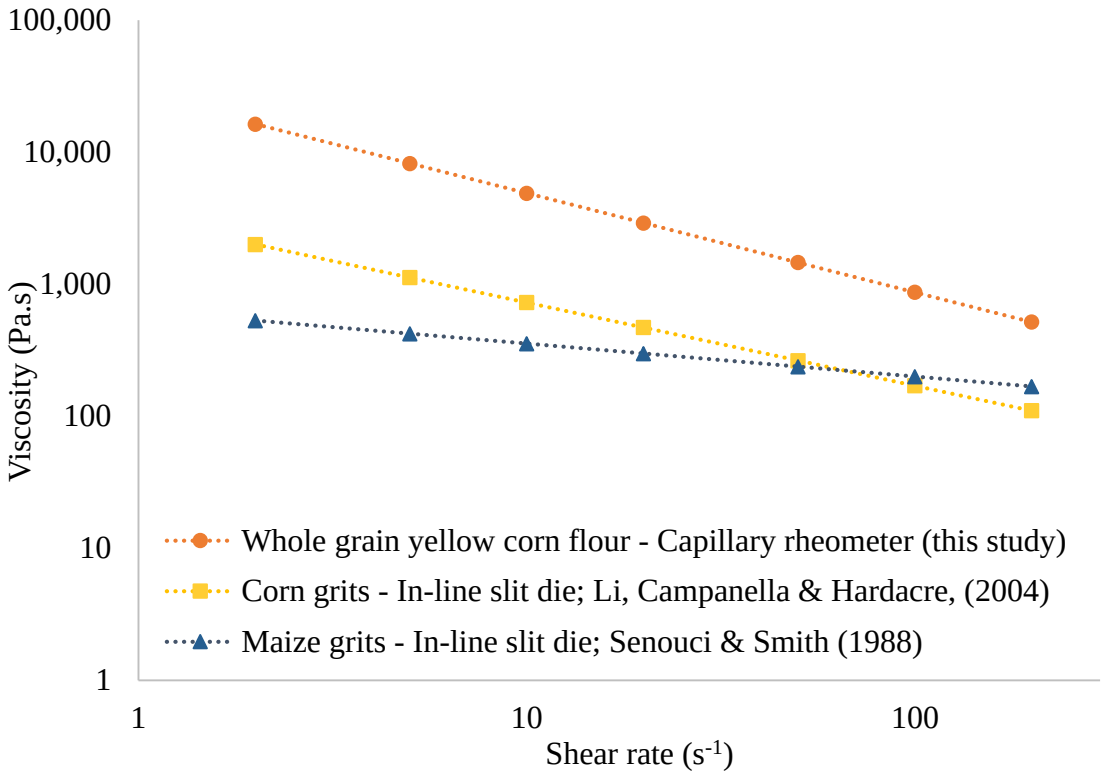

Figure 2.15. Comparison of viscosity model built for whole grain yellow corn flour in the current study with in-line rheometer models built for maize grits by Li et al. (2004) and Senouci and Smith (1988) at a reference temperature (120°C) and moisture content (35%).

From these comparisons made thus far, it is clear that the lack of shear degradation in the capillary rheometer leads to higher viscosity measurements compared to those made in an

extruder fed in-line rheometer. Hence, the application of off-line capillary rheometry for measuring viscosities of food/biopolymers needs to be further investigated for its applications and limitations, by more detailed studies comparing them with in-line rheometers in a range of extrusion conditions.

2.5 Conclusion

Challenges with pressure instability in off-line capillary rheometer during viscosity measurements of full fat soy bean flour at high temperature, shear rate and low moisture condition has been documented. Wall slip due to the accumulation of oil separated from the flour is hypothesized to lead to this pressure instability. Viscosity measurements for whole grain yellow and white corn flours have been successfully made with an off-line capillary rheometer. Power-law master curves were built for both the flours using the method of reduced variable. Multiple linear regression has also been used to fit the data in a mechanistic power law model reported in the literature. Comparison of the viscosity models of the two types of corn indicated that there was very little to no difference between them, which is in contradiction with their behavior in the extruder. But there is a possibility that the difference in extrusion condition is possible because of the raw material particle size and uniformity of particle size of the various components. Hence the effect of particle size on extrusion conditions also needs to be investigated. The lack of shear degradation in the off-line capillary rheometer compared to that of an extruder fed in-line rheometer is believed to result in higher viscosity measurements. Hence comparison of off-line and in-line viscosity measurement technique is needed for

food/biological materials at high temperature, shear and low moisture extrusion conditions.

2.6 References

Bagley, E.B., (1957). End corrections in the capillary flow of polyethylene. Journal of Applied Physics. 28(5), 624-627.

Bagley, E.B., Dintzis, F.R., Chakrabarti, S., (1998). Experimental and conceptual problems in the rheological characterization of wheat flour doughs. Rheologica Acta. 37(6), 556-565.

Bird, R.B., Armstrong, R.C., Hassager, O., (1987). *Dynamics of polymeric liquids: Volume 1 - Fluid Mechanics*. John Wiley & Sons, New York, USA.

Colonna, P., Doublier, J., Melcion, J., Monredon, F.D., Mercier, C., (1984). Extrusion cooking and drum drying of wheat starch. I. Physical and macromolecular modifications. Cereal chemistry (USA).

Dautant, F.J., Simancas, K., Sandoval, A.J., Muller, A.J., (2007). Effect of temperature, moisture and lipid content on the rheological properties of rice flour. Journal of Food Engineering. 78(4), 1159-1166.

de la Pena, E., Manthey, F.A., Patel, B.K., Campanella, O.H., (2014). Rheological properties of pasta dough during pasta extrusion: Effect of moisture and dough formulation. Journal of Cereal Science. 60(2), 346-351.

DellaValle, G., Colonna, P., Patria, A., Vergnes, B., (1996). Influence of amylose content on the viscous behavior of low hydrated molten starches. Journal of Rheology. 40(3), 347-362.

Fraiha, M., Biagi, J.D., Ferraz, A.C.d.O., (2011). Rheological behavior of corn and soy mix as feed ingredients. Food Science and Technology (Campinas). 31(1), 129-134.

Halliday, P.J., Smith, A.C., (1995). Estimation of wall slip velocity in the capillary-flow of potato granule pastes. Journal of Rheology. 39(1), 139-149.

Han, X.-Z., Campanella, O.H., Mix, N.C., Hamaker, B.R., (2002). Consequence of Starch Damage on Rheological Properties of Maize Starch Pastes 1. Cereal Chemistry. 79(6), 897-901.

Harper, J., Rhodes, T.P., Wanninger, L., (1971). Viscosity model for cooked cereal doughs, *Chemical Engineering Progress Symposium Series*, pp. 40-43.

Harper, J.M., (1981). *Extrusion of foods: Volume I*. CRC Press, Boca Raton, Florida.

Hatzikiriakos, S.G., (2012). Wall slip of molten polymers. Progress in Polymer Science. 37(4), 624-643.

Lai, L.S., Kokini, J.L., (1990). The effect of extrusion operating-conditions on the online apparent viscosity of 98-percent amylopectin Amioca) and 70-percent amylose (Hylon 7) corn starches during extrusion. Journal of Rheology. 34(8), 1245-1266.

Lai, L.S., Kokini, J.L., (1991). Physicochemical changes and rheological properties of starch during extrusion. Biotechnology Progress. 7(3), 251-266.

Leung, M., (2004). The effect of temperature, moisture content, oil content, and variety on rheology of soy, *Agricultural & Biological Engineering*. Purdue University, West Lafayette, Indiana.

Li, P.X., Campanella, O.H., Hardacre, A.K., (2004). Using an in-line slit-die viscometer to study the effects of extrusion parameters on corn melt rheology. Cereal Chemistry. 81(1), 70-76.

Liu, W.-C., Halley, P.J., Gilbert, R.G., (2010). Mechanism of degradation of starch, a highly branched polymer, during extrusion. Macromolecules. 43(6), 2855-2864.

Mackey, K.L., Ofoli, R.Y., (1990). Rheological modeling of corn starch doughs at low to intermediate moisture. Journal of Food Science. 55(2), 417-423.

Martin, O., Averous, L., Della Valle, G., (2003). In-line determination of plasticized wheat starch viscoelastic behavior: impact of processing. Carbohydrate Polymers. 53(2), 169-182.

Mercier, C., Linko, P., Harper, J.M., (1989). *Extrusion cooking*. American Association of Cereal Chemists, Inc., St. Paul, Minnesota, USA.

Mooney, M., (1931). Explicit formulas for slip and fluidity. Journal of Rheology. 2(2), 210-222.

Núñez, M., Della Valle, G., Sandoval, A.J., (2010). Shear and elongational viscosities of a complex starchy formulation for extrusion cooking. Food research international. 43(8), 2093-2100.

Remsen, C.H., Clark, J.P., (1978). A viscosity model for a cooking dough. Journal of Food Process Engineering. 2(1), 39-64.

Robin, F., Engmann, J., Tomasi, D., Breton, O., Parker, R., Schuchmann, H.P., Palzer, S., (2010). Adjustable Twin-Slit Rheometer for Shear Viscosity Measurement of Extruded Complex Starchy Melts. Chemical Engineering & Technology. 33(10), 1672-1678.

Sandoval, A.J., Barreiro, J.A., (2007). Off-line capillary rheometry of corn starch: Effects of temperature, moisture content and shear rate. Lwt-Food Science and Technology. 40(1), 43-48.

Senouci, A., Smith, A.C., (1988). An experimental study of food melt rheology. I. Shear viscosity using a slit die viscometer and a capillary rheometer. Rheologica Acta. 27(5), 546-554.

Singh, N., Smith, A.C., (1999). Rheological behaviour of different cereals using capillary rheometry. Journal of Food Engineering. 39(2), 203-209.

Vergnes, B., DellaValle, G., Tayeb, J., (1993). A sprcific slit die rheometer for extruded starchy products - Design, validation and application to maize starch. Rheologica Acta. 32(5), 465-476.

Vergnes, B., Villemaire, J.P., (1987). Rheological behavior of low moisture molten maize starch. Rheologica Acta. 26(6), 570-576.

Vergnes, B., Villemaire, J.P., Colonna, P., Tayeb, J., (1987). Interrelationships between thermomechanical treatment and macromolecular degradation of maize starch in a novel rheometer with preshearing. Journal of Cereal Science. 5(2), 189-202.

Wang, S.S., (1993). Gelatinization and melting of starch and tribochemistry in extrusion. Starch-Starke. 45(11), 388-390.

Wen, L.-F., Rodis, P., Wasserman, B., (1990). Starch fragmentation and protein insolubilization during twin-screw extrusion of corn meal. Cereal Chemistry. 67(3), 268-275.

Xie, F.W., Halley, P.J., Averous, L., (2012). Rheology to understand and optimize processibility, structures and properties of starch polymeric materials. Progress in Polymer Science. 37(4), 595-623.

Zheng, X.G., Wang, S.S., (1994). Shear-induced starch conversion during extrusion. Journal of Food Science. 59(5), 1137-1143.

CHAPTER 3. COMPARISON OF OFF-LINE CAPILLARY RHEOMETER AND IN-LINE EXTRUDER-FED CAPILLARY RHEOMETER AT HIGH TEMPERATURE, SHEAR AND LOW MOISTURE EXTRUSION CONDITIONS

3.1. Introduction

Various methods for understanding and quantifying the rheology of a raw material and the numerous transformations it undergoes during extrusion, originated from the polymer and plastics industry, similar to much of the advancements in extrusion processing technology itself. In most cases for plastics, viscosity is a simple and unique function of temperature and shear, hence off-line capillary rheometry can be successfully used to measure viscosity. But in the case of food/biopolymers, beside from the instantaneous temperature and shear, viscosity also becomes a function of temperature and shear history that the material has experienced, because of the physical and chemical changes that the macromolecules experience at extrusion conditions (Mercier et al., 1989).

Off-line capillary rheometry has been used successfully over the years in the polymers/plastics industry to understand the rheological behavior of various materials in a range of extrusion conditions (Bird et al., 1987; Morrison, 2001; Xie et al., 2012). Adaptation of this rheological method to the food/biopolymers industry is still in its early stages. Fundamental research is needed to validate and successfully adopt this technique from the polymer industry to the food industry. On the other hand, for food/biopolymers,

in-line rheometry techniques will allow to account for the temperature and shear history experience by a given material in an extruder before measuring viscosity.

3.2 Literature review

During polymer extrusion, the main objective is to melt the material which will facilitate its shaping with minimal degradation to the native structure of the material. Whereas in food extrusion, the complex biopolymer macromolecules undergo various levels of degradation, depending on the processing condition and desired final product. In high temperature extrusion, for example to produce puffed products or pre-cooked flours, the macromolecules are degraded by a combination of thermal and mechanical energy inputs. This can be further understood by analyzing the energy inputs for extrusion processing of different materials as shown in Figure 3.1.

The ineffectiveness of off-line capillary rheometry in predicting viscosities of food/biopolymers during extrusion at conditions similar to that described in Figure 3.1.(c) can be understood, since in a capillary rheometer, thermal degradation is the primary degradation, with minimal shear degradation at the die. While measuring the shear viscosity of commercial maize grits, potato powder and low density polyethylene using an extruder-fed in-line slit die viscometer and an off-line capillary rheometer, Senouci and Smith (1988) reported the strong dependence of viscosity of maize grits and potato powder on the processing history during extrusion.

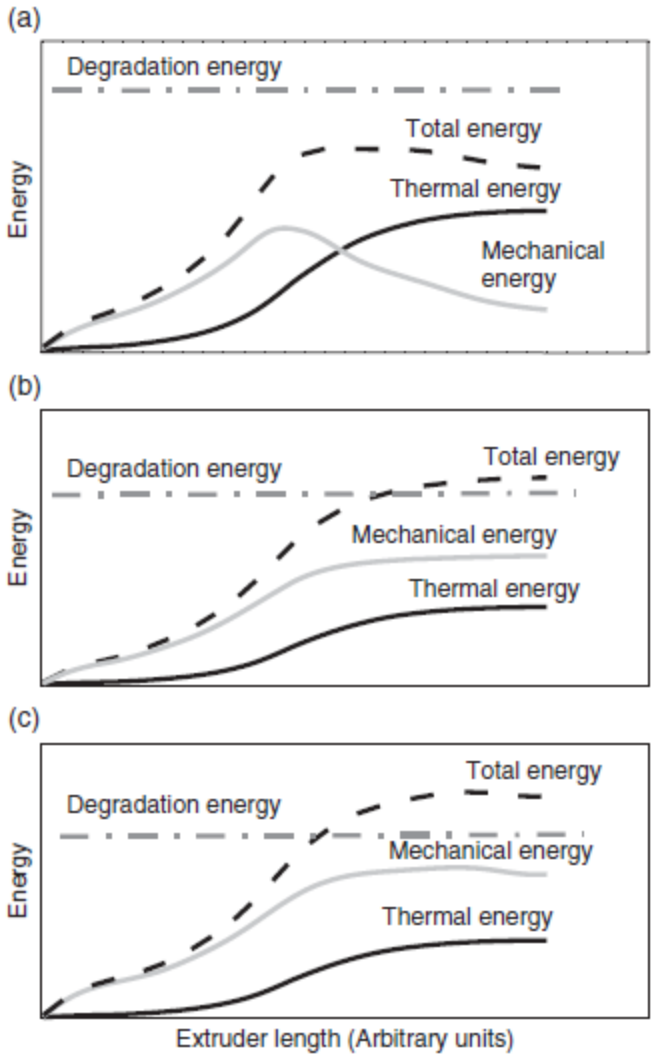

Figure 3.1. Different approaches used for the extrusion of plastic polymers and biomaterials in terms of thermal and mechanical energies profiles in the process. (a) Energy profile used for extruding plastic polymers. (b) Energy profile used for extruding biopolymers with minimum molecular degradation, e.g. extrusion of protein-based formulations. (c) Energy profile for extruding polymers where molecular degradation is sought, e.g. starch-based products with enhanced design. Reproduced from Bouvier and Campanella (2014).

Whereas, de la Pena et al. (2014) reported viscosity measurements for pasta dough with varying composition of semolina, whole wheat and flaxseed flour in a capillary rheometer and successfully used these measurements to calculate viscosity in a semi-commercial pasta extruder.

3.2.1 In-line rheometry techniques

Harper et al. (1971) were among the first to report the use of an in-line rheometer a for food material (cooked cereal dough – 80% corn grits and 20% oat flour at 30% moisture) viscosity modeling (Fig 3.2). They used a straight tube (capillary) viscometer with two pressure transducers and electric heaters (Fig 3.3) and the flow rate through the extruder was varied to measure viscosity at various shear rates. The data was modeled to account for the combined effect of temperature and moisture content on apparent viscosity (η) and fitted to Eq. 3.1 using multiple linear regression, to estimate the parameters for the different variables.

$$\eta = K_o \exp\left(\frac{E_a}{RT}\right) . \exp(-aMC) . (\dot{\gamma}_w)^{n-1} \quad (3.1)$$

where, K_o (Pa s^n) and a ($\%^{-1}$) are constants, E_a is the activation energy for a molten sample to flow (J/g mol), R is the universal gas constant (J/g mol/K), T is the absolute temperature (K) and MC is the moisture content of the sample (% wet weight basis).

Others have reported similar in-line viscosity measurement models without accounting for the variability in thermomechanical history using capillary viscometer (Cervone and Harper, 1978; Jao et al., 1978) and slit-die viscometer (Fletcher et al., 1985).

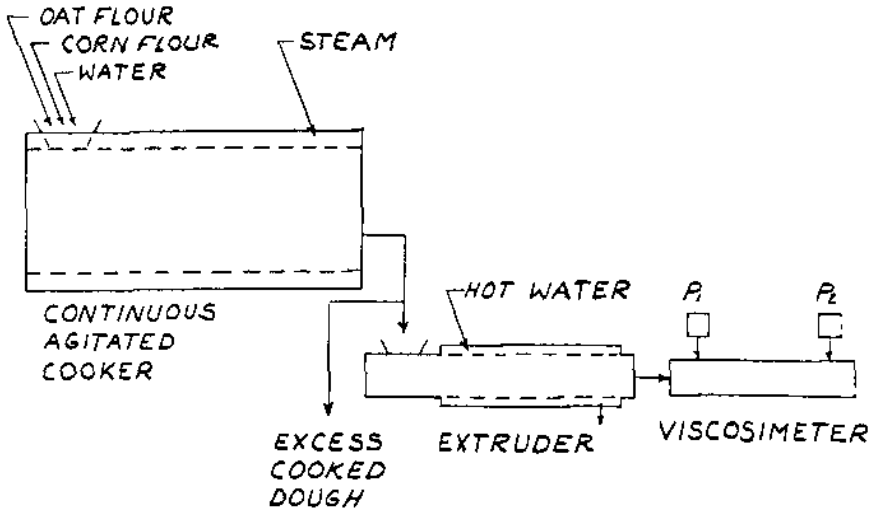

Figure 3.2. Experimental setup for in-line viscosity measurement of food dough by Harper et al. (1971).

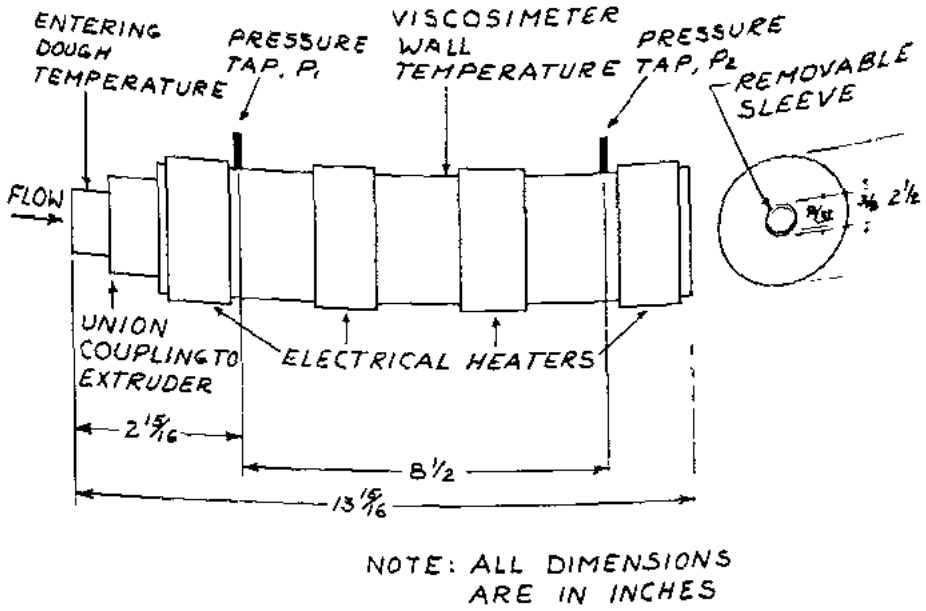

Figure 3.3. Schematic of the straight tube viscometer for in-line viscosity measurement of food dough by Harper et al. (1971).

With further understanding of the importance of thermomechanical history and product transformation in in-line viscosity measurements, few attempted to model for these changes. Senouci and Smith (1988) used a twin-screw extruder fed in-line slit die viscometer with multiple pressure transducers flush mounted along the length of the slit, which allows for accurate calculation of entrance and exit effects correction (Fig. 3.4). Along the effect of temperature and moisture content, the extruder screw speed was used to model the viscosity of maize grits and potato powder. Similarly, specific energy (Wang et al., 1990) and degree of gelatinization (Lai and Kokini, 1990) were used as parameters in addition to temperature and moisture content to model viscosity, to account for the thermomechanical history of the material.

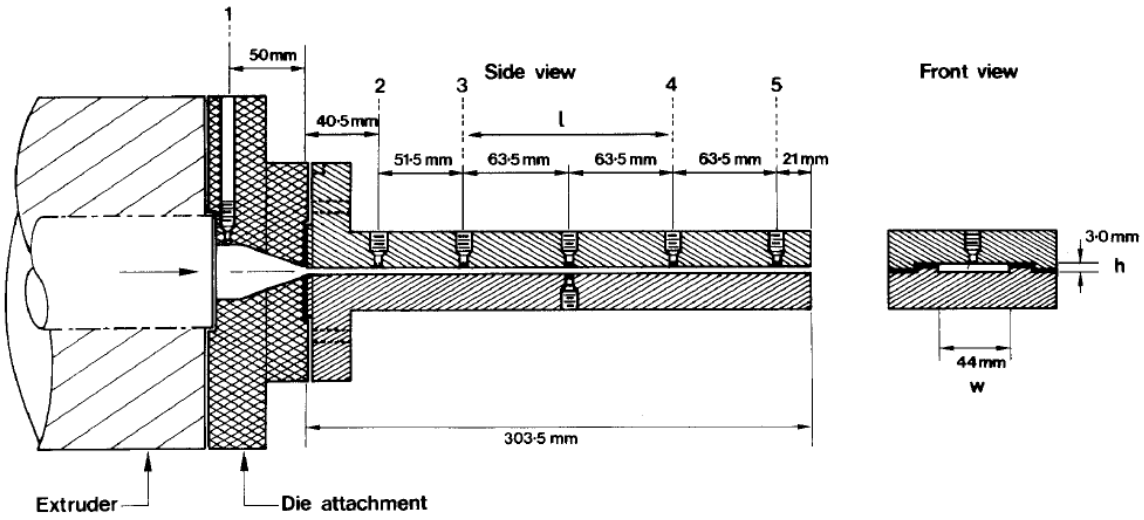

Figure 3.4. Schematic of the in-line slit die viscometer used in conjunction with a twin screw extruder by Senouci and Smith (1988).

The importance of the extrusion processing history and its impact on viscosity measurement and modeling was reported by Padmanabhan and Bhattacharya (1993) for corn meal who showed that changing extruder screw speed to vary shear rate through the die can result in erroneous viscosity curves, mainly in a single screw extruder. They demonstrated the use of a side stream valve near the extruder exit fitted with a slit die viscometer (Fig. 3.5) to measure viscosity at different shear rates instead of varying the extruder screw speed. In this approach even though the extruder screw speed was not changed, the level of opening of the side stream valve while measuring different shear rates, could cause changes in pressure in the extruder and the viscometer hence causing erroneous results.

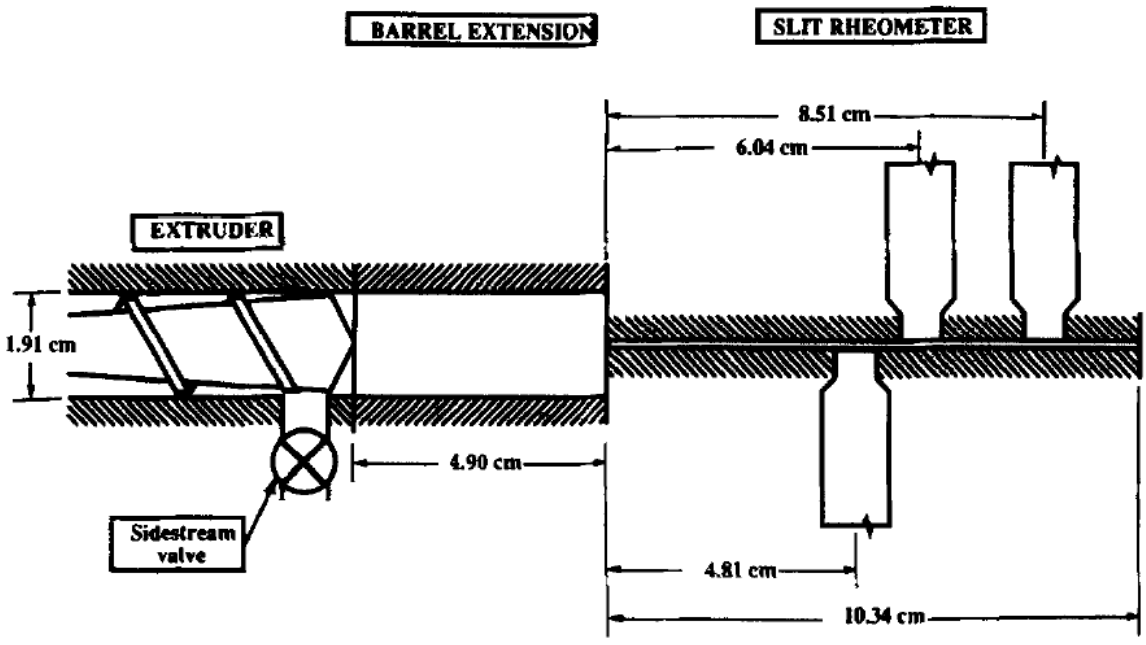

Figure 3.5. Schematic of the slit die rheometer attached to a single screw extruder with a side stream valve used by Padmanabhan and Bhattacharya (1993) for measuring corn meal rheology.

Similarly, Vergnes et al. (1993) developed a specific slit-die rheometer (Rheopac; Fig 3.6), which would allow to keep a constant flow conditions in the extruder while still allowing to vary the flow rate in the rheometer by using two flow channels (slits). But the extrusion die pressure was not monitored and the relationship between the slits had to be calculated to maintain same operating conditions (Li et al., 2004). Hence they were able to model the viscosity of molten melts for maize. The influence of amylose content on the viscosity of low moisture maize starch blends was also studied using this rheometer (DellaValle et al., 1996). Both these studies using the Rheopac in-line rheometer used specific mechanical energy as an additional parameter to model viscosity. They have also reported the dependence of the power law index (n) on temperature, moisture content and specific mechanical energy for certain materials.

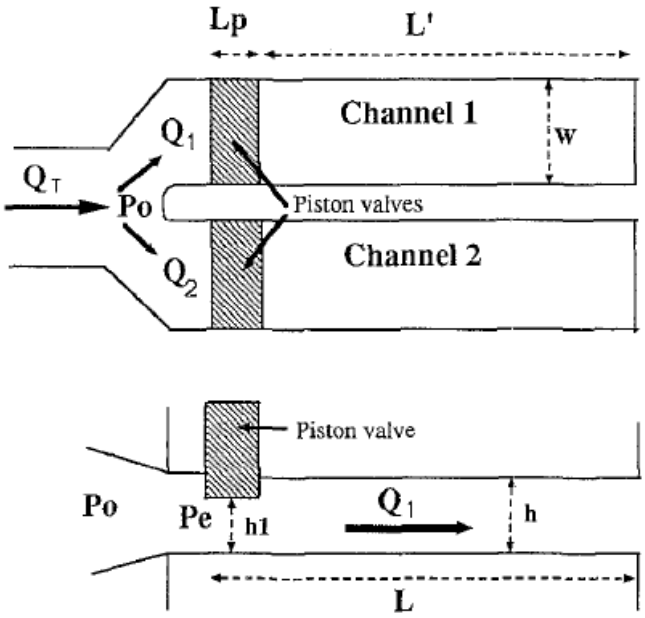

Figure 3.6. Schematic of the twin channel slit die Rheopac rheometer with balanced feed rate used by Vergnes et al. (1993) and DellaValle et al. (1996).

Another novel in-line slit-die rheometer system (Fig. 3.7) was developed by Li et al. (2004) which allowed for variation of shear rate in the in-line rheometer without changing the extruder operating conditions. The adapter section of the rheometer had an option to divert part of the flow from the extruder to the rheometer and discard the rest while maintaining a constant extruder back pressure and temperature which was monitored continuously, hence maintain a constant thermomechanical history at a given extrusion condition. The effect of various extrusion parameters on corn melt rheology was reported using this technique.

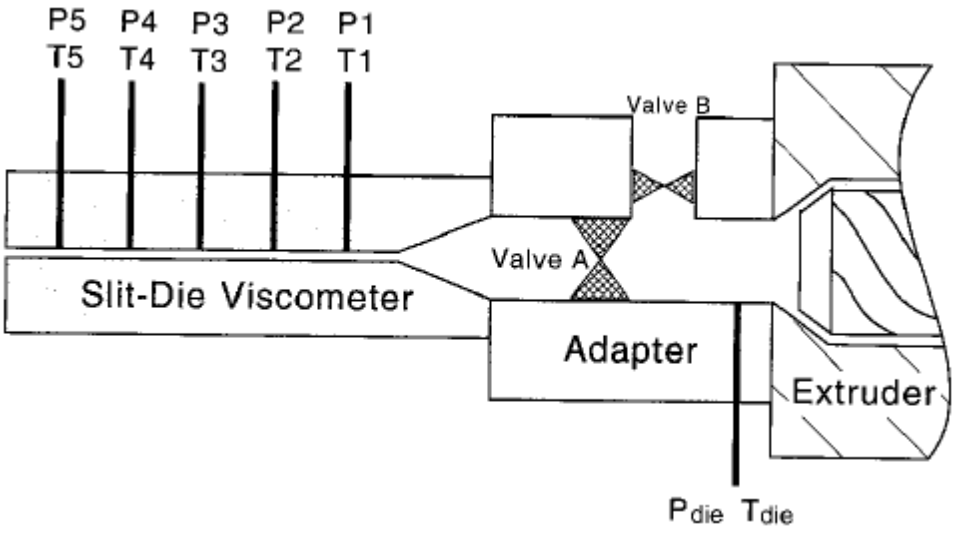

Figure 3.7. Schematic of the in-line slit-die viscometer used by Li et al. (2004).

More recently, Robin et al. (2010) reported the development of an innovative in-line twin-slit die rheometer with adjustable slit height, to vary flow rate and independent temperature controlled slits. The effect addition of bran to wheat flour and its impact on in-line viscosity was studied using this twin-slit rheometer (Robin et al., 2011; Robin et al., 2010).

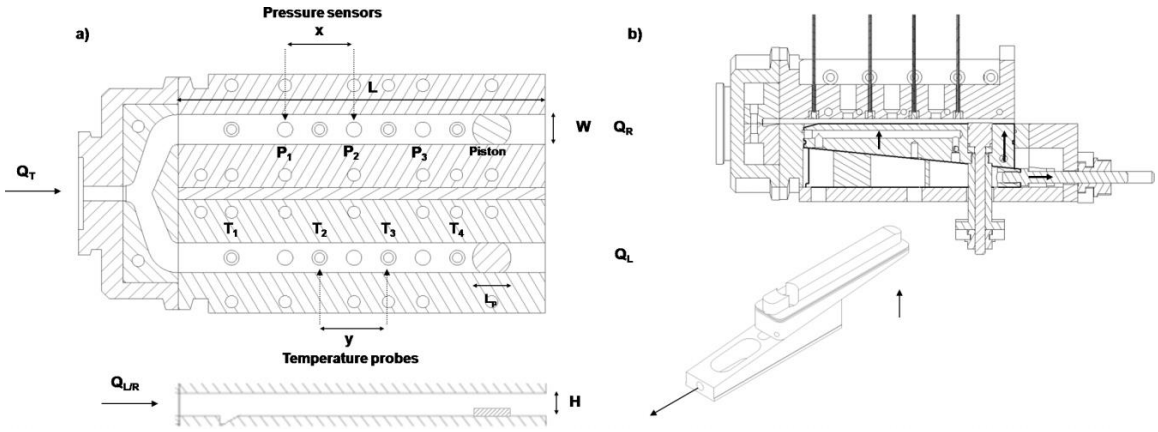

Figure 3.8. Schematic of twin-slit adjustable rheometer (a) and the principle of the rheometer's adjustable slits (b) used by (Robin et al., 2011); Robin et al. (2010).

Drozdek and Faller (2002) took a different approach to in-line viscosity measurement by using a dual orifice die (Figure 3.9) to quantify power law index for starchy foods by measuring only the flow rate at each die. This is a simpler approach to understanding the rheology of materials, but it has limitations, as the power law index is based only on two flow rates and any attempt to change the flow rates can be done only by changing the extruder screw speed, which changes the thermomechanical history of the product. Also extrusion pressure was not measured, so apparent viscosity of the material at different conditions cannot be calculated; only the effect of extrusion condition on power law index was reported. In another approach, while studying the behavior of pasta dough, de la Pena et al. (2014) measured the extrusion pressure before the die to calculate the shear stress at the die of the extruder and calculated shear rate from the volumetric flow rate of the pasta. These approaches offer new insights in to simpler techniques for in-line viscosity measurements.

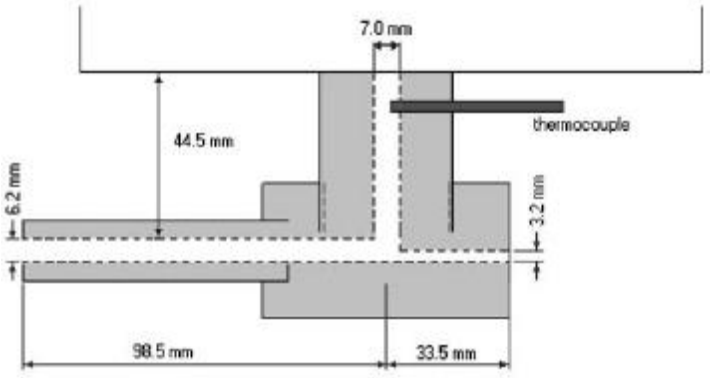

Figure 3.9. Schematic of bifurcated flow, dual orifice die used by Drozdek and Faller (2002).

3.2.2 Starch transformation during extrusion

Starch goes through several physicochemical and rheological changes during extrusion including gelatinization, melting and fragmentation (Lai and Kokini, 1991). Several analytical methods have been employed in understanding starch transformation during the extrusion process, including, pasting properties to understand change in pasting viscosities of starch (Al-Rabadi et al., 2011; Bouvier and Campanella, 2014; Doublier et al., 1986; Guha et al., 1998; Moussa et al., 2011), size exclusion chromatography to understand changes in molecular weight (Colonna et al., 1984; Liu et al., 2010; Moussa et al., 2011; Wen et al., 1990), intrinsic viscosity measurements which is affected by changes in molecular weight (Colonna et al., 1984), enzymatic methods to determine change in percentage of α-1,6 linkages in native and extruded starches (Colonna et al., 1984), iodine binding capacity to determine degree of gelatinization (Colonna et al., 1984; Lai and Kokini, 1990), differential scanning calorimetry (DSC) to quantify changes in enthalpy requirements (Donovan, 1979; Wang et al., 2010) and several types of

microscopy for qualitative observation of changes occurring in starch (Al-Rabadi et al., 2011; Colonna et al., 1984; Moussa et al., 2011; Wang et al., 2010).

Measuring the pasting properties of starch is a simple and effective method to quantify starch transformation during extrusion and has been proven to detect differences in thermomechanical processing variations. Bouvier and Campanella (2014) have documented the use of a Rapid Visco Analyzer which is typically used to study the pasting properties, to show effect of thermomechanical processing during extrusion. They have reported the use of pasting property to understand the effect of specific mechanical energy during the extrusion process and the effect of different screw profiles of the extruder.

3.3 Objective

The main goal of this study is to build viscosity models that will accurately predict the apparent viscosity of a material in a 60 lb/hr small-scale extruder (Insta-Pro International, now Technochem Inc., Boone, IA) with restrictions on screws and operates solely based on viscous dissipation of mechanical energy. The viscosity model built using an off-line capillary rheometer in the previous study over predicted apparent viscosity compared to models reported in literature. An appropriate in-line measurement technique is needed to compare and understand the differences between off-line capillary rheometer and in-line extruder-fed rheometer. The objective of this study is to measure viscosity off-line in a capillary rheometer and in-line in the small-scale extruder fed viscometer at high temperature, shear and low moisture extrusion conditions. These measurements are then compared to draw conclusions regarding the effect of thermomechanical history on the

viscosity of the material. In addition, to better understand the physicochemical changes experienced by the material in the small-scale extruder versus the capillary rheometer, pasting properties of the extrudates from both techniques is quantified.

3.4 Materials and methods

3.4.1 Raw material

Dehulled, degermed yellow corn meal (Degerminated fine yellow cornmeal M77) provided by Agricor Inc., (Marion, Indiana) was used for both in-line and off-line measurements in this study. The proximate composition and particle size of the cornmeal per the specifications provided are tabulated below (Table 3.1 and 3.2).

Table 3.1. Proximate composition of dehulled, degermed yellow cornmeal used in this study.

Component	Range
Moisture	11.0 – 13.5%
Protein	4.5 – 8.5%
Fat	1.25% maximum
Crude fiber	1.0% maximum
Ash	1.0% maximum

Table 3.2. Particle size of dehulled, degermed yellow cornmeal used in this study.

Held/Through	**US sieve size**	**Percentage**
Held	US #30 Screen	1% maximum
Held	US #40 Screen	20-50%
Held	US #80 Screen	45-75%
Through	US #80 Screen	5% maximum

For in-line extruder viscosity measurement, the cornmeal was used at the same particle size provided (Table 3.2). For off-line capillary rheometer measurement, the cornmeal was milled to fine flour using a pin mill (Alpine Augsburg 160Z, Augsburg, Germany).

3.4.2 Sample preparation

For in-line extruder fed viscosity measurement, the corn meal moisture was adjusted to 32.5, 35 and 37.5% wet basis by mixing a known amount of water initially at slow speed for 1 minute then at medium speed for 2 minutes, in a Hobart mixer (H-600T, Hobart Corporation, Troy, OH). For each extrusion run 18.1 kg (40lb) of corn meal was prepared, by mixing water in four 4.5 kg (10lb) batches individually at room temperature (21.7^{o}C). Then the moisture adjusted meals were stored in separate plastic buckets with a plastic liner (Open-top bags, 24” x 30”, 2 mils thick, FDA compliant polyethylene resin, McMaster-Carr, Elmhurst, IL) and kept in a cold room (7.2^{o}C) overnight for equilibration. On the day of the experiment, the samples were removed from the cold room and allowed to equilibrate to room temperature before the extrusion run.

For the off-line capillary rheometer measurement, the fine corn flour moisture was adjusted to the same levels (32.5, 35 and 37.5%) as the in-line measurement in benchtop

laboratory mixer (KitchenAid Mixer, Benton Harbor, Michigan) at room temperature (21.7^{o}C). The moisture adjusted samples were then packed in plastic bags (Ziploc bags, S.C. Johnson & son, Racine, Wisconsin) and kept in a cold room (7.2^{o}C) overnight for equilibration. On the day of the experiment, the samples were removed from the cold room and allowed to equilibrate to room temperature before the experiment. The moisture content of the samples was verified after equilibration by standard hot-air oven method for moisture determination (103^{o}C for 24hrs).

3.4.3 Off-line capillary rheometer measurements

A twin-bore Rosand RH2000 capillary rheometer (Bohlin Instruments, now Malvern Instruments Ltd., Worcestershire, UK) was used in this study. The experiments were carried out at three different bore wall temperatures (100, 110 and 120^{o}C). The bores were fitted with 4 mm capillaries of two different length/diameter (L/D) ratios of 4 and 8, respectively, for all experiments. Approximately, 110 g of sample was loaded in each bore, after the bore wall reached testing temperature. Using the Flowmaster® software (Version 8.5, Malvern Instrments), samples were initially compressed at a piston speed of 10 mm/min until the pressure transducers in each bore read a constant maximum pressure, then the piston was stopped and samples were equilibrated for 10 minutes at the test temperature. After equilibration, samples were compressed again at 10 mm/min until a constant maximum pressure was reached in each bore (product was flowing out of the capillaries in both compression steps). Immediately following this, two sweeps (high to low shear rate and vice versa) of viscosity measurements were made at pseudo wall shear rates of 100, 50, 20, 10, 5, 2 and 1 s^{-1}. The pressure recorded from each bore at each shear

rate was an average of 8 pressure readings (100 readings per minute) when variability was within 2%. All the experiments were done is triplicate.

Shear stress at the capillary wall was determined using the pressure measurements as,

$$\tau_w = \frac{\Delta P \,.D}{4\,.\,L} \tag{3.2}$$

The pseudo wall shear rate was calculated from,

$$\dot{\gamma}_{ow} = \frac{4\,.Q}{\pi\,.\,R^3} \tag{3.3}$$

where, Q is the volumetric flow rate, calculated from piston speeds and bore dimensions and R is the radius of the capillary. The true wall shear rate was then obtained by applying the Rabinowitsch correction as,

$$\dot{\gamma}_w = \left(\frac{3n+1}{4n}\right).\dot{\gamma}_{ow} \tag{3.4}$$

where, n = d(ln τ_w)/d (ln $\dot{\gamma}_{ow}$).

The apparent shear viscosity was calculated as,

$$\eta = \frac{\tau_w}{\dot{\gamma}_w} \tag{3.5}$$

Power-law model was used to determine the rheological behavior of the different samples:

$$\eta = k(\dot{\gamma}_w)^{n-1} \tag{3.6}$$

where n is the power law or flow behavior index and k is the consistency coefficient in $Pa.s^n$.

3.4.4 In-line extruder fed viscometer measurements

For in-line viscosity measurement at the exit of the small-scale extruder (Technochem Inc.), combining the ideas of Drozdek and Faller (2002) and de la Pena et al. (2014), a novel die with two capillary openings of different diameters (5mm and 3.4mm) and 17 mm length (same length as normal die used in the extruder) was used (Figure 3.10 (B)).

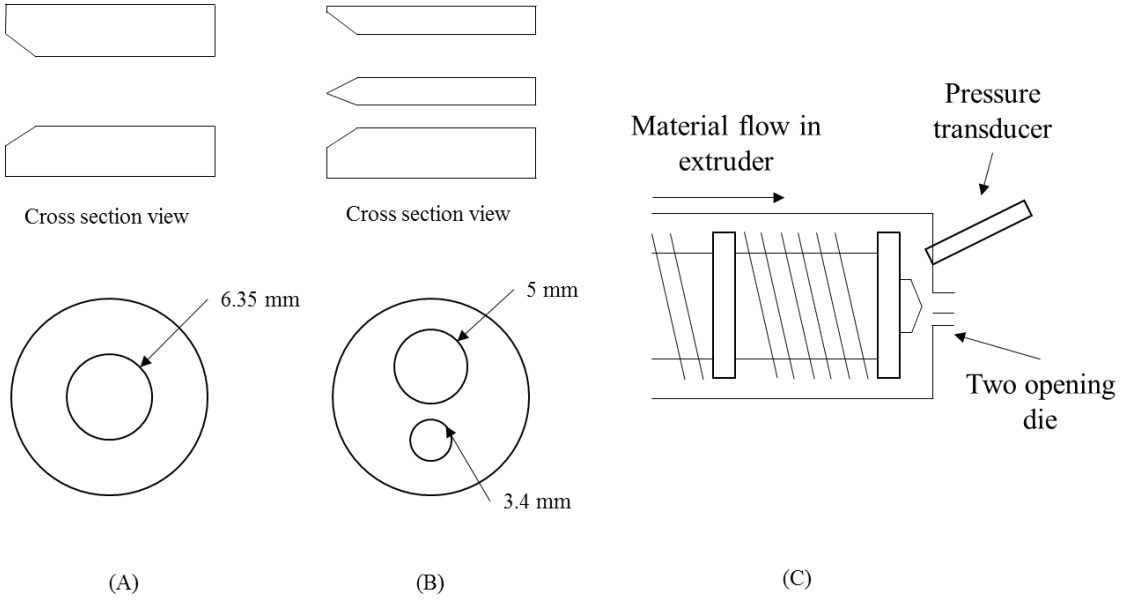

Figure 3.10. Schematic showing (A) Normal die used in the extruder; (B) Two capillary opening die used for in-line viscosity measurement in the extruder; (C) Experimental setup during in-line viscosity measurement.

The diameter of the two openings was initially calculated by matching their total cross sectional area with that of the normal die (Figure 3.10 (A)), then after preliminary

experiments it was adjusted based on flow ability of the material through the two openings. The entrance angle for each opening was designed to be 100 degrees, to avoid issues with uneven flow and to allow for fully developed flow through the two openings.

In-line viscosity was measured at three extruder speeds (100, 200 and 300 rpm) at each of three moisture contents of cornmeal (32.5, 35 and 37.5% wet basis; total 9 treatments). The extruder speed was measured using the non-contact (laser) option of a tachometer (HHT13, contact/non-contact pocket laser tachometer, Omega Engineering Inc., Stamford, CT) by fixing a laser reflective tape on a pulley attached to the extruder shaft behind the feeding section of the extruder. The extruder was starve-fed using a volumetric feeder (Dry materials feeder, serial no. 44126-01A-302, Accu-Rate Inc., Whitewater, WI); hence the mass flow rate was different at every treatment condition. From an operational standpoint, the extruder was run at one specific moisture content and the three screw speeds (100, 200 and 300 rpm), in that specific order, on each experimental day. Since temperature rise in the extruder is solely based on viscous dissipation of mechanical energy, randomizing the screw speeds was not an option, because there was no way to cool the barrels if switching from high to low speed. The extruder was allowed to equilibrate at each speed for at least 30 minutes before collecting data. Equilibrium was determined by stable pressure, temperature and motor current draw measurements at a given condition. Extrusion run at each treatment was replicated three times.

A digital ammeter attached to the 7.5hp motor (P21G6793B, Reliance motors, now Baldor, Fort Smith, AR) of the extruder was used to measure current drawn by the motor

at no load and when operating at a given condition. The current draw (ampere) readings were then converted power (watt) using the motor curves provided by Reliance motors (Table 3.3), using Eq. 3.7.

Table 3.3. Motor performance curve for 7.5hp motor (P21G6793B) by Reliance motors.

Current (A)	**Power (hp)**
5.38	0
5.8	1.88
6.9	3.76
8.15	5.62
10.5	7.51
12.8	9.37

$$\text{Power (watt)} = 0.4234\ (I)^2 + 7.6474\ (I) - 28.639 \qquad (3.7)$$

where I is current in ampere. Eq. 3.7 is a second degree polynomial fit of motor performance data from 5.38 to 8.15 amperes, since the current draw in the experiments in this study did not exceed 8 amperes. The power consumption, along with throughput was used to calculate specific mechanical energy at each treatment.

Temperature was measured using thermocouples at ports (1.6mm openings perpendicular to the direction of product flow) just before the exit on both the die openings. Temperature was recorded once equilibrium extrusion conditions were reached using a

data logger (HH309A 4-channel data logger thermometer, Omega Engineering Inc.) and transferred from the data logger to a spreadsheet using the software provided (SE309 V36). Thermocouples were removed after temperature was recorded, so it does not interfere with product flow rate and extrusion pressure measurements.

A 500 psi pressure transducer (Model PT462E, flexible stem melt pressure transducer, Dynisco, Franklin, MA) was flush mounted to the inner wall on the end plate just before the die openings. It was in direct contact with the material flowing through to measure extrusion pressure. The pressure transducer was connected to a digital display meter (TD502T, Transducers direct LLC, Cincinnati, OH). The digital meter had an Ethernet output port which was used to connect it to a desktop computer. An IP was assigned to the digital meter by the Device Installer software (Lantronix Inc., Irvine, CA) so the computer can communicate with the digital meter. Data logger software (Texmate Data Viewer 4.2.5.0, Tiger Controller Software, Texmate Inc., Escondido, CA) installed in the computer was used to collect the pressure data from the digital meter. The connection between the data logger software and the digital meter was setup using the IP address assigned to the digital meter. The pressure transducer was calibrated by two point calibration (0 and 400 psi) using a dead weight tester (Chandler engineering company, Tulsa, OK). The configuration utility software for the digital meter (Texmater Tiger Configurate Utility 2009.09.08, Texamte Inc.) was used to set the two point calibration. The live graphing option in the data logger software was used to monitor the extrusion pressure at the stages where the extruder was not equilibrium (at start-up and between two operation conditions). Once equilibrium was reached and in-line viscosity was ready

to be measured, the “batch test” option in the data logger software was used to save the pressure readings from the digital meter every 2 seconds. The time of each viscosity measurement was kept track and this was later used to calculate the extrusion pressure accurately from the saved data. The extrusion pressure was assumed to be equal across the two die openings. This was then used to calculate the wall shear stress at the two L/D using Eq. 3.2.

Mass flow rate was measured manually (five measurements in each replication) at equilibrium at each treatment condition. For each measurement, extrudate from the two openings were collected simultaneously for 30 seconds. They were allowed to cool down at room temperature before weighing. The cooled extrudate samples were immediately packed in plastic bags (Ziploc bags, S.C. Johnson & son, Racine, Wisconsin) to avoid further moisture loss. The moisture content of the weighed extrudate was measured by standard hot-air oven method at 103^{o}C for 72hrs. Dry matter content of the extrudate was then used to back calculate true mass flow rate through the extruder at the specific cornmeal moisture tested during that run. Volumetric metric flow rate was calculated by assuming a true density of 1250 kg/m^3 for corn.

The volumetric flow rate through the two die openings was used to calculate pseudo wall shear rate by using Eq. 3.3. The power law index (n) was calculated using this data which in turn was used to apply Rabinowitsch correction using Eq. 3.4.

Power law viscosity models were built at each operating condition of the extruder. These were then compared to the viscosity models built using the capillary rheometer to draw inferences. Temperature measured and specific mechanical energy calculated using the

power consumption based on current drawn by the motor (using Eq. 3.7) at each condition were also used to draw inferences.

3.4.5 Rheological modeling

Capillary rheometer data for the degermed dehulled corn flour was modeled using that proposed by Harper et al. (1971) in Eq. 3.1. Temperature effects were expressed using an Arrhenius relationship and moisture content effects were expressed using an exponential relationship.

For the in-line viscosity measurements, for the purpose of comparison of data in current study with data from literature, the data is fit in the model in Eq. 3.8 which is a slightly modified model from previous studies which used specific mechanical energy to account for thermomechanical history (DellaValle et al., 1996; Martin et al., 2003). In this model the specific mechanical energy effect is expressed using an exponential relationship, along with temperature and moisture content effects.

$$\eta = K_o \exp\left(\frac{E_a}{RT}\right). \exp(-aMC) . \exp(-bSME). (\dot{\gamma}_w)^{n-1} \quad (3.8)$$

where, K_o (Pa s^n), a ($\%^{-1}$), b (kg/kJ) are constants, E_a is the activation energy for a molten sample to flow (J/g mol), R is the universal gas constant (J/g mol/K), T is the absolute temperature (K), MC is the moisture content of the sample (% wet weight basis) and SME is the specific mechanical energy (kJ/kg).

3.4.6 Pasting property measurement

Extrudate collected from the two die openings at equilibrium during in-line viscosity measurement for different treatments were dried overnight at 50^{o}C. The dried samples were milled in a cyclone mill (CT 193 Cyclotec^{TM} sample mill, Foss, Hillerod, Denmark) fitted with a 0.5mm mesh screen. Then the samples were sieved through a 70 mesh screen (210μm). The moisture content of the material that passed through the screen was analyzed (103^{o}C for 24 hrs).

In case of the off-line viscosity measurement, since the capillary rheometer was operated at several shear rates within each run during the actual viscosity measurement, separate runs were carried out to generate samples for analyzing the pasting properties. Samples were generated at all the moisture contents tested (32.5, 35 and 37.5%) but only at the maximum bore temperature tested (120^{o}C) using only one bore fitted with the 16mm long, 4mm diameter die (since the L/D was closest to the L/D used in the in-line measurement). The capillary rheometer was operated at a maximum constant shear rate of 100s^{-1}, to create a uniform product. The samples were then dried, milled, sieved and analyzed for moisture content as before.

A Rapid Visco Analyzer (RVA; Perten Instruments, Hagersten, Sweden) was used to measure the pasting property of sample following the method described by Bouvier and Campanella (2014). All the measurements were performed with 29 g sample (dried sample + water) in the canister at a solid concentration of 11.86%. The moisture content measure for the individual sample, was used to determine accurately the amount of water to be added in order to maintain a constant solid concentration for all the RVA runs.

A standard temperature-time protocol was followed for all the runs. The run starts with an initial holding time of 6 minutes at 25^{o}C. The temperature is then raised to 95^{o}C over the next 4 minutes. The sample is held at that temperature for 6.5 minutes, then cooled down to 25^{o}C over the next 4.5 minutes. Finally the sample is held at 25^{o}C for 5 minutes. The sample is stirred at 960 rpm for the first 10 seconds and then stirred at 160 rpm throughout the rest of the test.

Peak, final and cold swell viscosity measurements and corresponding time and temperatures were calculated from the data collected and comparison between the in-line and off-line samples were made.

3.5 Results and discussion

3.5.1 Off-line capillary rheometer measurements

For all the temperature, moisture content, and shear rate combinations tested, pressure stability was reached in both bores of the capillary rheometer for the degermed, dehulled yellow corn flour. Based on the bore pressure measurements and preset piston speeds in the capillary rheometer, shear stress and pseudo wall shear rate calculations were made using Eqns. (3.2) and (3.3). Power law indicies (n) were calculated for each replicate from the slope of log-log plots of these values and actual wall shear rate was calculated by applying Rabinowitsch correction in Eq. (3.4). Bagley correction (Bagley, 1957) was not applied for the data analysis (only data from L/D = 4 is analyzed), in order to allow for comparison of data with in-line measurements where there was no provision for

Bagley correction. The data for each replicate was fit to a power law model described in Eq. (3.6), to calculate consistency index (k).

As expected the corn flour displayed a psedoplastic behavior at all the conditions tested (Figure 3.11). Increase in moisture content and temperature led to a decrease in viscosity, under the conditions tested, agreeing with conclusions reported by several others who studied similar food/biological systems at these extrusion conditions, using off-line and in-line rheometers (Dautant et al., 2007; de la Pena et al., 2014; Fraiha et al., 2011; Halliday and Smith, 1995; Harper et al., 1971; Lai and Kokini, 1990; Li et al., 2004; Núñez et al., 2010; Sandoval and Barreiro, 2007; Senouci and Smith, 1988; Vergnes and Villemaire, 1987).

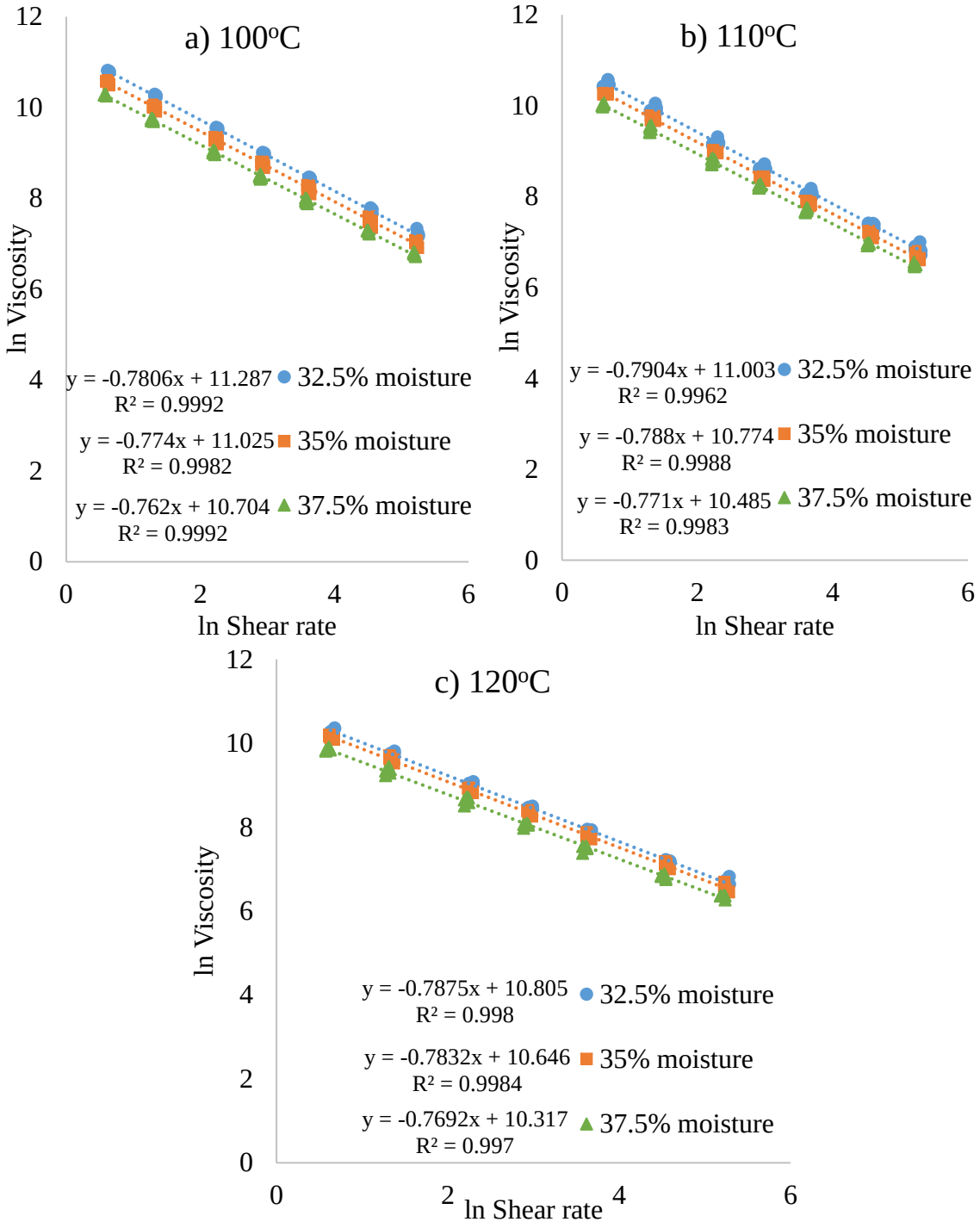

Figure 3.11. Off-line viscosity vs shear rate (natural log) plots of degermed, dehulled yellow corn flour at temperature a) 100°C, b) 110°C and c) 120°C and 32.5%, 35% and 37.5% moisture contents.

Table 3.4. Power law indices (n) and consistency coefficients (k) for degermed, dehulled yellow corn flour, at different temperatures and moisture contents measured in an off-line capillary rheometer.

Temperature (^oC)	Moisture content (% wet basis)	n	k ($kPa.s^n$)
100	32.5	0.22	79.7
100	35	0.22	61.5
100	37.5	0.24	44.5
110	32.5	0.21	60.2
110	35	0.21	47.8
110	37.5	0.23	35.8
120	32.5	0.21	49.4
120	35	0.22	42.0
120	37.5	0.23	30.3

The consistency coefficient, k, also decreased with increasing temperature and moisture content whereas the power law index, n, did not follow a particular trend, as shown in Table 3.4. This is also in agreement with rheological studies conducted on food materials by several others (Dautant et al., 2007; Fraiha et al., 2011; Sandoval and Barreiro, 2007).

The viscosity data for was also fit in Harper's model (Eq. 3.1) using multiple linear regression analysis. The parameter estimates for this model is shown in Table 3.5 for the degermed, dehulled corn flour.

Table 3.5. Estimated values of parameters using multiple linear regression for the power law viscosity model represented by Eq. 3.1 for degermed dehulled yellow corn flour.

	K_o	**E_a/R**	**a**	**n**
Degermed dehulled yellow corn	5.70	3218	0.09497	0.23

K_o in Pa. s^n

a in $\%^{-1}$

E_a/R in K

3.5.2 In-line extruder-fed viscometer measurements

Extrusion pressure and volumetric flow rate measurement from the two openings of the die attached to the extruder were used to calculate shear stress and pseudo wall shear rate respectively, using Eqns 3.2 and 3.3. Power law indicies (n) were calculated from the individual set of shear stress and pseudo wall shear rate values calculated for the large and small die. The actual wall shear was then calculated by applying Rabinowitsch correction in Eq. 3.4. All the data from each extrusion condition was then fit to a power law model described in Eq. 3.6, to calculate consistency index (k).

Similar to the off-line measurement, during the in-line measurement, the corn meal displayed a pseudoplastic behavior at all the extrusion conditions tested which can be inferred from the power law indicies (n) in Table 3.6. The power law index (n) did not seem to be depend on the extrusion conditions since there was no specific trend observed,

which is in agreement with the study by Li et al. (2004), but contrary with the study by Vergnes et al. (1993). The consistency coefficient on the other hand decreased with increasing screw speed at specific moisture content and showed interaction effects with increasing moisture contents at a specific screw speed (explained further under the section "effect of moisture content" later in this discussion), which is in agreement with previous literature (Li et al., 2004; Padmanabhan and Bhattacharya, 1993; Vergnes et al., 1993).

Table 3.6. Power law indices (n) and consistency coefficients (k) for degermed, dehulled yellow corn flour, at various moisture contents and extruder screw speeds measured in an in-line extruder fed two-opening die viscometer.

Moisture content (% wet basis)	Screw speed (rpm)	n	k ($kPa.s^n$)
32.5	100	0.17	33.5
32.5	200	0.19	10.6
32.5	300	0.20	8.9
35	100	0.19	38.9
35	200	0.21	28.0
35	300	0.21	22.6
37.5	100	0.16	33.4
37.5	200	0.17	23.7
37.5	300	0.19	18.4

Temperature recorded at die exit for both the large and small die openings have been tabulated in Table 3.7. Temperature recorded at the small die exit was consistently lower compared to the large die at all extrusion conditions. A maximum difference in temperature of 8^{o}C between the two dies was recorded at 32.5% moisture content and extruder speeds of 200 and 300 rpm. The lack of a heating system at the die is believed to cause this product cool down in the small die. The temperature recorded at the large die exit is used as the actual material temperature for further analysis in this study.

Table 3.7. Die exit temperature at the large and small dies for degermed, dehulled yellow corn flour, at various moisture contents and extruder screw speeds measured in an in-line extruder fed two-opening die viscometer.

		Temperature (^{o}C)	
Moisture content (% wet basis)	Screw speed (rpm)	Large die	Small die
32.5	100	123	116
32.5	200	139	131
32.5	300	145	137
35	100	112	105
35	200	123	118
35	300	128	125
37.5	100	105	100
37.5	200	119	115
37.5	300	127	123

Specific mechanical energy (SME) and total throughput (combined throughput from the two openings) recorded during in-line viscosity measurements are reported in Table 3.8. Since the extruder was starve-fed in a manner to fill the barrel to the point where there was no material backing in to the feed section during the measurement, the throughput was varied at each extrusion condition. At 32.5% moisture content, there was significantly higher back flow near the feed section because the material was too dry and it was easily being pushed back thorough the barrel grooves at the screw restriction closest to the feed section. In order to prevent this back flow the throughput at 32.5% had to be dropped significantly lower to get stable flow and pressure readings at the die. This in turn is reflected as higher SME at all screw speeds compared to other moisture contents tested. SME increased with increase in screw speed at a given moisture content, similar to observations made in literature (Li et al., 2004). Although it must be noted that since the flow rate was different at each extrusion condition, inferences drawn using SME must be considered cautiously.

3.5.2.1 Effect of screw speed

At a specific moisture content, the viscosity of cornmeal decreased with increasing extruder screw speed. This was consistent across all the moisture contents tested (Figures 3.12, 3.13 and 3.14) and in agreement with previous studies (Li et al., 2004; Padmanabhan and Bhattacharya, 1993; Vergnes et al., 1993). Increase in screw speed leads to increased conversion of mechanical energy to thermal energy, hence the product temperature increases which in turn lowers viscosity. The increased conversion of mechanical energy is also indicated by the increase in SME with increase in screw speed

at specific moisture content (Table 3.8), but it should also be noted that the throughput was different at each condition so the inference with regard to SME should be considered cautiously.

Table 3.8. Specific mechanical energy (SME) and total throughput for degermed, dehulled yellow corn flour, at various moisture contents and extruder screw speeds measured in an in-line extruder fed two-opening die viscometer.

Moisture content (% wet basis)	Screw speed (rpm)	SME (kJ/kg)	Total throughput (kg/hr)
32.5	100	86	4.1
32.5	200	149	4.7
32.5	300	225	6.6
35	100	67	5.5
35	200	95	11.0
35	300	180	15.7
37.5	100	82	4.5
37.5	200	140	7.8
37.5	300	165	10.9

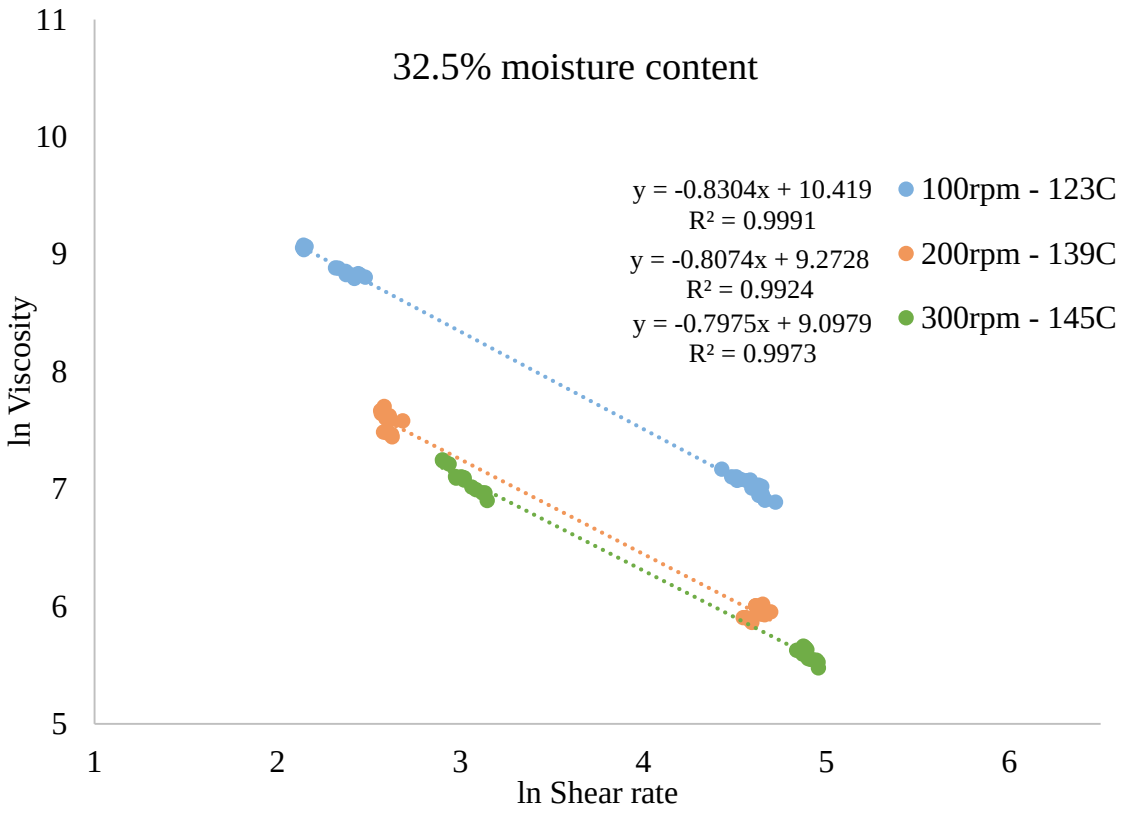

Figure 3.12. In-line viscosity vs shear rate (natural log) plots of degermed, dehulled yellow cornmeal at extruder screw speeds of 100, 200 and 300 rpm and moisture content of 32.5% (wet basis).

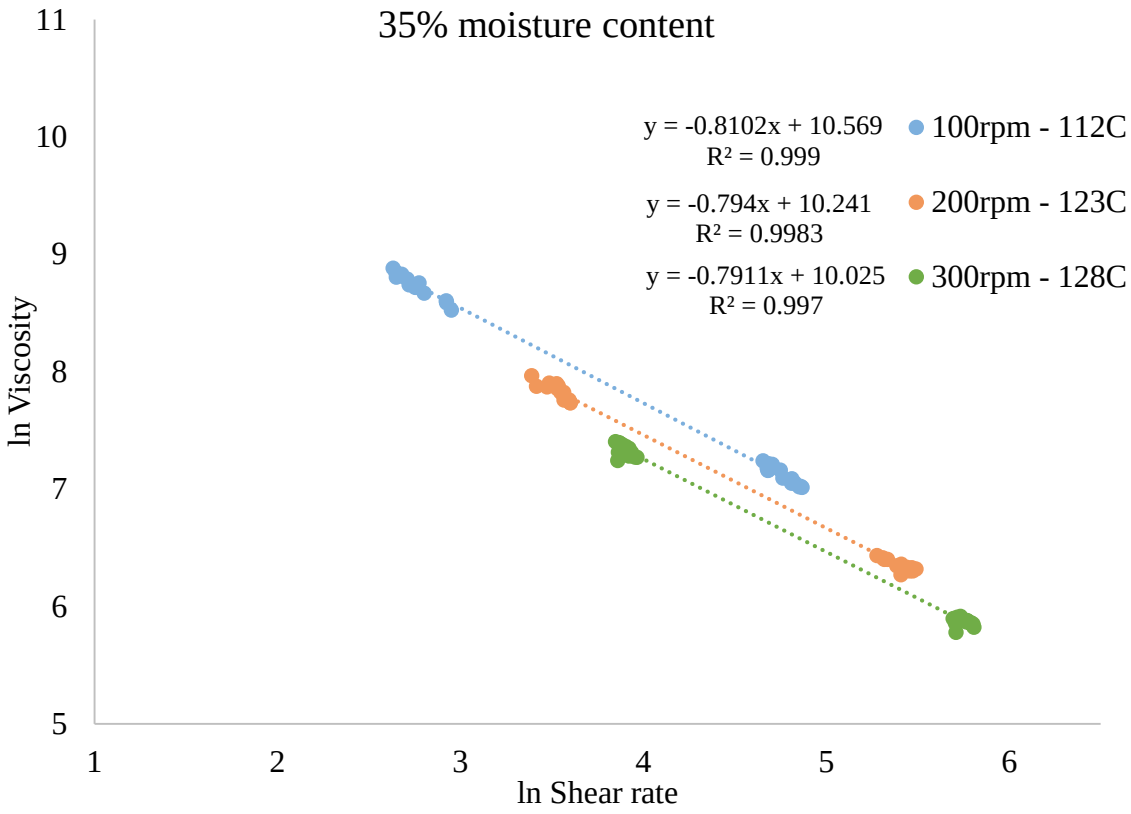

Figure 3.13. In-line viscosity vs shear rate (natural log) plots of degermed, dehulled yellow cornmeal at extruder screw speeds of 100, 200 and 300 rpm and moisture content of 35% (wet basis).

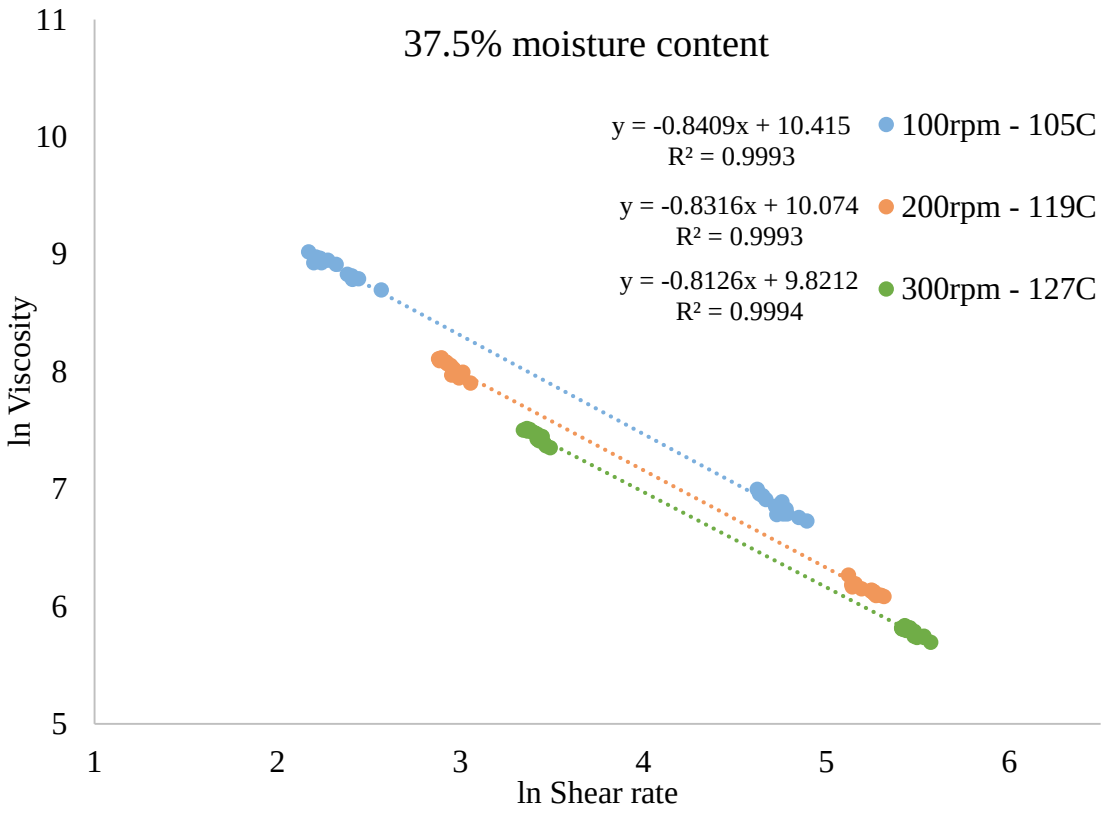

Figure 3.14. In-line viscosity vs shear rate (natural log) plots of degermed, dehulled yellow cornmeal at extruder screw speeds of 100, 200 and 300 rpm and moisture content of 37.5% (wet basis).

3.5.2.2 Effect of moisture content

The same data is plotted to see the effect of moisture content at different screw speeds in Figures 3.15, 3.16 and 3.17. Due to the differences in throughput and hence die temperature and SME, interaction effects arise in explaining the effect of moisture content. Theoretically, one would expect at a set extruder speed (and throughput), viscosity decreases with increasing moisture content, as reported by other studies (Li et al., 2004; Vergnes et al., 1993). But in this study, at 100 rpm, 32.5% moisture cornmeal has a lower viscosity compared to 35% moisture cornmeal, this can be attributed to the high die temperature (123^{o}C vs 112^{o}C) which was likely caused by low throughput (4.1 vs 5.5 kg/hr) and high SME (85 vs 67 kJ/kg) at 32.5% vs 35% moisture content.

At 200 rpm and 300 rpm, 32.5% moisture cornmeal has a lower viscosity compared to both 35% and 37.5% moisture cornmeal. Here again, the 32.5% moisture cornmeal is at higher temperature (Table 3.7), SME and lower throughput (Table 3.8) compared to the other moisture contents. Hence the interaction between moisture content and temperature terms arise in the use of a single screw extruder fed viscometer because of the variability in throughput at different moisture contents and extruder screw speeds.

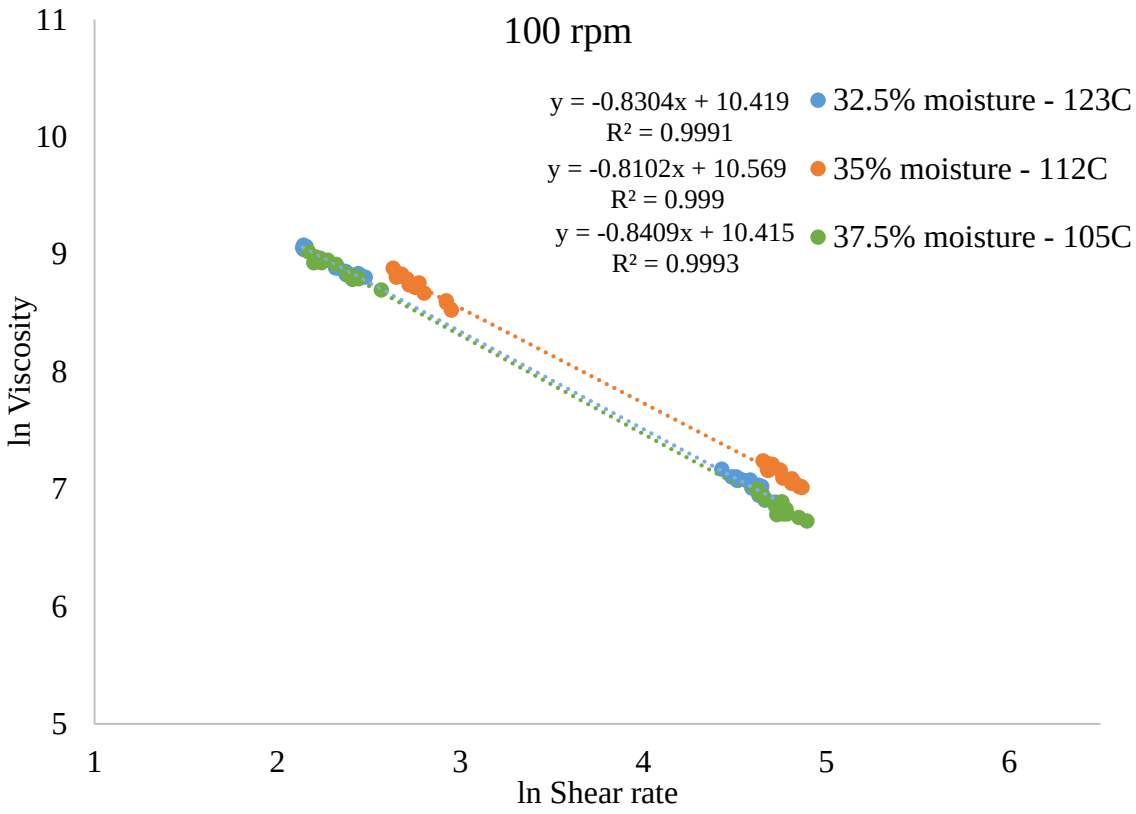

Figure 3.15. In-line viscosity vs shear rate (natural log) plots of degermed, dehulled yellow cornmeal at moisture contents of 32.5, 35 and 37.5% (wet basis) and extruder screw speed of 100 rpm.

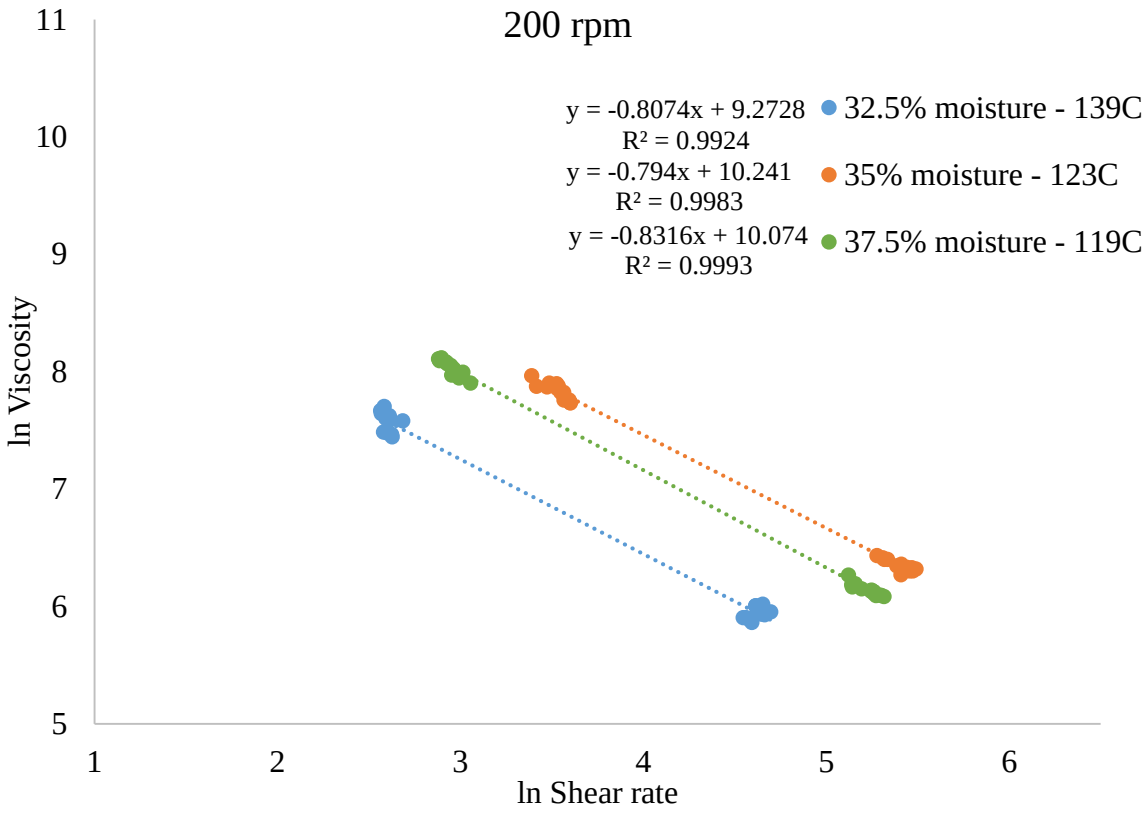

Figure 3.16. In-line viscosity vs shear rate (natural log) plots of degermed, dehulled yellow cornmeal at moisture contents of 32.5, 35 and 37.5% (wet basis) and extruder screw speed of 200 rpm.

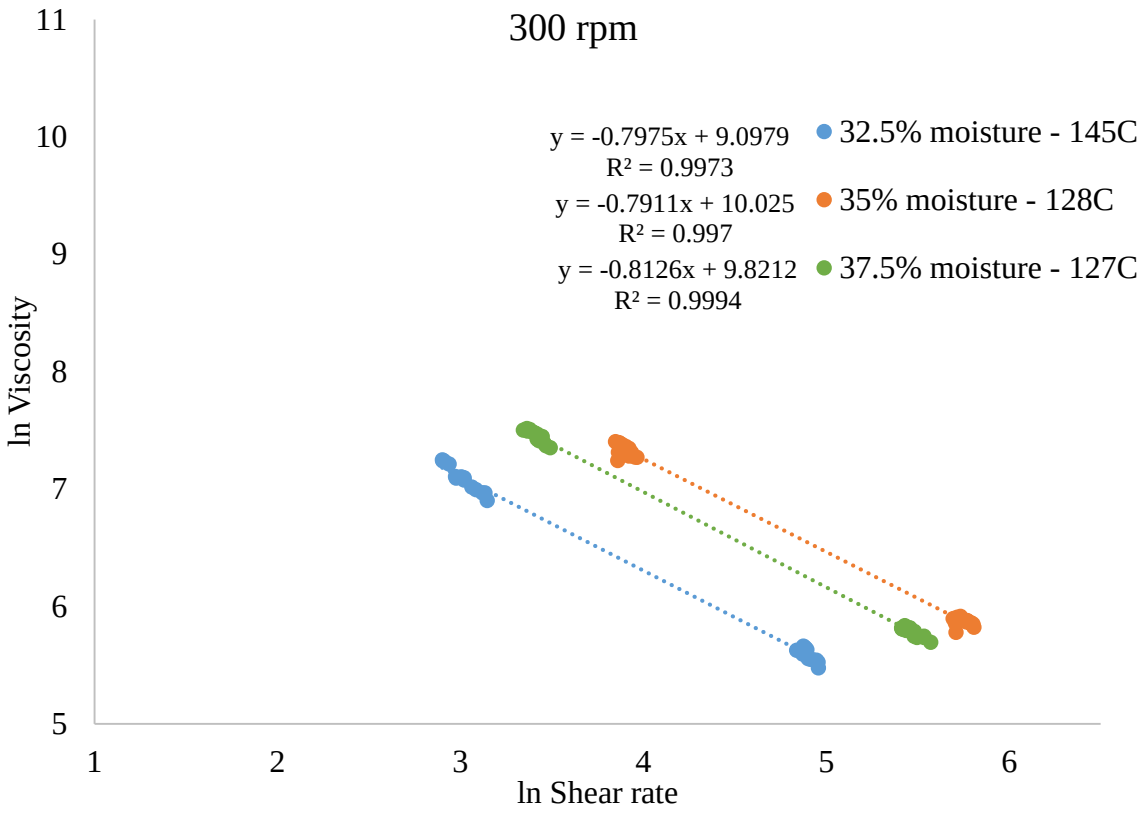

Figure 3.17. In-line viscosity vs shear rate (natural log) plots of degermed, dehulled yellow cornmeal at moisture contents of 32.5, 35 and 37.5% (wet basis) and extruder screw speed of 300 rpm.

3.5.3 Comparison of in-line versus off-line measurements

Plots comparing in-line versus off-line viscosity measurements show that in-line measurements are consistently lower compared to off-line measurements at specific moisture contents and comparable temperatures (Figures 3.18, 3.19 and 3.20). The effect of shear degradation on the viscosity of cornmeal extruded at high temperature, shear and low moisture conditions has been shown by this comparison of off-line and in-line viscosity measurements. This is in agreement with past research comparing off-line versus in-line measurements on food/biopolymers at similar extrusion conditions – high temperature, shear and low moisture conditions (Mackey and Ofoli, 1990; Senouci and Smith, 1988; Vergnes et al., 1993; Vergnes and Villemaire, 1987). Senouci and Smith (1988) compared in-line and off-line viscosity of LDPE, maize grits and potato powder at high temperature, shear and low moisture conditions. They found that viscosity data for LDPE at 200^{o}C from in-line extruder fed slit die viscometer at different screw speeds and off-line capillary rheometer at similar shear rates were in good agreement. But in the case of the maize grits (31.5% moisture wet basis) and potato powder (39.2% moisture wet basis), at 80^{o}C to 140^{o}C, the melt viscosities decreased with increasing extruder speeds, at the same temperature and moisture contents compared to the off-line capillary rheometer. This clearly showed that food/biopolymers such as maize grits and potato powder are susceptible to shear/mechanical degradation at the conditions tested and off-line techniques cannot predict (will over predict) melt viscosities in an extruder at these conditions. The current study is added evidence to these conclusions. These extrusion conditions can also be thought of as the conditions where the sum of the thermal and

mechanical energy supplied to the food/biopolymer is greater than the degradation energy of the material as visualized by Bouvier and Campanella (2014) in Figure 3.1(c).

On the contrary, de la Pena et al. (2014) while studying the effect of moisture content and formulation on pasta dough during pasta extrusion made a similar comparison of off-line capillary rheometer measurements and in-line extruder viscosity measurements and concluded that at the conditions tested in their study, there is a possibility of using a capillary rheometer to determine moisture content of a formulation before extruding pasta. The extrusion temperature in this study was 45^{o}C, at 30 to 34% moisture contents and at wall shear rates ranging between 41.6 to 90.8 s^{-1}. Pasta extrusion is a forming process where the sum of the thermal and mechanical energy supplied is lower than the degradation energy of a material and hence there is minimal degradation experienced by the material, which can be compared to the visualization by Bouvier and Campanella (2014) in Figure 3.1(a).

The results from this study show that the lack of shear degradation in a capillary rheometer, in the moisture content and temperature ranges tested, will lead to higher viscosity measurements and hence are not representative of the viscosity of a food/biopolymer material which is sensitive to shear degradation at these extrusion conditions. This research challenges the reports of several other researchers who have suggested the use of capillary rheometer as an effective off-line technique at high temperature/shear extrusion conditions for food/biopolymers (Dautant et al., 2007; Fraiha et al., 2011; Sandoval and Barreiro, 2007; Singh and Smith, 1999).

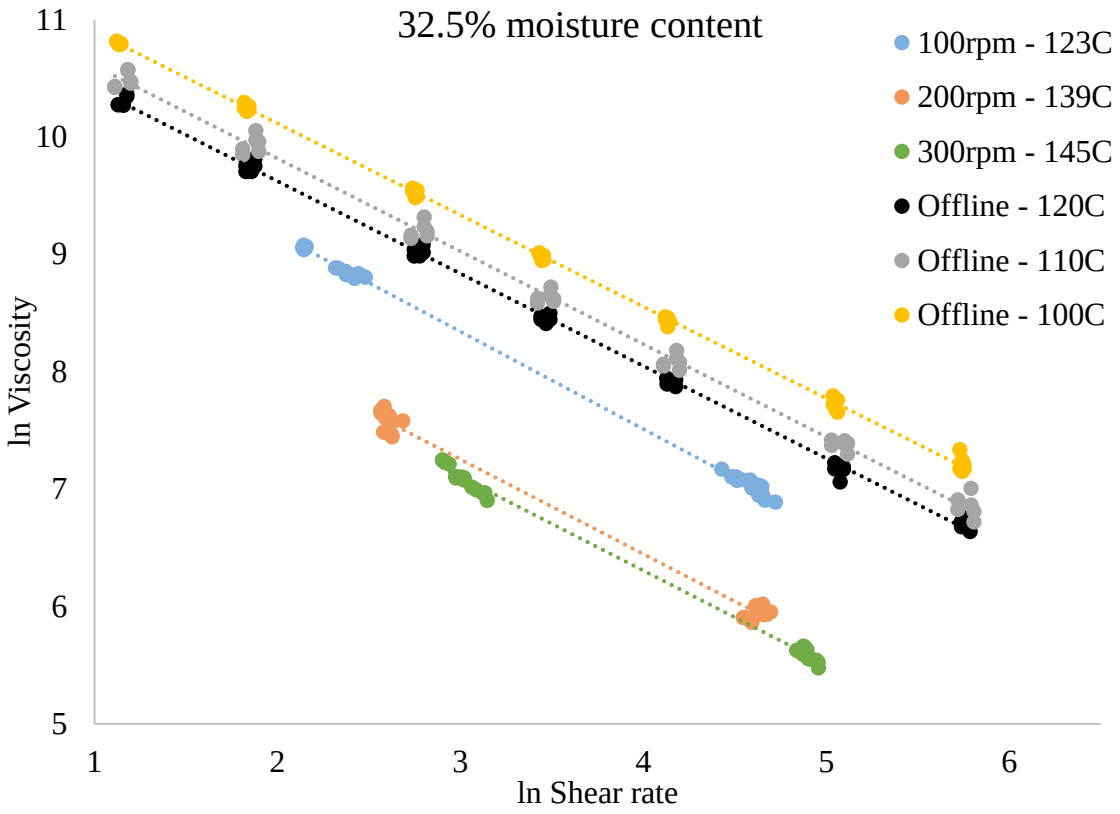

Figure 3.18. In-line vs off-line viscosity vs shear rate (natural log) plots of degermed, dehulled yellow cornmeal at extruder screw speeds of 100, 200 and 300 rpm and capillary bore wall temperatures 100, 110 and 120°C at moisture content of 32.5% (wet basis).

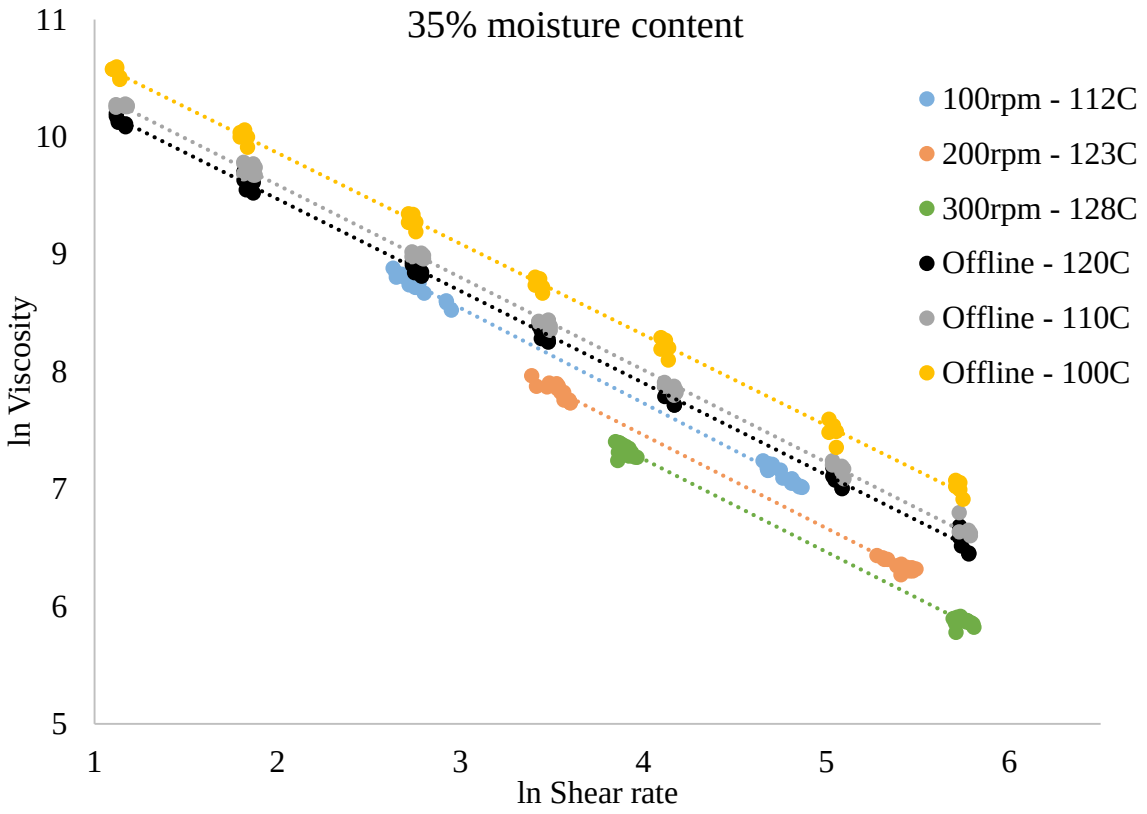

Figure 3.19. In-line vs off-line viscosity vs shear rate (natural log) plots of degermed, dehulled yellow cornmeal at extruder screw speeds of 100, 200 and 300 rpm and capillary bore wall temperatures 100, 110 and 120°C at moisture content of 35% (wet basis).

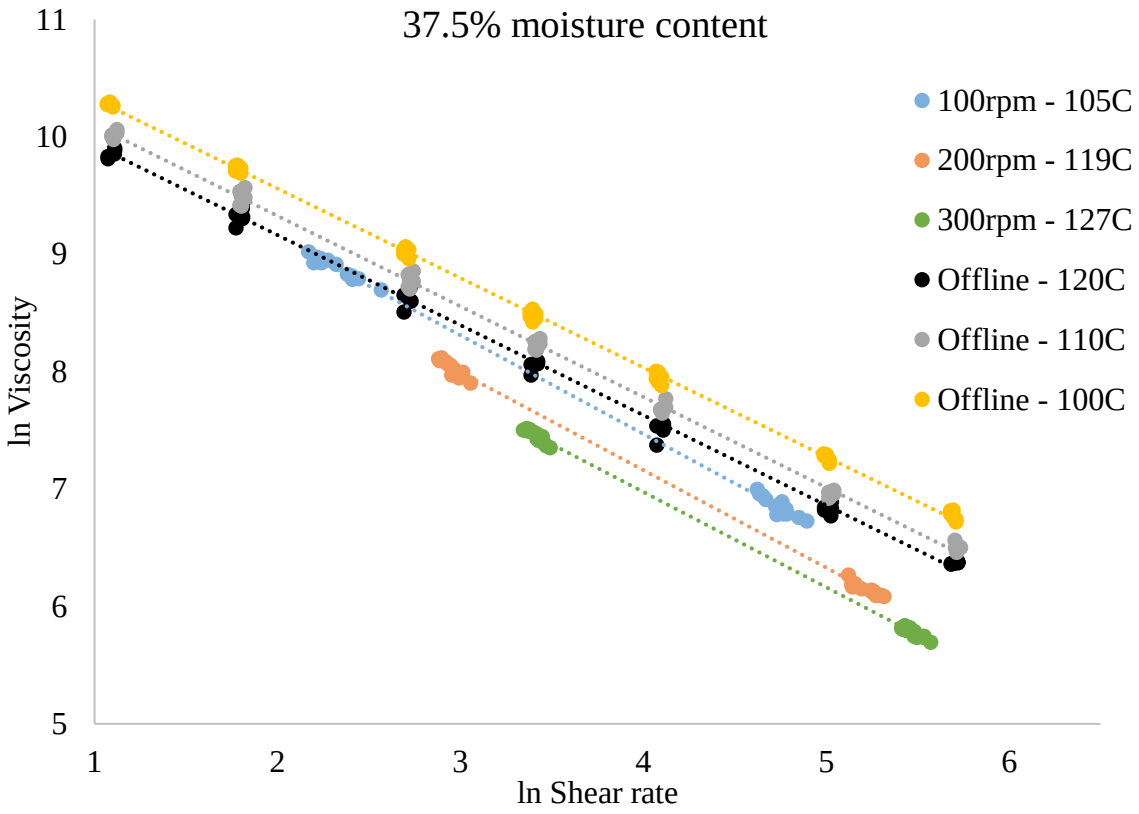

Figure 3.20. In-line vs off-line viscosity vs shear rate (natural log) plots of degermed, dehulled yellow cornmeal at extruder screw speeds of 100, 200 and 300 rpm and capillary bore wall temperatures 100, 110 and 120°C at moisture content of 37.5% (wet basis).

3.5.4 Comparison of material transformation using pasting property

RVA pasting profiles of samples collected in-line and off-line provide additional evidence to the inferences made from the viscosity data collected. But they also raise new questions which help further the understanding of the in-line and off-line techniques.

First, looking at the effect of the extrusion conditions on the in-line viscosity measurements, similar to the inference made on the effect of screw speed, at a given moisture content, with increase in screw speed (and therefore temperature and SME), the final viscosity of the paste decreases (Figures 3.21, 3.22 and 3.23). This is in agreement with results reported in literature studying the effect of extrusion conditions using pasting property (Al-Rabadi et al., 2011; Bouvier and Campanella, 2014; Moussa et al., 2011) or other techniques such as, size exclusion chromatography (DellaValle et al., 1996; Liu et al., 2010; Moussa et al., 2011), intrinsic viscosity (Vergnes et al., 1993) and microscopy (Al-Rabadi et al., 2011; Moussa et al., 2011).

Second, no research has been reported on comparing the material transformation between in-line and off-line viscosity measurement techniques. In this study based on literature, the initial hypothesis for the pasting property study was that the off-line capillary rheometer samples would have higher final viscosities compared to the in-line samples, because the off-line samples did not have any mechanical degradation. But from figures 3.21, 3.22 and 3.23, it can be seen that the pasting profiles of the off-line samples collected at the different moisture contents (at 120^{o}C and 100 s^{-1} pseudo wall shear rate) consistently have the lowest final viscosity. This can be attributed to difference in the amount of thermal energy received by the samples during in-line versus off-line

measurements. The residence time in an extruder is typically under a minute (Harper, 1981; Mercier et al., 1989), whereas in the case of the capillary rheometer there was a 3 minute sample loading time and an added 10 minute equilibration time at the temperature at which viscosity measurements were made. Hence, the off-line samples received significantly higher thermal energy due to the increased residence time in the capillary rheometer and this can explain low final viscosities in the RVA pasting profiles.

However, the off-line melt viscosities of corn meal were higher than in-line measurements (figures 3.18, 3.19 and 3.20). While measuring viscosities of corn starch with an off-line pre-shearing rheometer called a Rheoplast, Vergnes and Villemaire (1987) noted that the disruption of starch granules increases the melt viscosity whereas the depolymerization of the molecules decreases it. This observation can be used to interpret the results from the current study. In the capillary rheometer, the material is receiving excessive thermal energy which only disrupts the starch granule and not depolymerize it, hence the higher melt viscosities. Whereas, in the extruder, there is higher mechanical energy which depolymerizes the starch molecules and hence result in a lower melt viscosity.

This inference however must be confirmed with an appropriate analytical method to quantify molecular weight change, such as size exclusion chromatography, between the two techniques to validate it.

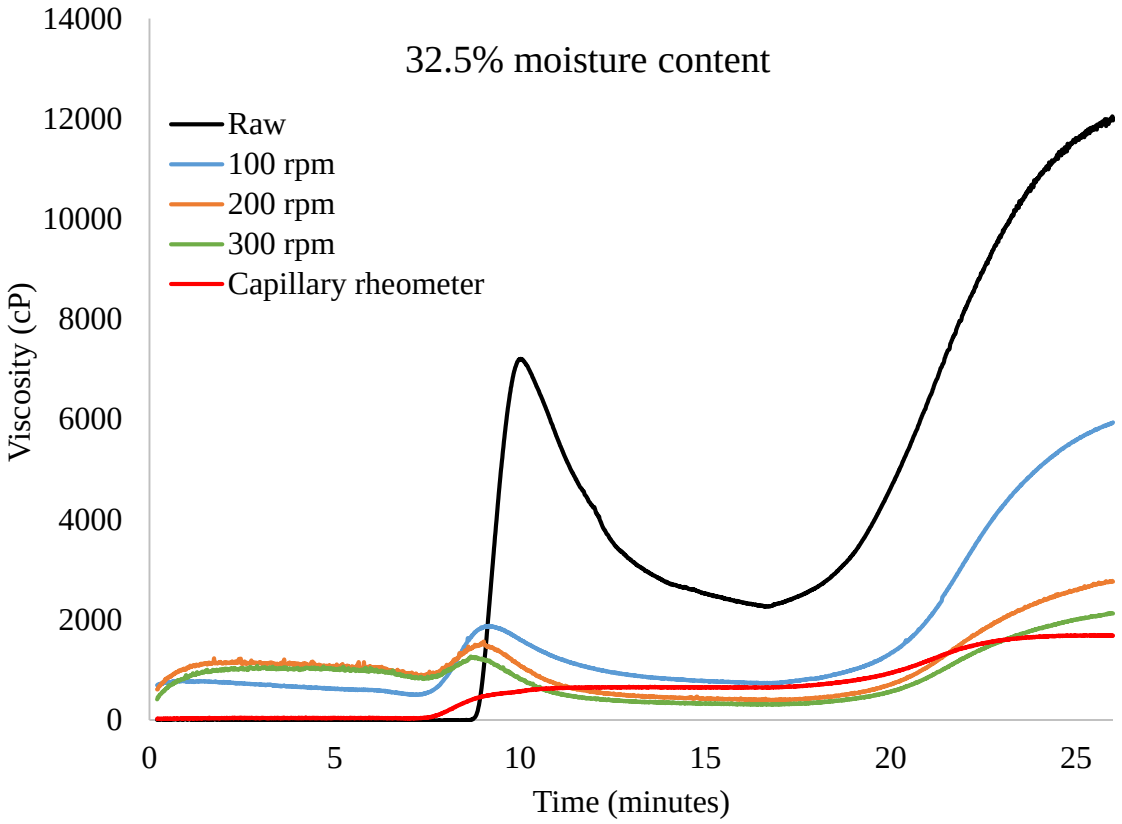

Figure 3.21. RVA pasting profiles of dried, sieved extrudate of degermed, dehulled yellow cornmeal, raw, collected in-line at extruder screw speeds of 100, 200 and 300 rpm and collected off-line at 120ºC capillary bore wall temperature and 100 s^{-1} pseudo wall shear rate, at 32.5% moisture content.

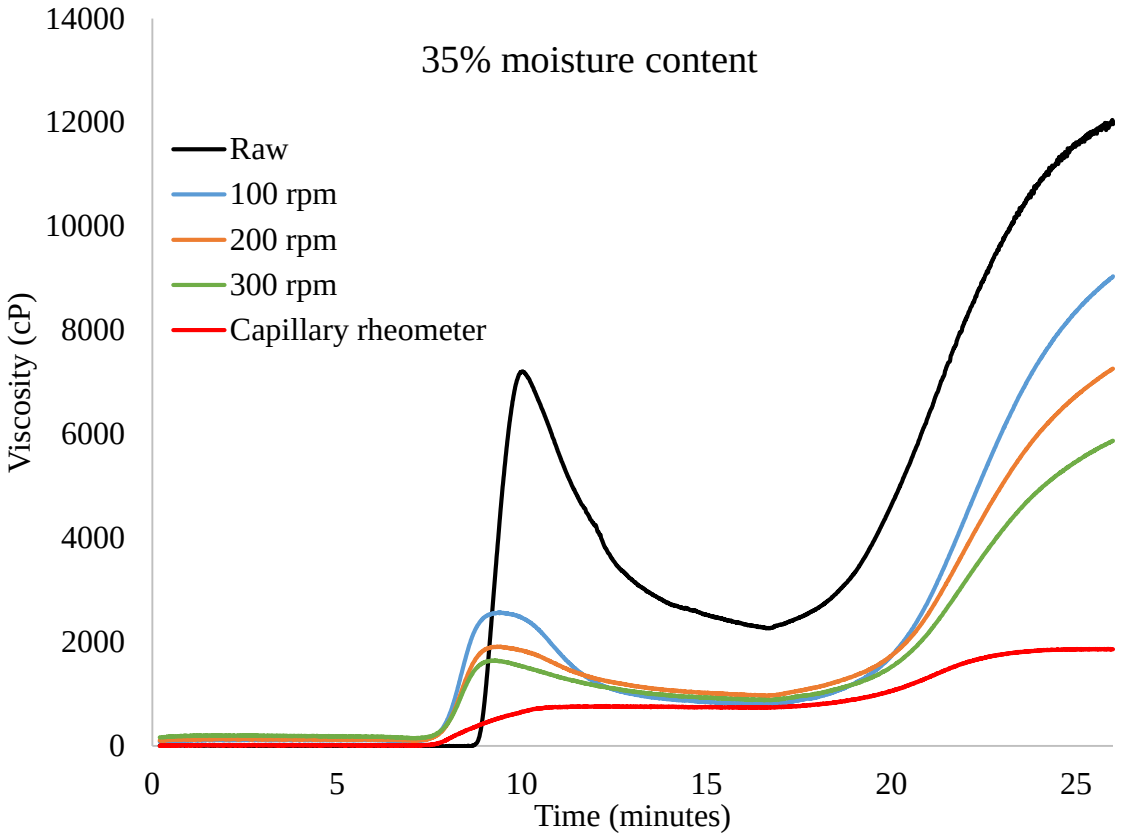

Figure 3.22. RVA pasting profiles of dried, sieved extrudate of degermed, dehulled yellow cornmeal, raw, collected in-line at extruder screw speeds of 100, 200 and 300 rpm and collected off-line at 120ºC capillary bore wall temperature and 100 s^{-1} pseudo wall shear rate, at 35% moisture content.

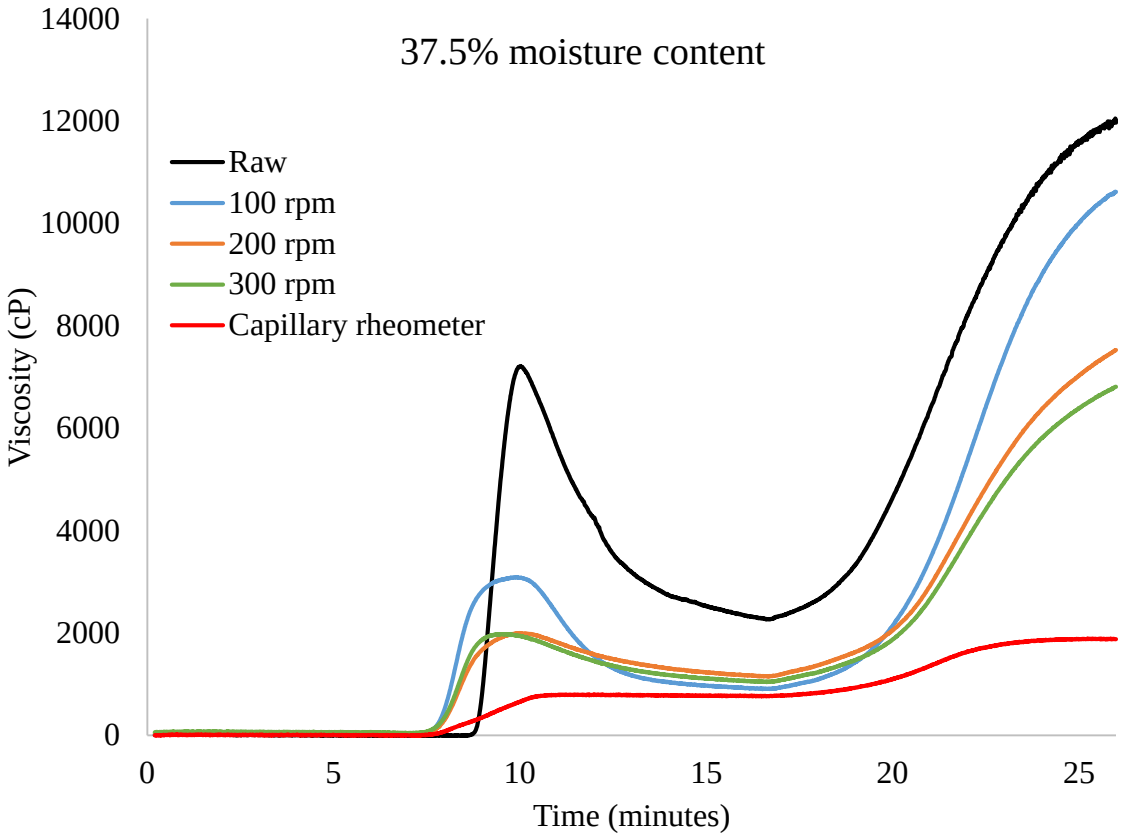

Figure 3.23. RVA pasting profiles of dried, sieved extrudate of degermed, dehulled yellow cornmeal, raw, collected in-line at extruder screw speeds of 100, 200 and 300 rpm and collected off-line at 120ºC capillary bore wall temperature and 100 s^{-1} pseudo wall shear rate, at 37.5% moisture content.

3.5.5 Challenges observed

Even though this study successfully showed that off-line measurements are over-predicting melt viscosities due to the lack of shear degradation, by comparing with a unique two-opening die in-line viscosity measurement technique for a small-scale extruder, there are some challenges observed with the in-line measurement technique.

In order to explain these challenges and solely for the purpose of comparison with viscosity models for corn meals/maize grits from the literature, the in-line data from the current study is modeled using Eq. 3.8 which uses SME to account for shear history in the extruder. The model parameters by fitting the data in Eq. 3.8 are listed in table 3.9.

Table 3.9. Estimated values of parameters using multiple linear regression for the power law viscosity model represented by Eq. 3.8 for in-line viscosity of degermed dehulled yellow corn flour.

	K_o	**E_a/R**	**a**	**b**	**n**
Degermed dehulled yellow corn	-0.888	4942	0.0406	0.0023	0.23

K_o in Pa. s^n

E_a/R in K

a in $\%^{-1}$

b in kg/kJ

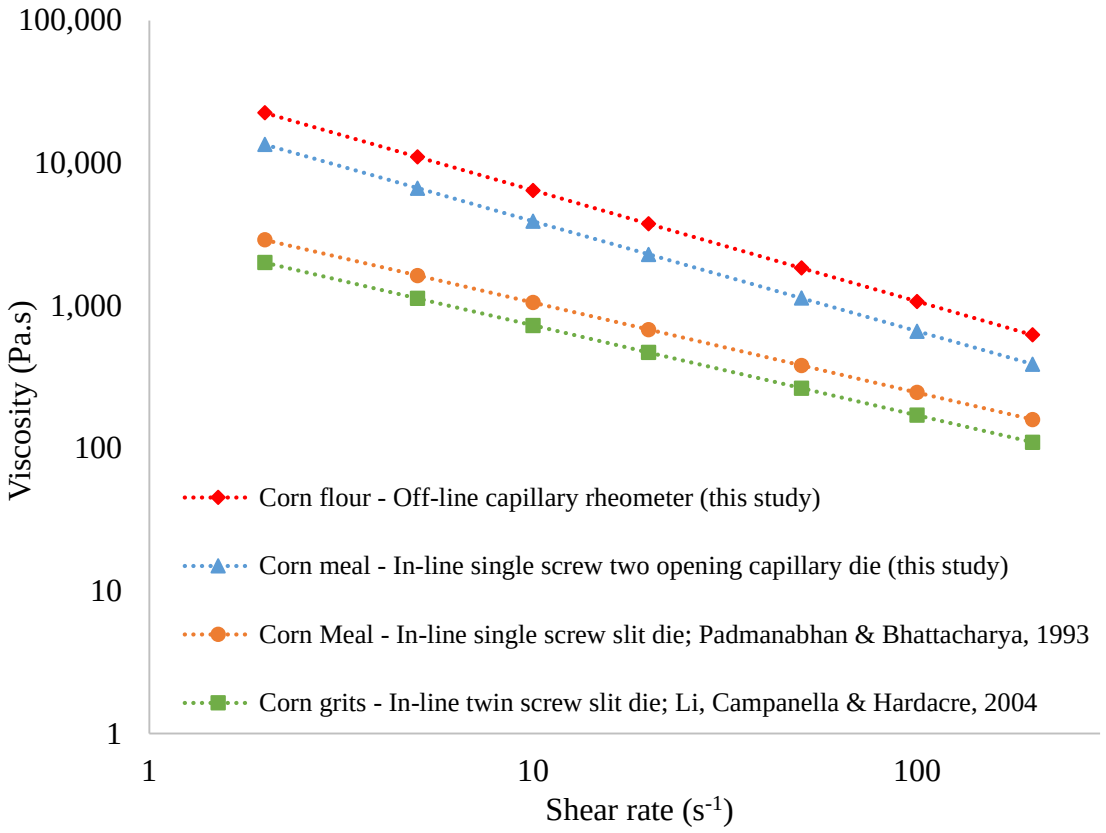

Figure 3.24. Comparison of off-line and in-line power law viscosity models of cornmeal from current study with in-line models reported for corn meal and grits by Padmanabhan and Bhattacharya (1993) and Li et al. (2004), respectively, at a reference temperature of 120^{o}C, 35% moisture content and 100 kJ/kg SME (where applicable).

On comparing the in-line power law viscosity model which accounts for the effect of temperature, moisture content, and SME on the consistency index from the current study with similar in-line models reported in literature (Li et al., 2004; Padmanabhan and Bhattacharya, 1993), it can be noted that model in the current study is over predicting viscosity by almost an order of magnitude, provided the difference in raw material and test conditions used in these studies. This is important to understand, because the melt

viscosity is a key parameter to quantify viscous dissipation in a mechanistic model for the extruder and if the melt viscosity is over predicted then this would lead to erroneous viscous dissipation calculations.

On further analyzing the technique used for measuring in-line viscosity in this study, two key observations were made. First, the consistent temperature difference between the large and small die measurements indicate that there is significant product cooling at the die and this will certainly influence flow rate and hence viscosity calculation. Secondly, using the two-opening die setup, there is no way to account for Bagley correction to correct for entrance and exit effects and this can have also have a significant effect on viscosity calculations. In order to address these challenges a new setup has to be designed to correct for both these challenges observed for in-line viscosity measurement on the small-scale extruder.

3.6 Conclusion

Melt viscosity of degermed, dehulled yellow corn meal was quantified using an off-line capillary rheometer technique and a novel in-line technique where a two-opening die was used in the small-scale single screw extruder. Corn meal melt followed a pseudoplactic behavior at all the conditions test and viscosity decreased with increase in temperature and moisture content in both the techniques as reported in literature. Increased screw speed reduced viscosity due to increase in temperature at given moisture content in the in-line technique. Whereas interaction effects arose while inferring the effect of moisture content at a given screw speed, which was attributed to the variation in throughput and specific mechanical energy between the different conditions tested. Comparison of off-

line versus in-line measurements consistently revealed that off-line measurements were over predicting viscosity, as reported in literature. Hence this challenges the use of an off-line capillary rheometer technique to quantify melt viscosity of a food/biopolymer material which is sensitive to shear degradation at the high temperature, shear and low moisture conditions tested. Pasting properties of extrudates were successfully used to show the effect of extrusion conditions on the material during in-line viscosity measurements. But comparison of pasting properties of in-line versus off-line technique samples revealed interesting observations, which needs to be followed up with further analysis of samples. Furthermore, comparison of power law viscosity model built from in-line measurements in the current study with models reported in literature reveals that the model in the current study is over predicting viscosity by almost an order of magnitude and this need to be addressed by taking appropriate measures in future studies.

3.7 References

Al-Rabadi, G.J., Torley, P.J., Williams, B.A., Bryden, W.L., Gidley, M.J., (2011). Particle size of milled barley and sorghum and physico-chemical properties of grain following extrusion. Journal of Food Engineering. 103(4), 464-472.

Bagley, E.B., (1957). End corrections in the capillary flow of polyethylene. Journal of Applied Physics. 28(5), 624-627.

Bird, R.B., Armstrong, R.C., Hassager, O., (1987). *Dynamics of polymeric liquids: Volume 1 - Fluid Mechanics*. John Wiley & Sons, New York, USA.

Bouvier, J., Campanella, O.H., (2014). *Extrusion processing technology: food and non-food biomaterials*. John Wiley & Sons, Ltd, West Sussex, UK.

Cervone, N.W., Harper, J.M., (1978). Viscosity of an intermediate moisture dough. Journal of Food Process Engineering. 2(1), 83-95.

Colonna, P., Doublier, J., Melcion, J., Monredon, F.D., Mercier, C., (1984). Extrusion cooking and drum drying of wheat starch. I. Physical and macromolecular modifications. Cereal chemistry (USA).

Dautant, F.J., Simancas, K., Sandoval, A.J., Muller, A.J., (2007). Effect of temperature, moisture and lipid content on the rheological properties of rice flour. Journal of Food Engineering. 78(4), 1159-1166.

de la Pena, E., Manthey, F.A., Patel, B.K., Campanella, O.H., (2014). Rheological properties of pasta dough during pasta extrusion: Effect of moisture and dough formulation. Journal of Cereal Science. 60(2), 346-351.

DellaValle, G., Colonna, P., Patria, A., Vergnes, B., (1996). Influence of amylose content on the viscous behavior of low hydrated molten starches. Journal of Rheology. 40(3), 347-362.

Donovan, J.W., (1979). Phase-transitions of the starch-water system. Biopolymers. 18(2), 263-275.

Doublier, J., Colonna, P., Mercier, C., (1986). Extrusion cooking and drum drying of wheat starch. II. Rheological characterization of starch pastes. Cereal Chem. 63(3), 240-246.

Drozdek, K.D., Faller, J.F., (2002). Use of a dual orifice die for on-line extruder measurement of flow behavior index in starchy foods. Journal of Food Engineering. 55(1), 79-88.

Fletcher, S., McMaster, T., Richmond, P., Smith, A., (1985). Rheology and extrusion of maize grits. Chemical Engineering Communications. 32(1-5), 239-262.

Fraiha, M., Biagi, J.D., Ferraz, A.C.d.O., (2011). Rheological behavior of corn and soy mix as feed ingredients. Food Science and Technology (Campinas). 31(1), 129-134.

Guha, M., Ali, S.Z., Bhattacharya, S., (1998). Effect of barrel temperature and screw speed on rapid viscoanalyser pasting behaviour of rice extrudate. International Journal of Food Science & Technology. 33(3), 259-266.

Halliday, P.J., Smith, A.C., (1995). Estimation of wall slip velocity in the capillary-flow of potato granule pastes. Journal of Rheology. 39(1), 139-149.

Harper, J., Rhodes, T.P., Wanninger, L., (1971). Viscosity model for cooked cereal doughs, *Chemical Engineering Progress Symposium Series*, pp. 40-43.

Harper, J.M., (1981). *Extrusion of foods: Volume I*. CRC Press, Boca Raton, Florida.

Jao, Y., Chen, A., Lewandowski, D., Irwin, W., (1978). Engineering analysis of soy dough rheology in extrusion. Journal of Food Process Engineering. 2(1), 97-112.

Lai, L.S., Kokini, J.L., (1990). The effect of extrusion operating-conditions on the online apparent viscosity of 98-percent amylopectin Amioca) and 70-percent amylose (Hylon 7) corn starches during extrusion. Journal of Rheology. 34(8), 1245-1266.

Lai, L.S., Kokini, J.L., (1991). Physicochemical changes and rheological properties of starch during extrusion. Biotechnology Progress. 7(3), 251-266.

Li, P.X., Campanella, O.H., Hardacre, A.K., (2004). Using an in-line slit-die viscometer to study the effects of extrusion parameters on corn melt rheology. Cereal Chemistry. 81(1), 70-76.

Liu, W.-C., Halley, P.J., Gilbert, R.G., (2010). Mechanism of degradation of starch, a highly branched polymer, during extrusion. Macromolecules. 43(6), 2855-2864.

Mackey, K.L., Ofoli, R.Y., (1990). Rheological modeling of corn starch doughs at low to intermediate moisture. Journal of Food Science. 55(2), 417-423.

Martin, O., Averous, L., Della Valle, G., (2003). In-line determination of plasticized wheat starch viscoelastic behavior: impact of processing. Carbohydrate Polymers. 53(2), 169-182.

Mercier, C., Linko, P., Harper, J.M., (1989). *Extrusion cooking*. American Association of Cereal Chemists, Inc., St. Paul, Minnesota, USA.

Morrison, F.A., (2001). *Understanding rheology*. Oxford University Press, Inc., New York, USA.

Moussa, M., Qin, X., Chen, L.F., Campanella, O.H., Hamaker, B.R., (2011). High-quality instant sorghum porridge flours for the West African market using continuous processor cooking. International Journal of Food Science & Technology. 46(11), 2344-2350.

Núñez, M., Della Valle, G., Sandoval, A.J., (2010). Shear and elongational viscosities of a complex starchy formulation for extrusion cooking. Food research international. 43(8), 2093-2100.

Padmanabhan, M., Bhattacharya, M., (1993). Effect of extrusion processing history on the rheology of corn meal. Journal of Food Engineering. 18(4), 335-349.

Robin, F., Bovet, N., Pineau, N., Schuchmann, H.P., Palzer, S., (2011). Online shear viscosity measurement of starchy melts enriched in wheat bran. Journal of Food Science. 76(5), E405-E412.

Robin, F., Engmann, J., Tomasi, D., Breton, O., Parker, R., Schuchmann, H.P., Palzer, S., (2010). Adjustable Twin-Slit Rheometer for Shear Viscosity Measurement of Extruded Complex Starchy Melts. Chemical Engineering & Technology. 33(10), 1672-1678.

Sandoval, A.J., Barreiro, J.A., (2007). Off-line capillary rheometry of corn starch: Effects of temperature, moisture content and shear rate. Lwt-Food Science and Technology. 40(1), 43-48.

Senouci, A., Smith, A.C., (1988). An experimental study of food melt rheology. I. Shear viscosity using a slit die viscometer and a capillary rheometer. Rheologica Acta. 27(5), 546-554.

Singh, N., Smith, A.C., (1999). Rheological behaviour of different cereals using capillary rheometry. Journal of Food Engineering. 39(2), 203-209.

Vergnes, B., DellaValle, G., Tayeb, J., (1993). A specific slit die rheometer for extruded starchy products - Design, validation and application to maize starch. Rheologica Acta. 32(5), 465-476.

Vergnes, B., Villemaire, J.P., (1987). Rheological behavior of low moisture molten maize starch. Rheologica Acta. 26(6), 570-576.

Wang, J., Yu, L., Xie, F., Chen, L., Li, X., Liu, H., (2010). Rheological properties and phase transition of cornstarches with different amylose/amylopectin ratios under shear stress. Starch-Stärke. 62(12), 667-675.

Wang, S., Bouvier, J., Gelus, M., (1990). Rheological behaviour of wheat flour dough in twin-screw extrusion cooking. International Journal of Food Science & Technology. 25(2), 129-139.

Wen, L.-F., Rodis, P., Wasserman, B., (1990). Starch fragmentation and protein insolubilization during twin-screw extrusion of corn meal. Cereal Chemistry. 67(3), 268-275.

Xie, F.W., Halley, P.J., Averous, L., (2012). Rheology to understand and optimize processibility, structures and properties of starch polymeric materials. Progress in Polymer Science. 37(4), 595-623.

CHAPTER 4. MECHANISTIC MODEL FOR A SMALL-SCALE SINGLE SCREW EXTRUDER WITH RESTRICTIONS ON THE SCREW

4.1 Introduction

Modeling extrusion process is critical in understanding the fundamental operation and behavior of the process using basic engineering and scientific principles. It also allows for improving productivity, making modifications to the process based on change in raw material formulation, designing optimal equipment for specific purposes and scaling-up or scaling-down processes (Harper, 1981).

4.2 Literature review

Modeling the food extrusion process, similar to rheological techniques, was based on the models developed from the plastic industry (Carley et al., 1953; Carley and Strub, 1953). Although there are similarities between food and polymer extrusion, there are also vast differences in terms of material behavior. The heterogeneity of the food/biopolymer matrix creates complications in accurately quantifying their rheological properties during extrusion conditions since their components go through various physiochemical and biochemical changes such as starch gelatinization and protein degradation. Hence modeling food extrusion is much more complex compared to plastics extrusion (Harper, 1981).

The basic mechanistic model for a single screw extruder is that of the metering section where the screw is considered as a long continuous channel peeled off the screw root and approximating it to a two dimensional plane Couette flow (Figure 4.1).

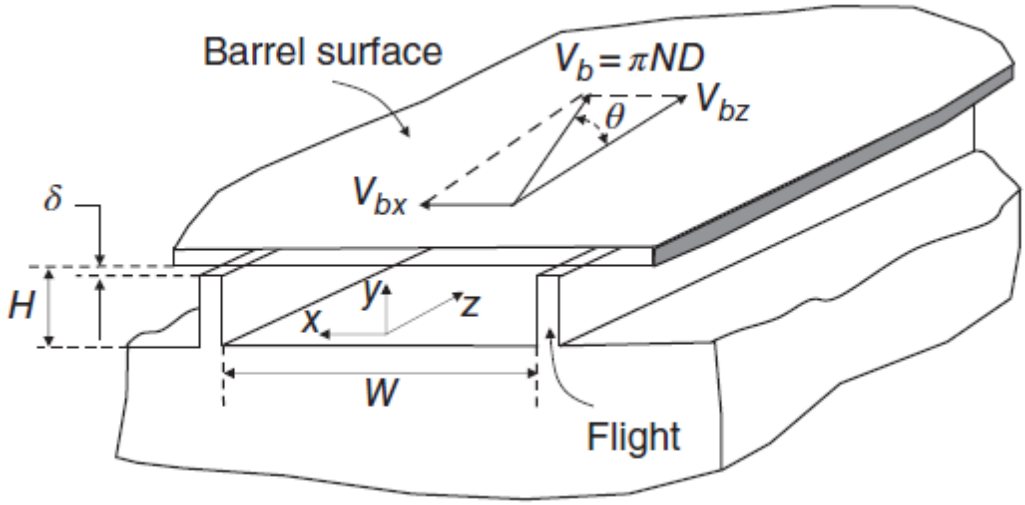

Figure 4.1. Unwound channel of a single screw extruder indicating main geometric characteristics and velocity components from Bouvier and Campanella (2014) originally reported by Tadmor and Klein (1970).

Velocity profiles in the screw channel, operating characteristics of the extruder such as flow rate and pressure build-up at the die, leakage flow due to clearance between the barrel and screw channel, presence of barrel grooves and tapered channels in specialized extruders have been accounted for by this approach, for Newtonian fluids. In the case of non-Newtonian fluids, complications arise in the solution of the equation of motion, hence often, they are carefully approximated as Newtonian within certain defined conditions and assumptions (Harmann and Harper, 1974; Harper, 1981; Li and Hsieh, 1996; Tsao et al., 1978). In the case of foods/biopolymers, during extrusion processing,

they undergo a structural transformation in a short period of time. Hence, along with the non-Newtonian behavior, the raw material undergo various transformations such as starch gelatinization or melting, protein degradation, binding of macromolecules and other such transformations which complicate modeling their behavior under various extrusion conditions. Advanced modeling techniques such as finite element methods have been used to model single screw extruders to account for some these material transformations (Wang et al., 2004). LeRoux et al. (1995) modeled pasta extrusion in a single screw extruder by using a combination of a modified analytical single screw extruder model and finite element methods. Numerous other approaches to account for the aforementioned challenges with food/biopolymer extrusion modeling have been documented in several texts (Bouvier and Campanella, 2014; Kokini et al., 1992; Mercier et al., 1989).

4.3 Objective

Harper (1979) documented the several designs of the screws used in single screw extruders (Figure 4.2). In the first four designs, the screw is a continuous channels whereas in the last design (Figure 4.2, 5) the screw channel is interrupted by multiple restrictions perpendicular the direction of flow.

All the models built thus far for single screw extruders consider the screw as a continuous channel. But there is a lack of literature in analytical modelling for single screw extruders with restrictions on the screw, such as the small scale extruder being currently studied (Figure 1.1). Hence the objective of this study is to develop a simple analytical model to simulate the flow through such an extruder.

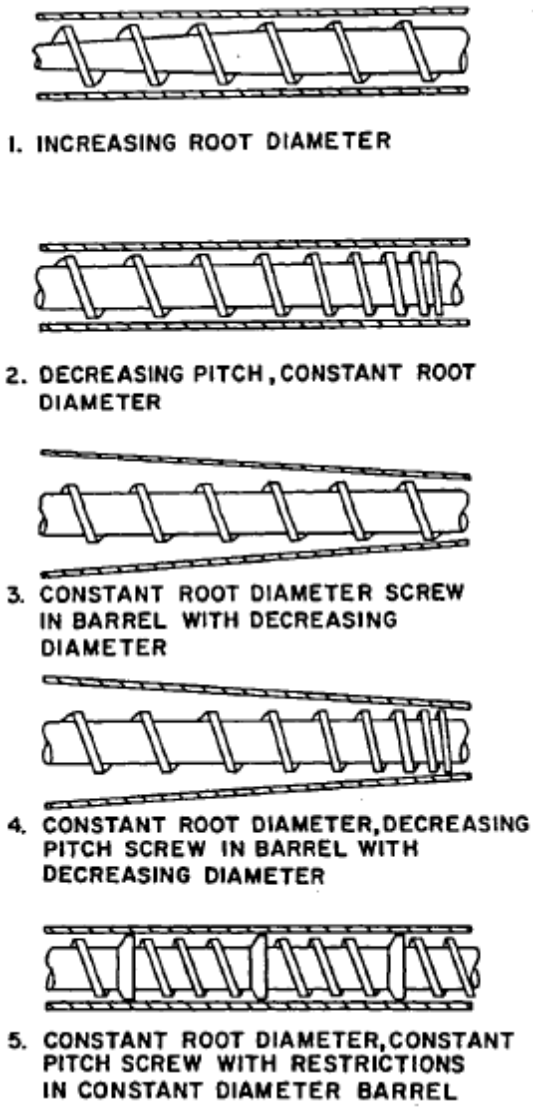

Figure 4.2. Various configurations of screw and barrel to achieve compression in single screw extruders from Harper (1979).

The small scale extruder in the current study was designed to be a high shear extruder. Hence the depth to width ratio of the double flight screw sections is high comparable to most single screw extruder models that have been developed. Couette flow of a fluid, where a fluid flows between two plates - one moving and one stationary, has been the

most simple and common setup that has been used for developing mechanistic models for single screw extruders. In the past, researchers have looked at several cases of Couette flow, for Newtonian and non-Newtonian fluids. But there is limited research on viscous dissipation in Couette flow of Newtonian and non-Newtonian fluid with and without heat fluxes at either one of the plates (Aydin and Avci, 2006; Mondal and Mukherjee, 2014; Sheela-Francisca and Tso, 2012; Sheela-Francisca et al., 2012). All the researchers have also considered a simple geometry of infinitely long parallel plates with a uniform gap between the plates. This study looks at a special geometry to account for the restrictions on the screw of the small scale extruder being studied, by considering two different gaps between the plates. Also, constant but different heat fluxes are considered at both the plates. The mass, momentum and energy equations are solved to find expressions for velocity and temperature profiles for the flow of a Newtonian fluid.

4.4 Analysis

For developing a simple analytical model for one screw section followed by a restriction (shear bushing) and a die in the extruder, a one-dimensional Couette flow of a Newtonian fluid between parallel plates consisting of two regions with two different gaps (step change in gap) between the plates, with back pressure from the die, is considered, as shown in Figure 4.3.

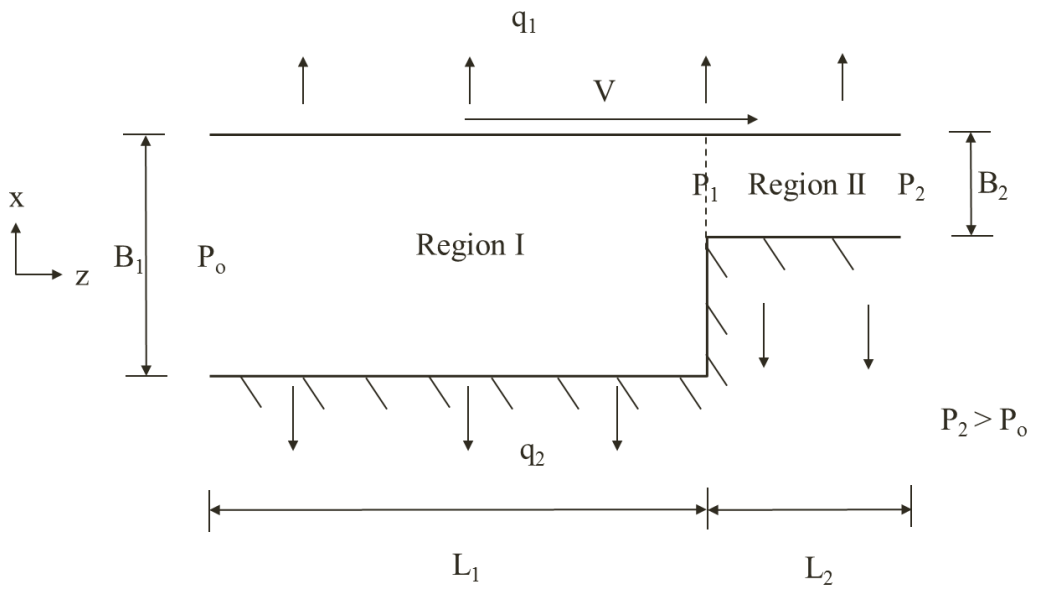

Figure 4.3. Couette flow setup between parallel plates with a step change in gap.

The distance between the parallel plates is B_1 and B_2 in region I and region II respectively with lengths L_1 and L_2, in an x-z coordinate system chosen as shown. The variation in gap is based only on the geometry of the bottom plate (screw), which is fixed. The top plate (barrel) is considered as infinitely long and moving at a constant velocity V.

The flow through the plates is assumed to be fully developed both hydro-dynamically and thermally, with a negligible transition region at the entrance of region I. The temperature of the fluid entering region I is assumed to be T_o. The apparent viscosity of the fluid is assumed to be constant within the region but not between the regions. Fluid properties including thermal conductivity, specific heat and density are assumed to be constant between the two regions. Both the top and bottom plates are kept at constant but different heat fluxes, q_1 and q_2, respectively.

In order to understand the effect of viscous dissipation on the flow through this setup, the momentum and energy equations are solved individually for the two regions, using dimensionless analysis. Mass and energy balance at the interface of the two regions and overall mass and energy balance for the system is used to find unknowns and hence the velocity and temperature profiles.

4.4.1 Velocity profile

In region I, considering one dimensional flow, the equation of continuity simplifies to:

$$\frac{dV_z^{\,I}}{dz} = 0 \tag{4.1}$$

Based on the assumptions made and equation (4.1), the momentum equation in the z-direction simplifies to,

$$0 = -\frac{dp}{dz} + \mu_1\left(\frac{d^2V_z^{\,I}}{dx^2}\right) \tag{4.2}$$

Using the dimensionless terms,

$$V_z^{\,*\,I} = \frac{V_z^{\,I}}{V} \qquad\qquad x^* = \frac{x}{B_1}$$

and defining, $\frac{dp}{dz} = \frac{P_1 - P_o}{L_1} = \frac{\Delta P_1}{L_1}$, where ΔP_1 is positive since $P_1 > P_o$, due to back pressure from the die

Equation (4.2) simplifies to,

$$\frac{d^2V_z^{*I}}{dx^{*2}} = \frac{\Delta P_1 B_1^2}{L_1 \mu_1 V} \tag{4.3}$$

Now, introducing a dimensionless term,

$$\Lambda_1 = \frac{\Delta P_1 B_1^2}{L_1 \mu_1 V}$$

and applying the boundary conditions, at $x^* = 0$; $V_z^{*I} = 0$ and at $x^* = 1$; $V_z^{*I} = 1$, the velocity profile (V_z^{*I}) for region I is solved from equation (4.3) as,

$$\boxed{V_z^{*I} = \frac{\Lambda_1}{2} x^{*2} + \left(1 - \frac{\Lambda_1}{2}\right) x^*} \tag{4.4}$$

Similarly for region II, introducing the dimensionless terms,

$$V_z^{*II} = \frac{V_z^{II}}{V} \quad \text{and} \quad \Lambda_2 = \frac{\Delta P_2 B_1^2}{L_2 \mu_2 V}$$

defining, $\frac{dp}{dz} = \frac{P_2 - P_1}{L_2} = \frac{\Delta P_2}{L_2}$ where ΔP_2 is positive since $P_2 > P_1$, due to back pressure from the die and applying the boundary conditions, at $x^* = 0$; $V_z^{*II} = 0$ and at $x^* = B_2/B_1$; $V_z^{*II} = 1$, the velocity profile (V_z^{*II}) for region II is solved as,

$$\boxed{V_z^{*II} = \frac{\Lambda_2}{2} x^{*2} + \left(\frac{B_1}{B_2}\right)\left(1 - \frac{\Lambda_{12}}{2} \cdot \left(\frac{B_2}{B_1}\right)\right) x^*} \tag{4.5}$$

To solve for the velocity profile, Λ_1 and Λ_2 are needed. The relationship between Λ_1 and Λ_2 is given by,

$\Lambda_1 = \Lambda_2(\frac{\Delta P_2}{\Delta P_1})(\frac{L_1}{L_2})(\frac{\mu_1}{\mu_2})$, where μ_1 and μ_2 are the apparent viscosities in region I and II respectively

To solve for Λ_1 and Λ_2, two conditions are imposed,

a. Total pressure difference across the two regions ($\Delta P = P_2 - P_o$) is equal to the sum of the pressure differences (ΔP_1 and ΔP_2) across the individual regions. Substituting the dimensionless terms, we get,

$$\Lambda = \Lambda_1 + \Lambda_2(\frac{L_2}{L_1})(\frac{\mu_2}{\mu_1}) \tag{4.6}$$

where, $\Lambda = \frac{\Delta P {B_1}^2}{L_1 \mu_1 V}$

b. Mass balance at the interface of region I and II, indicating an equal volumetric flow through the two regions gives,

$$\frac{1}{2} - \frac{\Lambda_1}{12} = \frac{1}{2}\left(\frac{B_2}{B_1}\right) - \frac{\Lambda_2}{12}\left(\frac{B_2}{B_1}\right)^3 \tag{4.7}$$

With known die characteristics, volumetric flow rate and fluid viscosity at the die, the total ΔP can be determined and hence Λ. From equations 4.6 & 4.7 Λ_1 and Λ_2 are calculated. And the velocity profiles of the individual regions are obtained from equations 4.4 & 4.5.

4.4.2 Temperature profile

Based on the one-dimensional flow assumption made, the energy equation with the viscous dissipation term for a Newtonian fluid in region I simplifies to,

$$\rho_1 c_{p1} V_z{}^{I} \frac{\delta T_1}{\delta z} = \frac{k_1 \delta^2 T_1}{\delta x^2} + \mu_1 \left(\frac{\delta V_z{}^{1}}{\delta x} \right)^2 \tag{4.8}$$

Due the inclusion of the viscous dissipation term, the temperature gradient in the z direction is included in the energy equation, but assumed to be an unknown constant within the individual regions.

Defining generalized dimensionless temperature as,

$$T^{*} = \frac{T - T_o}{T_o} = \Theta(x^{*}) + \frac{d\Theta}{dz} z^{*} \tag{4.9}$$

where T_o is the mean fluid temperature entering region I

Substituting the various dimensionless terms, equation (4.8) becomes,

$$\frac{d^2\Theta^{I}}{dx^{*2}} = \frac{\rho_1 c_{p1} V B_1{}^{2}}{k_1 L_1} \left(\frac{d\Theta^{I}}{dz^{*}} \right) V_z{}^{*I} - \frac{\mu_1 V^2}{k_1 T_o} \left(\frac{\delta V_z{}^{1}}{\delta x} \right)^2 \tag{4.10}$$

Now introducing new dimensionless terms,

$$\beta_1 = \frac{\rho_1 c_{p1} V B_1{}^{2}}{k_1 L_1} \quad \text{and} \quad Br_1 = \frac{\mu_1 V^2}{k_1 T_o}$$

where β_1 is a dimensionless constant and Br_1 is Brinkman number

and defining temperature gradient in the z directions as,

$$a_1 = \frac{d\Theta^{I}}{dz^{*}}$$

Equation (4.10) simplifies to,

$$\frac{d^2\Theta^I}{dx^{*2}} = \beta_1 a_1 V_z{}^{*I} - Br_1\left(\frac{\delta V_z{}^1}{\delta x}\right)^2 \tag{4.11}$$

Now substituting for $V_z{}^{*I}$ from equation (4.4) and applying the boundary conditions, at $x^* = 0$; $d\Theta^I/dx^* = q_2{}^*$ and at $x^* = 1$; $d\Theta^I/dx^* = -q_1{}^*$, where dimensionless heat flux is defined as, $q_i{}^* = \frac{B_1 q_i}{k_1 T_o}$

The constant temperature gradient in the z-direction, a_1 is determined as,

$$\boxed{a_1 = \left[\frac{1}{\beta_1\left(\frac{1}{2} - \frac{\Lambda_1}{12}\right)}\right] * \left[Br_1\left(1 + \frac{\Lambda_1{}^2}{12}\right) - q_2{}^* - q_1{}^*\right]} \tag{4.12}$$

And the temperature profile in the x-direction for region I is determined as,

$$\boxed{\begin{aligned}\Theta^I = \beta_1 a_1 &\left[\frac{\Lambda_1}{24} x^{*4} + \frac{1}{6}\left(1 - \frac{\Lambda_1}{2}\right) x^{*3}\right] \\ &- Br_1\left[\frac{\Lambda_1{}^2}{12} x^{*4} + \frac{1}{6}(2\Lambda_1 - \Lambda_1{}^2) x^{*3} + \frac{1}{2}\left(\frac{\Lambda_1{}^2}{4} - \Lambda_1 + 1\right) x^{*2}\right] \\ &+ q_2{}^* + c_1\end{aligned}} \tag{4.13}$$

where c_1 is an unknown constant of integration.

Similarly, the temperature profile for region II is determined by applying the boundary conditions, at $x^* = 0$; $d\Theta^I/dx^* = q_2{}^*.(k_2/k_1)$ and at $x^* = B_2/B_1$; $d\Theta^I/dx^* = -q_1{}^*$, and defining the terms,

$$\beta_2 = \frac{\rho_2 c_{p2} V B_1{}^2}{k_2 L_1} \qquad Br_2 = \frac{\mu_2 V^2}{k_2 T_o} \qquad a_2 = \frac{d\Theta^{II}}{dz^*}$$

The constant temperature gradient in the z-direction, a_2 for region II is determined as,

$$a_2 = \left[\frac{1}{\beta_2\left(\frac{1}{2}\left(\frac{B_2}{B_1}\right) - \frac{\Lambda_2}{12}\left(\frac{B_2}{B_1}\right)^3\right)}\right] * \left[Br_2\left(\left(\frac{B_1}{B_2}\right) + \frac{{\Lambda_2}^2}{12}\left(\frac{B_2}{B_1}\right)^3\right) - {q_2}^*\left(\frac{k_2}{k_1}\right) - {q_1}^*\left(\frac{k_2}{k_1}\right)\right] \quad (4.14)$$

And the temperature profile in the x-direction for region II is determined as,

$$\begin{aligned}\Theta^{II} = {} & \beta_2 a_2\left[\frac{\Lambda_2}{24}{x^*}^4 + \frac{1}{6}\left(\frac{B_1}{B_2}\right)\left(1 - \frac{\Lambda_2}{2}\left(\frac{B_2}{B_1}\right)^2\right){x^*}^3\right] \\ & - Br_2\left[\frac{{\Lambda_2}^2}{12}{x^*}^4 + \frac{1}{6}\left(2\Lambda_2\left(\frac{B_1}{B_2}\right) - {\Lambda_2}^2\left(\frac{B_2}{B_1}\right)^2\right){x^*}^3\right. \\ & \left. + \frac{1}{2}\left(\frac{{\Lambda_2}^2}{4}\left(\frac{B_2}{B_1}\right)^2 - \Lambda_2 + \left(\frac{B_1}{B_2}\right)^2\right){x^*}^2\right] + {q_2}^*\left(\frac{k_2}{k_1}\right) \\ & + c_2\end{aligned} \quad (4.15)$$

where c_2 is an unknown constant of integration.

To determine c_1 and c_2, two conditions are imposed:

a. Overall energy balance for the system:

Energy generated in Region I and II – Energy leaving through the top and bottom plates in Region I and Region II = Energy leaving the system at the end of Region II – Energy entering the system at the entrance of Region I. This is represented by equation 4.16.

$$\begin{aligned}&\left[\mu_1\int\left(\frac{dV_z{}^I}{dx}\right)^2 dx\right]L_1 + \left[\mu_2\int\left(\frac{dV_z{}^{II}}{dx}\right)^2 dx\right]L_2 - L_1q_1 - L_1q_2 \\ &\qquad = c_{p2}\rho_2\left[\int Vz^{II}T^{II}dx\right] - c_{p1}\rho_1\left[\int Vz^{I}T_o dx\right]\end{aligned} \quad (4.16)$$

b. Temperature continuity at the interface:

$$\int T^{I} V z^{I} dx = \int T^{II} V z^{II} dx \tag{4.17}$$

In equation 4.17, T^{I} is calculated at z=L_1, and T^{II} is calculated at z=0, which represent the interface in terms of length for the two regions based on how they are defined earlier.

Using the dimensionless terms defined earlier and substituting for known terms, c_2 is obtained from equation 4.16 as,

$$\begin{aligned} c_2 = & \left[\frac{1}{\frac{1}{2}\left(\frac{B_2}{B_1}\right) - \frac{\Lambda_2}{12}\left(\frac{B_2}{B_1}\right)^3}\right] \cdot \left\{\frac{1}{\beta_1}\left[\left[1 + \frac{\Lambda_1}{12}\right] + Br_1\left(\frac{L_2}{L_1}\right)\left[\frac{B_1}{B_2} + \frac{{\Lambda_2}^2}{12}\left(\frac{B_2}{B_1}\right)^3\right]\right.\right. \\ & \left. - {q_1}^*\left(1 + \left(\frac{L2}{L1}\right)\right) + {q_2}^*\left(1 + \left(\frac{L2}{L1}\right)\right)\right] \\ & - \left(1 + a2\left(\frac{L2}{L1}\right)\right)\left[\frac{1}{2}\left(\frac{B_2}{B_1}\right) - \frac{\Lambda_2}{12}\left(\frac{B_2}{B_1}\right)^3\right] \\ & - \beta_2 a_2\left[\frac{{\Lambda_2}^2}{1120}\left(\frac{B_2}{B_1}\right)^7 - \frac{\Lambda_2}{80}\left(\frac{B_2}{B_1}\right)^5 + \frac{1}{30}\left(\frac{B_2}{B_1}\right)^3\right] \\ & - Br_2\left[\frac{3{\Lambda_2}^3}{2240}\left(\frac{B_2}{B_1}\right)^7 - \frac{3{\Lambda_2}^2}{160}\left(\frac{B_2}{B_1}\right)^5 + \frac{17\Lambda_2}{240}\left(\frac{B_2}{B_1}\right)^3 - \frac{1}{8}\left(\frac{B_2}{B_1}\right)\right] \\ & \left. - {q_2}^*\left[\frac{1}{3}\left(\frac{B_2}{B_1}\right)^2 - \frac{\Lambda_2}{24}\left(\frac{B_2}{B_1}\right)^4\right] + \left[\frac{1}{2} - \frac{\Lambda_1}{12}\right]\right\} \end{aligned} \tag{4.18}$$

And c_1 is obtained from equation 4.17 as,

$$c_1 = \left[\frac{1}{\frac{1}{2}-\frac{\Lambda_1}{12}}\right].\left\{(1-c_2)\left[\frac{1}{2}\left(\frac{B_2}{B_1}\right)-\frac{\Lambda_2}{12}\left(\frac{B_2}{B_1}\right)^3\right] + \beta_2 a_2\left[\frac{{\Lambda_2}^2}{1120}\left(\frac{B_2}{B_1}\right)^7-\frac{\Lambda_2}{80}\left(\frac{B_2}{B_1}\right)^5+\frac{1}{30}\left(\frac{B_2}{B_1}\right)^3\right] + Br_2\left[\frac{3{\Lambda_2}^3}{2240}\left(\frac{B_2}{B_1}\right)^7-\frac{3{\Lambda_2}^2}{160}\left(\frac{B_2}{B_1}\right)^5+\frac{17\Lambda_2}{240}\left(\frac{B_2}{B_1}\right)^3-\frac{1}{8}\left(\frac{B_2}{B_1}\right)\right] - \beta_1 a_1\left[\frac{{\Lambda_1}^2}{1120}-\frac{\Lambda_1}{80}+\frac{1}{30}\right] - Br_1\left[\frac{3{\Lambda_1}^3}{2240}-\frac{3{\Lambda_1}^2}{160}+\frac{17\Lambda_1}{240}-\frac{1}{8}\right] - {q_2}^*\left[\frac{1}{3}\left(\frac{B_2}{B_1}\right)^2-\frac{\Lambda_2}{24}\left(\frac{B_2}{B_1}\right)^4-\frac{1}{3}+\frac{\Lambda_1}{24}\right] - (1+a_1)\left[\frac{1}{2}-\frac{\Lambda_1}{12}\right]\right\} \quad (4.19)$$

Hence the various components of temperature profiles for region I and II have been determined. These values are then substituted in equations 4.13 and 4.15 to plot temperature profiles.

4.5 Results and discussion

For analysis of the velocity and temperature profiles at various conditions, for simplicity, the following conditions/assumptions are made:

1. $L_2/L_1 = 0.1$, based on the dimensions of the extruder in the current study.
2. Dimensionless terms, β_1 and β_2 are assumed to be equal to 1.
3. Dimensionless heat fluxes leaving the top and bottom plate, q_1^* and q_2^* are considered equal.
4. Dimensionless heat flux leaving the top plate is defined as a fraction of Brinkman number (which represents heat generated) in region I, $q_1^* = x^* Br_1$.

4.5.1 Effect of screw restriction

In order to show the effect of screw restriction, two cases of the original Couette flow setup are considered:

Case 1: The gap between the top and bottom plates in Region I and Region II are equal, therefore $B_2/B_1 = 1$. This is represented in Figure 4.4. The viscosity between the two regions is also considered equal, therefore $\mu_2/\mu_1 = 1$.

Case 2: The gap between the plates in Region II is half of the gap between the plates in Region I, therefore $B_2/B_1 = 0.5$. This is similar to the original representation of the setup, as in Figure 4.3. The viscosity ratio between the two regions is assumed to be independent of the consistency index, for the sake of simplicity and just dependent on the power law index (n=0.23) from the corn meal model in the previous study is used, therefore, $\mu_2/\mu_1 = (B_1/B_2)^{\wedge}0.77$.

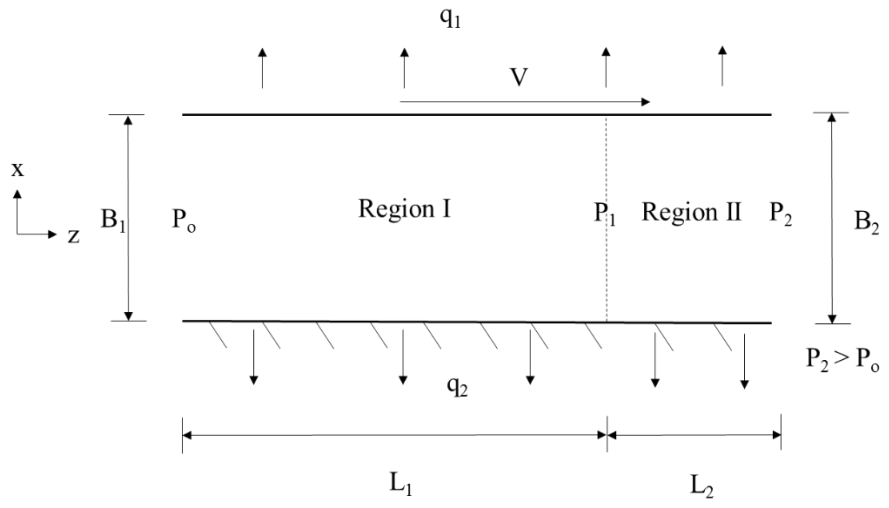

Figure 4.4. Couette flow setup between parallel plates with equal gap between Region I and Region II to represent Case 1.

Based on the assumptions made thus far, the parameter that influences velocity profile is overall pressure difference across the two regions which is directly related to the dimensionless term Λ. The parameters that influence temperature profile are a) overall pressure difference (related to Λ), b) viscous dissipation (related to Brinkman number) and c) heat fluxes leaving the system (q_1^* and q_2^*). To see the effect of these parameters on velocity and temperature profiles, one parameter will be changed at a time while the others are kept constant. Temperature profiles are plotted at the end of region I and end of region II.

4.5.1.1 Effect of overall pressure difference

To show the effect of overall pressure difference across the two regions, Λ is set to three levels (0.05, 0.5 and 1), while viscous dissipation (Br_1=1) and heat flux (q_1^*=0.1*Br_1) are kept constant. The effect of Λ on velocity profile in Region I and Region II of the two setups, case 1 and case 2, are shown in figures 4.5 and 4.6, respectively.

When the gaps between the plates in the two regions are equal, it can be seen that the velocity profile in the two regions are identical (Figure 4.5 a & b). As Λ increases, the non-linearity of the drag flow increases, indicating the effect of increase in pressure difference. Whereas when the gap in region II is reduced, the non-linearity further increases in region I (Figure 4.6 a), but in region II, the peak velocity is not at the top plate but at a region slightly below it and the velocity itself is higher than the top plate velocity (Figure 4.6 b). A closer look at the analysis reveals that this is due to the mass balance condition imposed at the interface of the two regions.

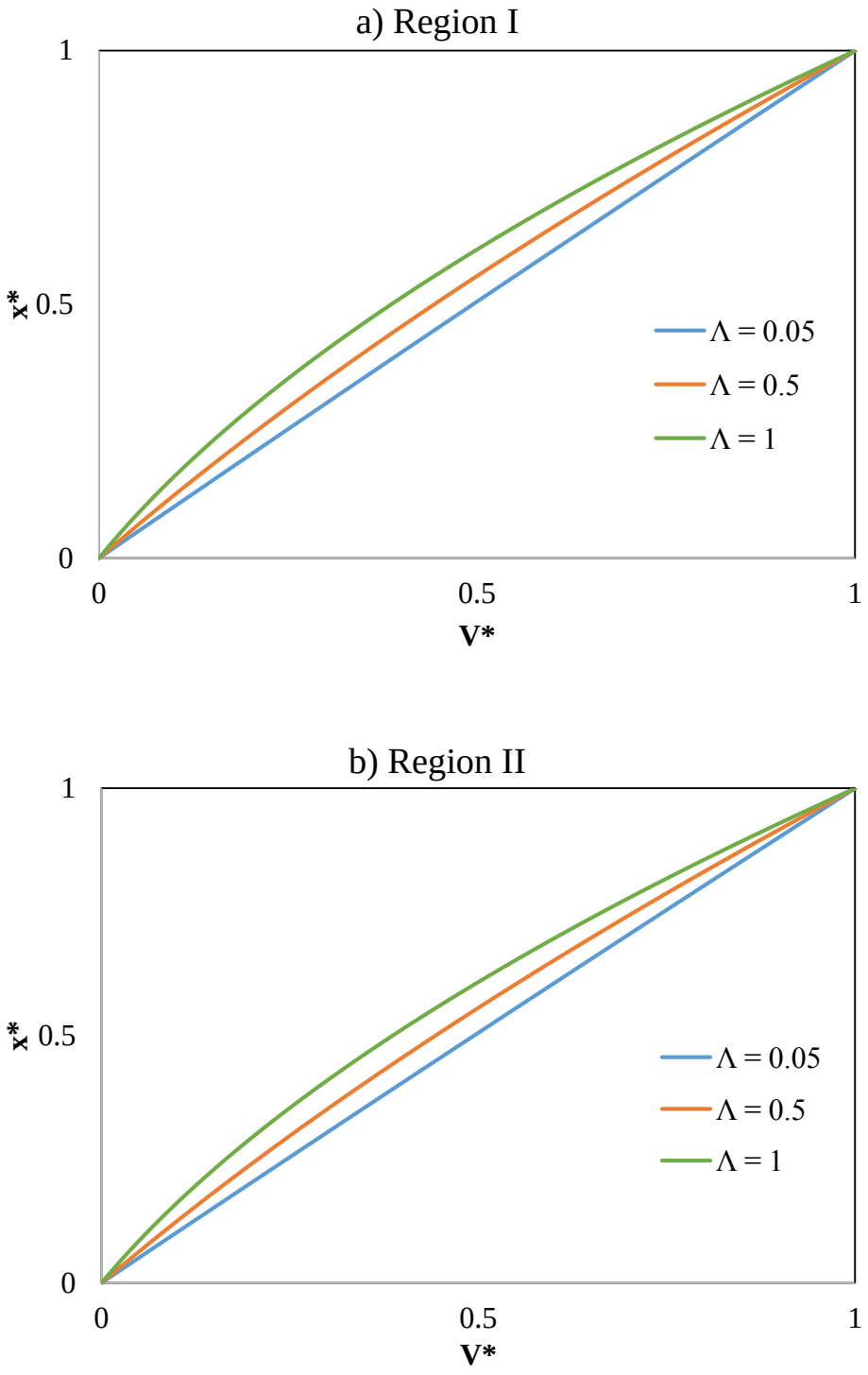

Figure 4.5. Dimensionless velocity profiles in a) Region I and b) Region II for case 1 ($B_2/B_1 = 1$) at different overall pressure difference across the two regions (Λ).

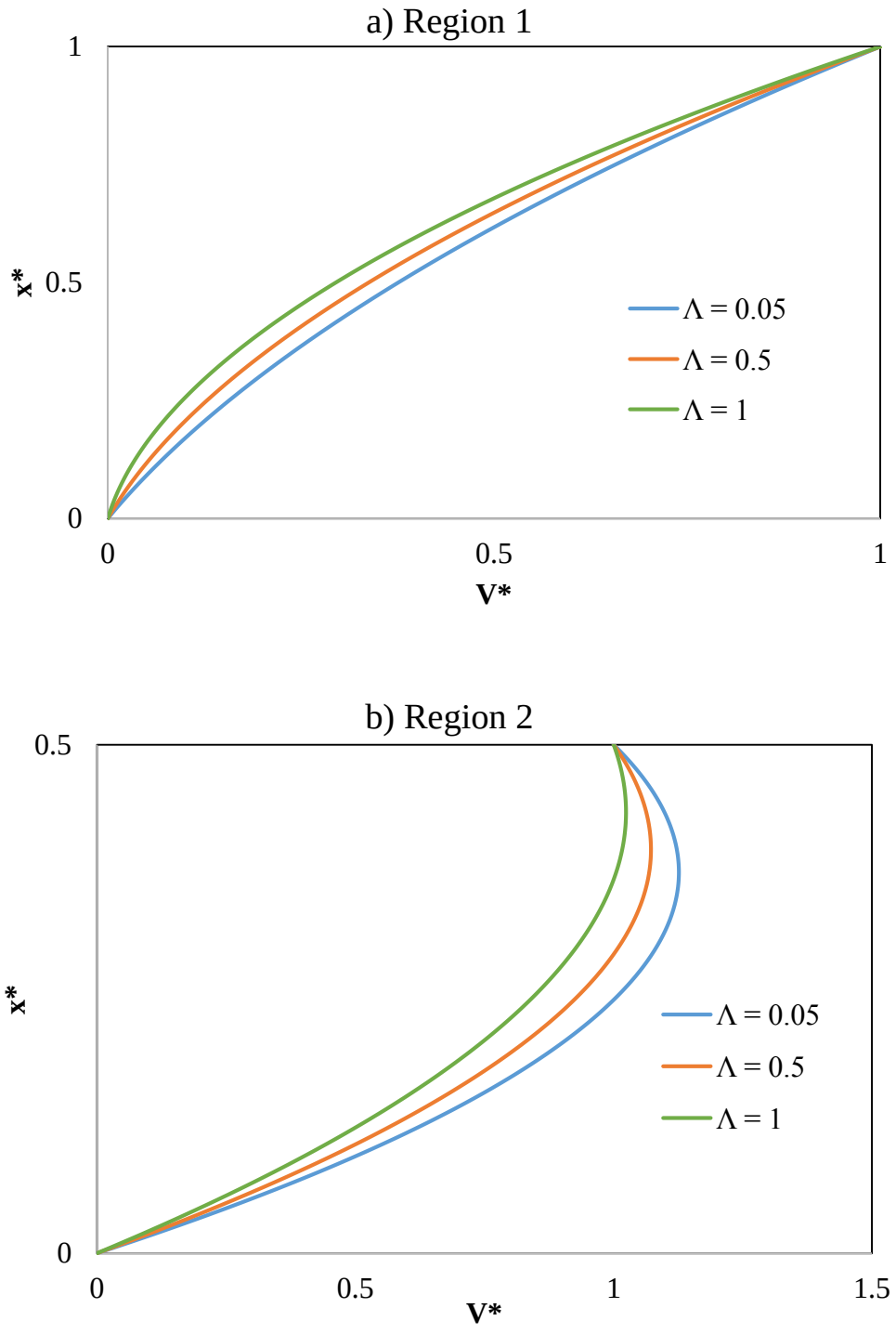

Figure 4.6. Dimensionless velocity profiles in a) Region I and b) Region II for case 2 ($B_2/B_1 = 0.5$) for different overall pressure difference across the two regions (Λ).

Now looking at the effect of Λ on temperature profile in Region I and Region II of the two setups, case 1 and case 2, are shown in figures 4.7 and 4.8, respectively.

Similar to the velocity profiles, the temperature profiles between region I and II are identical in case 1 where the gaps are equal (Figure 4.7). But on comparing the dimensionless temperatures at the end of regions, region II has a higher temperature than region I because of the added viscous dissipation along the z-direction as the product flows through region II. And as Λ increases dimensionless temperature increases accordingly at the exit of both the regions, indicating that as extrusion pressure increases, the temperature also increases.

In case 2, due to presence of a smaller gap in region II, the temperature rise is much higher for the same Λ compared to case 1 (Figure 4.8), indicating the effect of the presence of screw restriction. Also in region II (Figure 4.8 b), the temperature profile near the bottom plate is higher than the top plate. This can be explained by looking at the velocity profile at the same conditions in Figure 4.6 b. Since viscous dissipation is directly related to the square of the slope of velocity profile, the higher slope in velocity profile near the bottom place leads to higher viscous dissipation, hence the temperature rise near the bottom plate is much higher compared to the top plate.

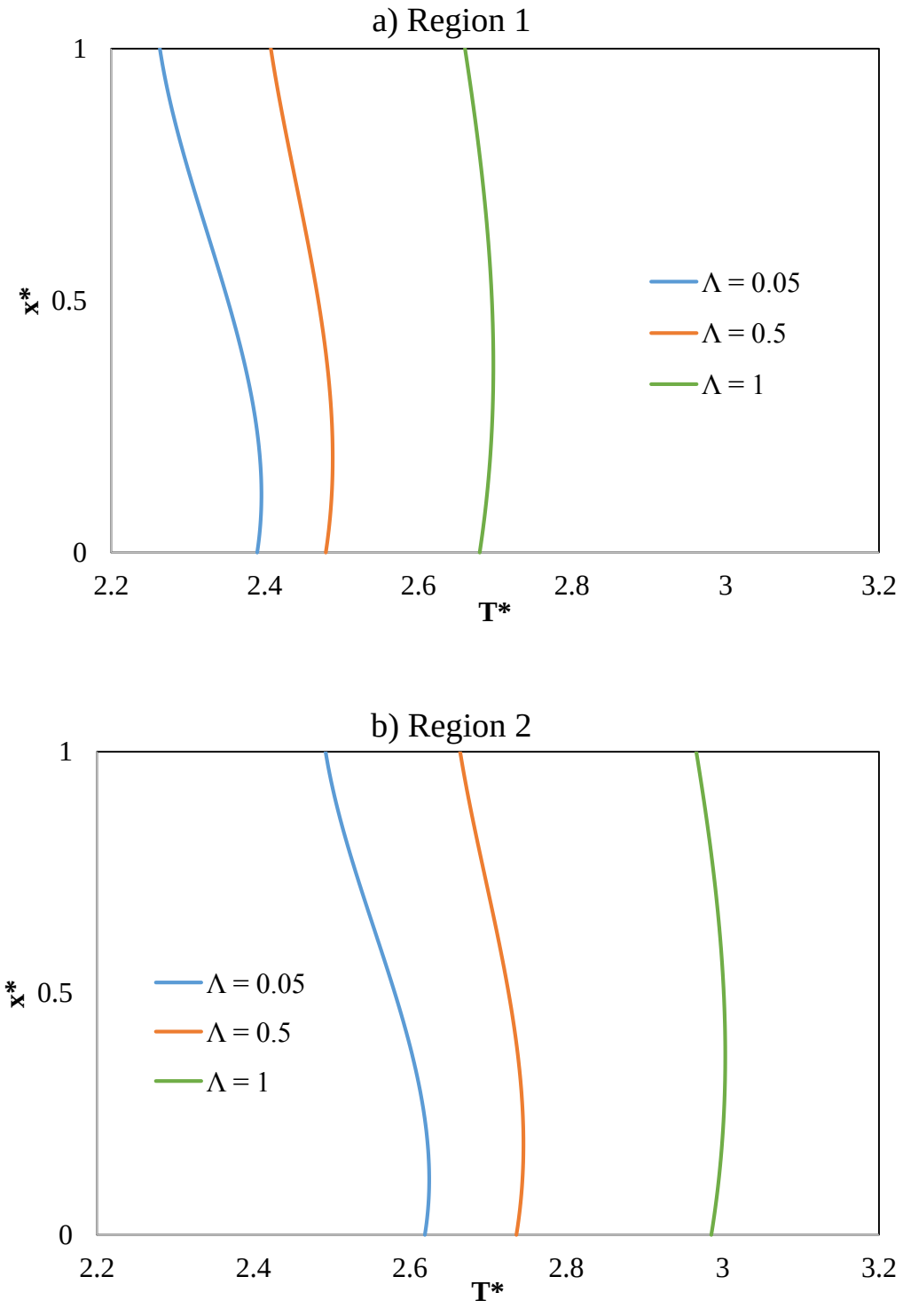

Figure 4.7. Dimensionless temperature profiles at the end of a) Region I and b) Region II for case 1 ($B_2/B_1 = 1$) at different overall pressure difference across the two regions (Λ).

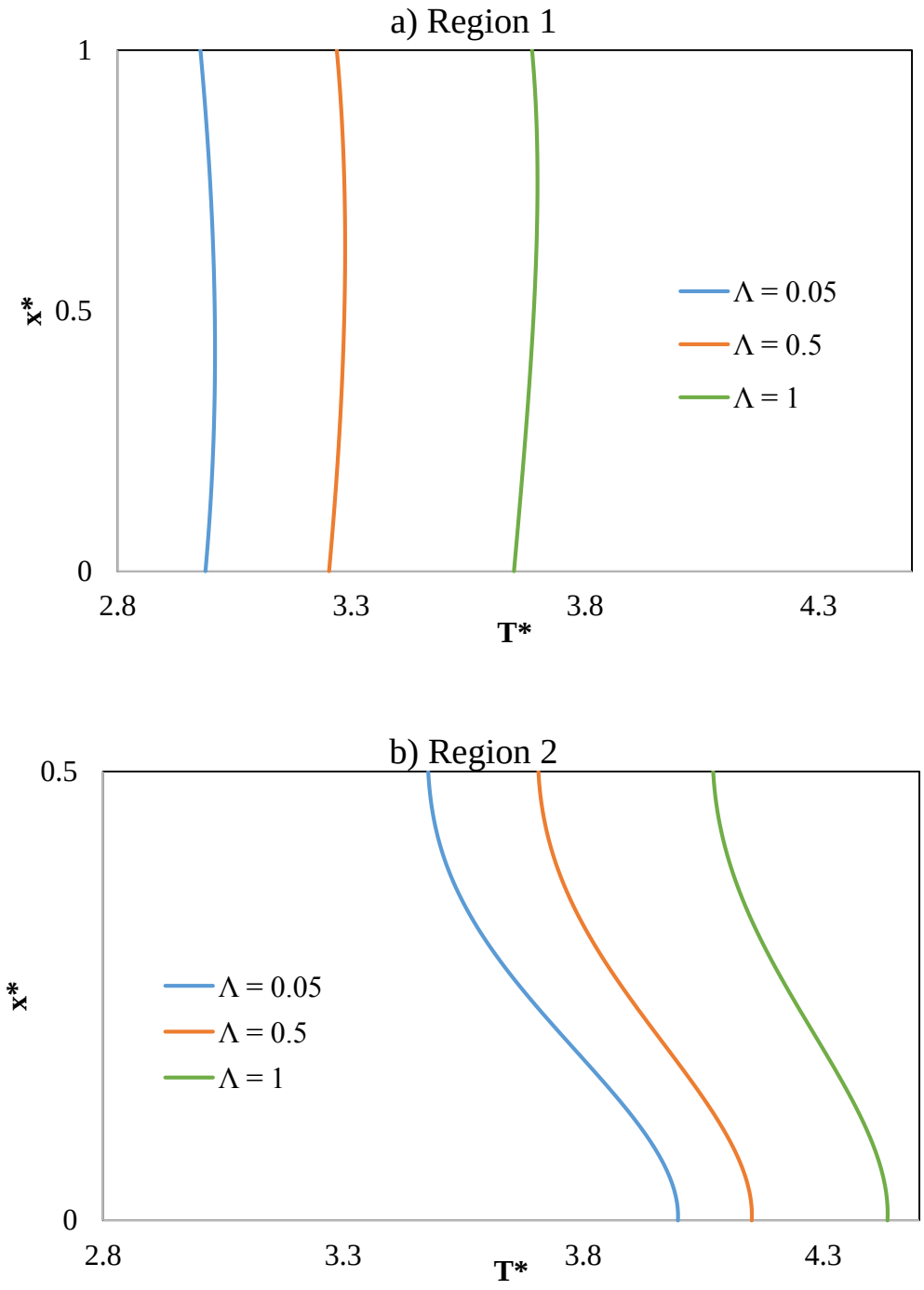

Figure 4.8. Dimensionless temperature profiles at the end of a) Region I and b) Region II for case 2 ($B_2/B_1 = 0.5$) for different overall pressure difference across the two regions (Λ).

4.5.1.2 Effect of viscous dissipation

To show the effect of viscous dissipation, Br_1 is set to three levels (0.1, 0.5 and 1), while the overall pressure difference (Λ =0.05) and heat flux (q_1^*=0.1*Br_1) are kept constant. The effect of Br_1 on temperature profile in region I and region II of the two setups, case 1 and case 2, are shown in figures 4.9 and 4.10, respectively.

In both cases, as Br_1 increases, dimensionless temperature at the end of a region increases, indicating that viscous dissipation is higher for a fluid with a higher viscosity, as expected. Region II has a higher temperature than region I at the end, because of the additional viscous dissipation generated in region II as the product flows through it. Comparing the temperature rise between the two cases, the presence of a screw restriction clearly indicates a higher rise in temperature (Figure 4.9 and 4.10).

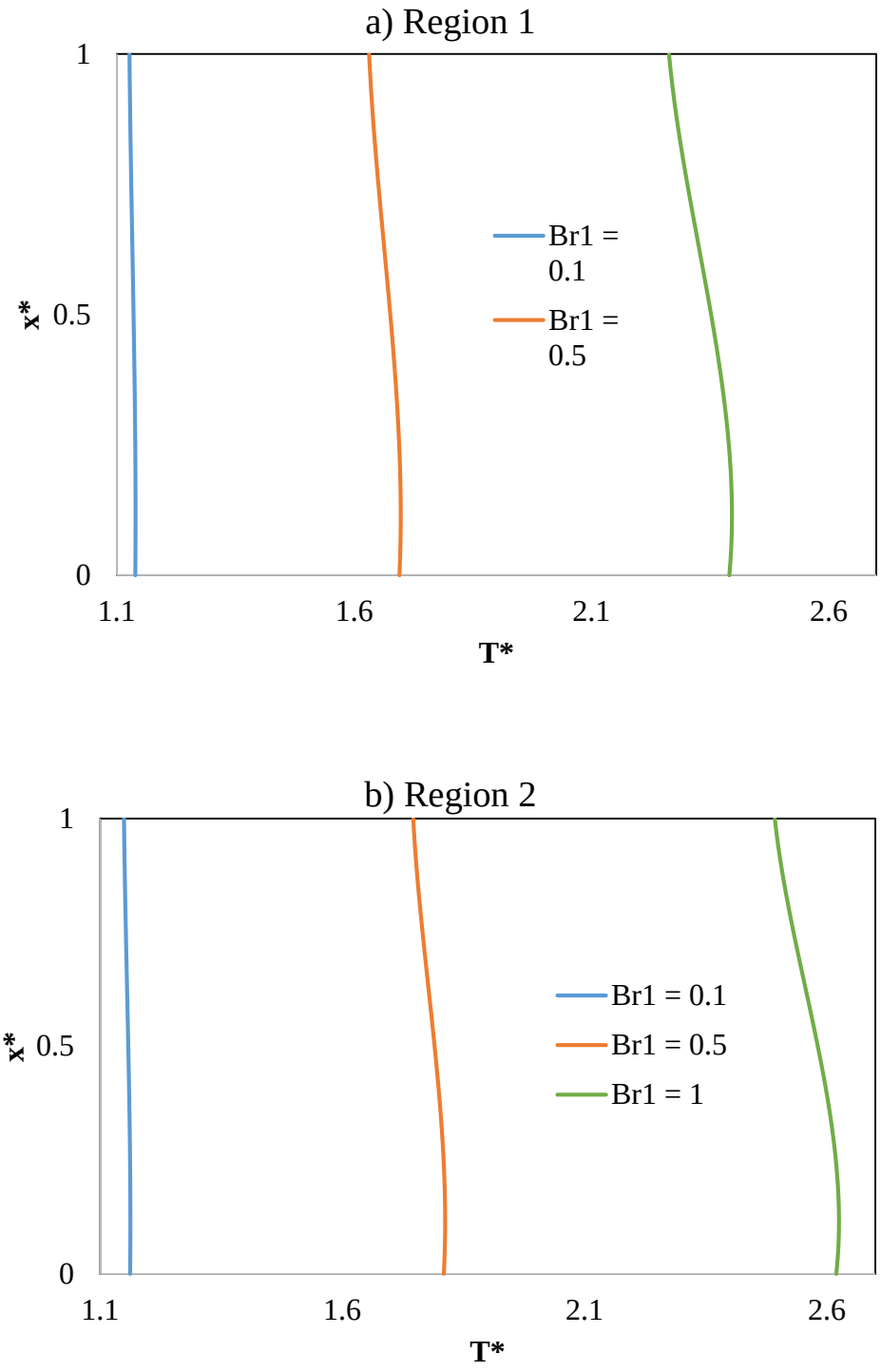

Figure 4.9. Dimensionless temperature profiles at the end of a) Region I and b) Region II for case 1 ($B_2/B_1 = 1$) at different viscous dissipation (Br_1).

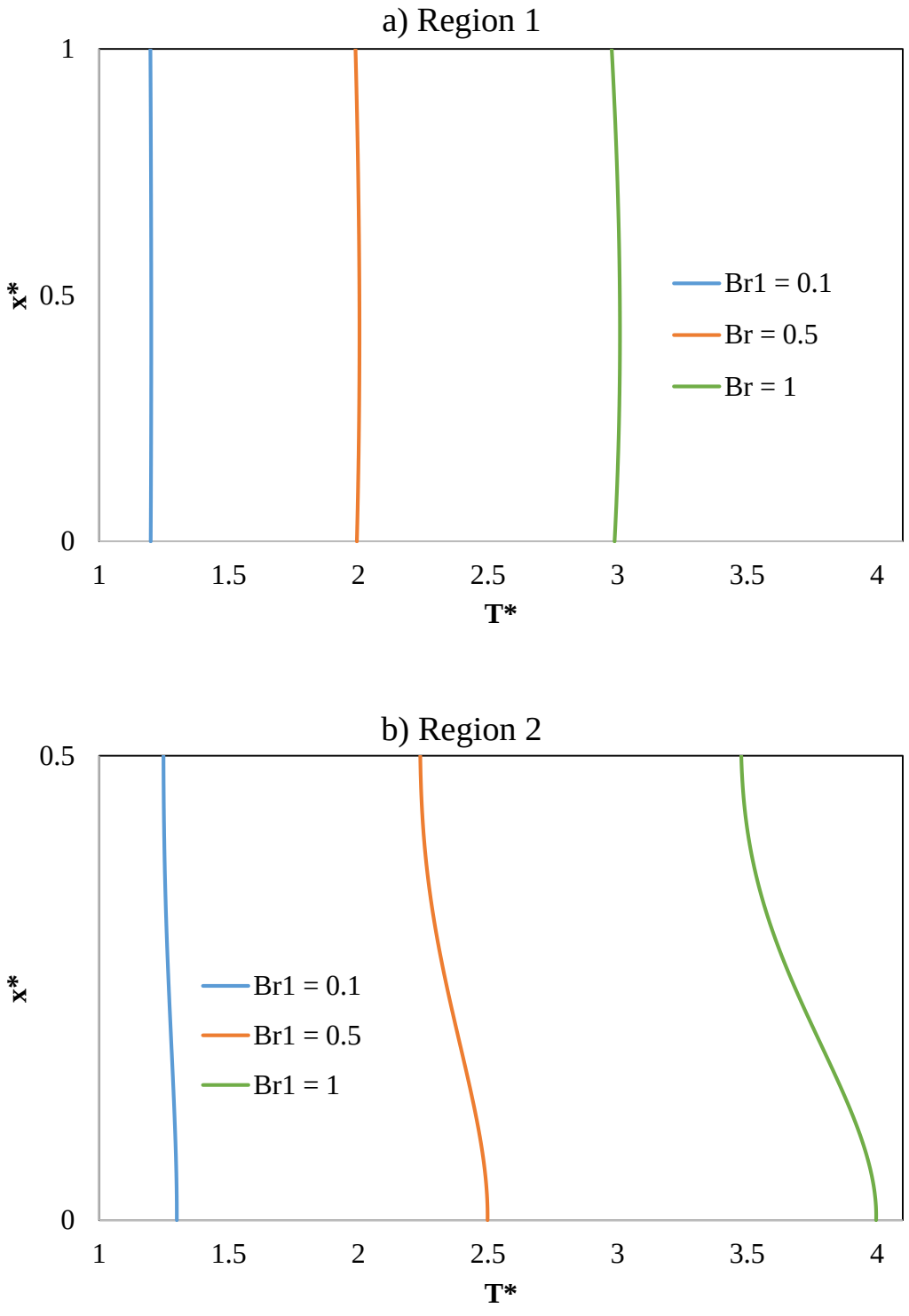

Figure 4.10. Dimensionless temperature profiles at the end of a) Region I and b) Region II for case 2 ($B_2/B_1 = 0.5$) at different viscous dissipation (Br_1).

4.5.1.3 Effect of heat flux leaving the system

To show the effect of heat flux leaving the system, q_1^* is set to three levels (0.1, 0.2 and $0.3*Br_1$), while the overall pressure difference (Λ =0.05) and viscous dissipation (Br_1=1) are kept constant. The effect of q_1^* on temperature profile in region I and region II of the two setups, case 1 and case 2, are shown in figures 4.11 and 4.12, respectively.

Heat flux in this model is setup as a fraction of Brinkman number which indicates the level of viscous dissipation. As the heat flux leaving the system increases, the dimensionless temperature at the end of a region decreases as expected, in both the setups (Figure 4.11 and 4.12). In the presence of a screw restriction, the overall temperature rise is much higher compared to having an equal gap between the plates.

The interaction between the various parameters used to show their effect on velocity and temperature profile plays a crucial role in understanding the application of this mechanistic model to a single screw extruder with screw restrictions.

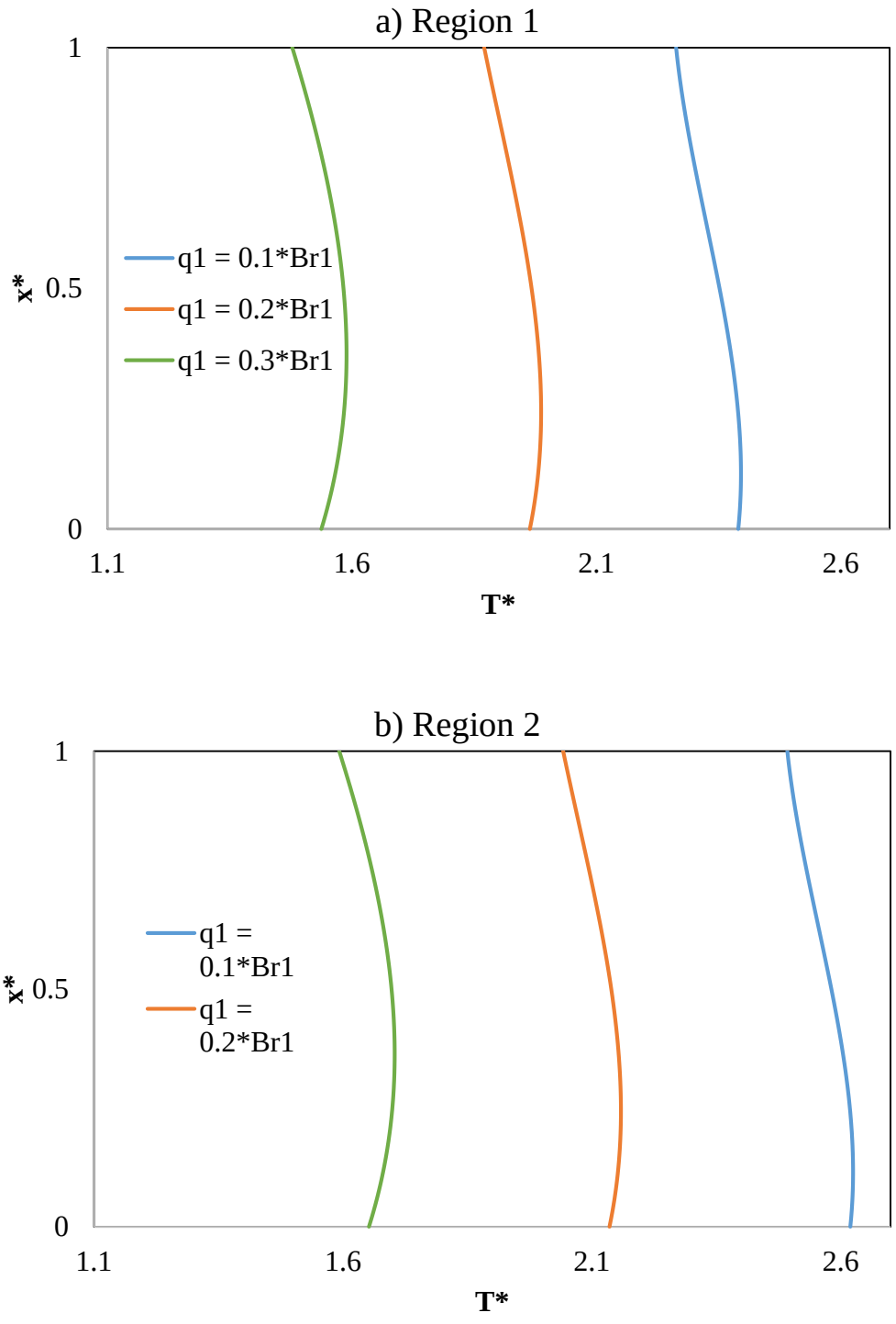

Figure 4.11. Dimensionless temperature profiles at the end of a) Region I and b) Region II for case 1 ($B_2/B_1 = 1$) at different heat fluxes (q_1^*).

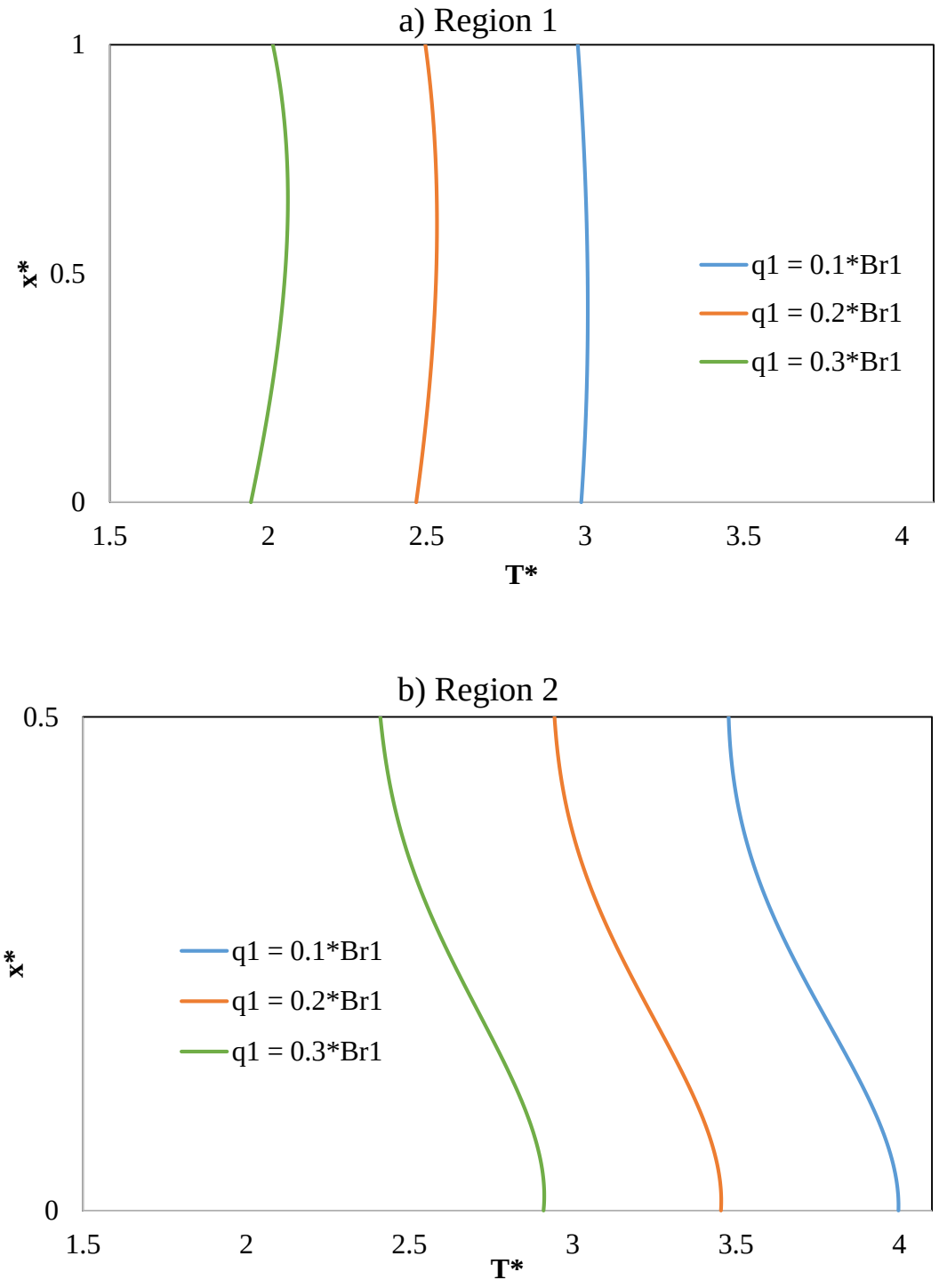

Figure 4.12. Dimensionless temperature profiles at the end of a) Region I and b) Region II for case 2 ($B_2/B_1 = 0.5$) at different heat fluxes (q_1^*).

4.5.2. Quantitative analysis

In order to give an example of how quantitative results can be generated from the current model, one of the conditions used in in-line viscosity measurement of corn meal from the previous study is used here. 35% moisture content corn meal was extruded at 300rpm to give a die temperature rise of 128^{o}C.

Only the last screw, screw restriction and die are considered for this example. The physical dimensions of the screw, shear bushing and die were used to calculate the various dimensions of the setup. The extruder screw speed (300 rpm) was used to calculate the velocity of the top moving plate and hence the shear rate experienced in region I and II.

The power-law viscosity model developed for the corn meal in the previous study was used to calculate viscosity of the fluid in the individual regions. Since it is known that the viscosity model is over predicting the viscosity of the fluid, it was adjusted by a factor of 10. For viscosity calculations, an average temperature at the entrance of region I was assumed and to be 90^{o}C. Based on these parameters, Λ was calculated to be 0.028.

In order to determine temperature rise, Brinkman number was calculated based on extruder data and viscosity calculated from the power-law model to be 0.75. Then the heat flux leaving the system was adjusted as an unknown variable to match the actual temperature rise in the extruder (128^{o}C). Since heat flux was defined as a fraction of Brinkman, the multiplying factor of 0.45 gave the required temperature rise at the exit of region II in the model. But this needs to be further validated with experimental data.

4.6 Conclusion

A mechanistic model for one screw, one restriction and die, of a single screw extruder with restrictions on its screw was built using a modified Couette flow between two parallel plates with two regions or varying gaps. In order to understand the effect of viscous dissipation on the flow through this setup, the momentum and energy equations are solved individually for the two regions, using dimensionless analysis. Mass and energy balance at the interface of the two regions and overall mass and energy balance for the system is used to find unknowns and hence the velocity and temperature profiles in the two regions. To show the effect of the presence of a screw restriction on velocity and temperature profiles, two setups, one with and without screw restriction are compared. The effect of overall pressure difference across the two regions, viscous dissipation and heat fluxes leaving the system were documented. In all the cases, the presence of a screw restriction leads to a larger temperature rise in the system. The proposed model could be used to calculate unknown variables to fit experimental data and predict operating conditions of an extruder but still needs to be validated with experimental data.

4.7 References

Aydin, O., Avci, M., (2006). Laminar forced convection with viscous dissipation in a Couette-Poiseuille flow between parallel plates. Applied Energy. 83(8), 856-867.

Bouvier, J., Campanella, O.H., (2014). *Extrusion processing technology: food and non-food biomaterials*. John Wiley & Sons, Ltd, West Sussex, UK.

Carley, J., Mallouk, R., McKelvey, J., (1953). Simplified flow theory for screw extruders. Industrial & Engineering Chemistry. 45(5), 974-978.

Carley, J., Strub, R., (1953). Basic concepts of extrusion. Industrial & Engineering Chemistry. 45(5), 970-973.

Harmann, D.V., Harper, J.M., (1974). Modeling a forming foods extruder. Journal of Food Science. 39(6), 1099-1104.

Harper, J.M., (1979). Food Extrusion. Critical Reviews in Food Science and Nutrition. 11(2), 155-215.

Harper, J.M., (1981). *Extrusion of foods: Volume I*. CRC Press, Boca Raton, Florida.

Kokini, J.L., Ho, C., Karwe, M.V., (1992). *Food extrusion science and technology*. Marcel Dekker, Inc., New York, New York.

LeRoux, D., Vergnes, B., Chaurand, M., Abecassis, J., (1995). A thermomechanical approach to pasta extrusion. Journal of Food Engineering. 26(3), 351-368.

Li, Y., Hsieh, F., (1996). Modeling of flow in a single screw extruder. Journal of Food Engineering. 27(4), 353-375.

Mercier, C., Linko, P., Harper, J.M., (1989). *Extrusion cooking*. American Association of Cereal Chemists, Inc., St. Paul, Minnesota, USA.

Mondal, P.K., Mukherjee, S., (2014). Thermodynamically consistent limiting Nusselt number in the viscous dissipative non-Newtonian Couette flows. Industrial & Engineering Chemistry Research. 53(1), 402-414.

Sheela-Francisca, J., Tso, C.P., (2012). An Analysis of a Viscous Dissipation Flow, in: Wahid, M.A., Samion, S., Sheriff, J.M., Sidik, N.A.C. (Eds.), *4th International Meeting of Advances in Thermofluids*, pp. 392-399.

Sheela-Francisca, J., Tso, C.P., Hung, Y.M., Rilling, D., (2012). Heat transfer on asymmetric thermal viscous dissipative Couette-Poiseuille flow of pseudo-plastic fluids. Journal of Non-Newtonian Fluid Mechanics. 169, 42-53.

Tadmor, Z., Klein, I., (1970). *Engineering principles of plasticating extrusion*. Van Nostrand Reinhold Co.

Tsao, T., Harper, J., Repholz, K., (1978). The effects of screw geometry on extruder operational characteristics, *AIChE Symp. Ser*, p. 142.

Wang, L., Ganjyal, G., Jones, D., Weller, C., Hanna, M., (2004). Finite Element Modeling of Fluid Flow, Heat Transfer, and Melting of Biomaterials in a Single-screw Extruder. Journal of Food Science. 69(5), E212-E223.

CHAPTER 5. FUTURE WORK

Based on the conclusions made from the current work, the following future work are proposed/recommended:

- Accurate in-line measurement of melt viscosity: Based on the observations made from the current study, lack of temperature control and inability to correct for entrance and exit effects (Bagley correction) at the capillary die could possibly result in over-prediction of viscosity during in-line viscosity measurement. To address these challenges, a new in-line viscometer to match the scale of the small-scale extruder should be designed with temperature control and ability to make measurements for Bagley correction. Although such rheometers already exist on a larger scale, designing one to work with the small scale extruder will be a challenge.
- Further understanding of material transformation during in-line versus off-line measurements and extrusion (for food/biopolymers sensitive to thermal/mechanical degradation): Pasting property measurements made on extrudates from the current study clearly show the difference in material transformation between in-line and off-line viscosity measurement techniques. It is essential to utilize additional analytical techniques such as size exclusion

chromatography to further the understanding of material transformation. This is could also help understand and explain the difference in transformation based on the amount of thermal versus mechanical energy supplied to a material during different extrusion processes.

- Validation of mechanistic model for single screw extruders with screw restrictions: In order to validate the basic one-dimensional model proposed in this study, it has to be tested with experimental data collected at a range of extrusions conditions and with a range of raw materials. Since the model is based for one screw and restriction, possibilities of using multiple such sections in series should be explored. For example, the small-scale extruder used in the current study has three such sections in series (excluding the feed section) before the die. Methods to quantify melt viscosities, temperature rises and heat fluxes within each section should also be explored in order to build a robust model.

VITA

VITA

Amudhan Ponrajan received his undergraduate degree in Food Process Engineering from Tamil Nadu Agricultural University in 2007. Then he started graduate study at the University of Georgia where he received a M.S. in Food Science in 2010. During his M.S. he completed a summer internship in 2009 at Frito-Lay R&D, PepsiCo. Following that, he worked at Frito-Lay R&D, PepsiCo for 2 years from summer 2010 to 2012 as a R&D Scientist. Then he joined Purdue University in summer 2012 to purse his Ph.D. in the Department of Agricultural & Biological Engineering under the guidance of Dr. Martin Okos, with a focus on extrusion and rheology. He is headed to General Mills after his Ph.D. to work as a R&D Engineer.